Dynamic modelling of trace metal speciation in anaerobic digestion

An extended ADM1-based mechanistic model framework

SUSAN GEORGE

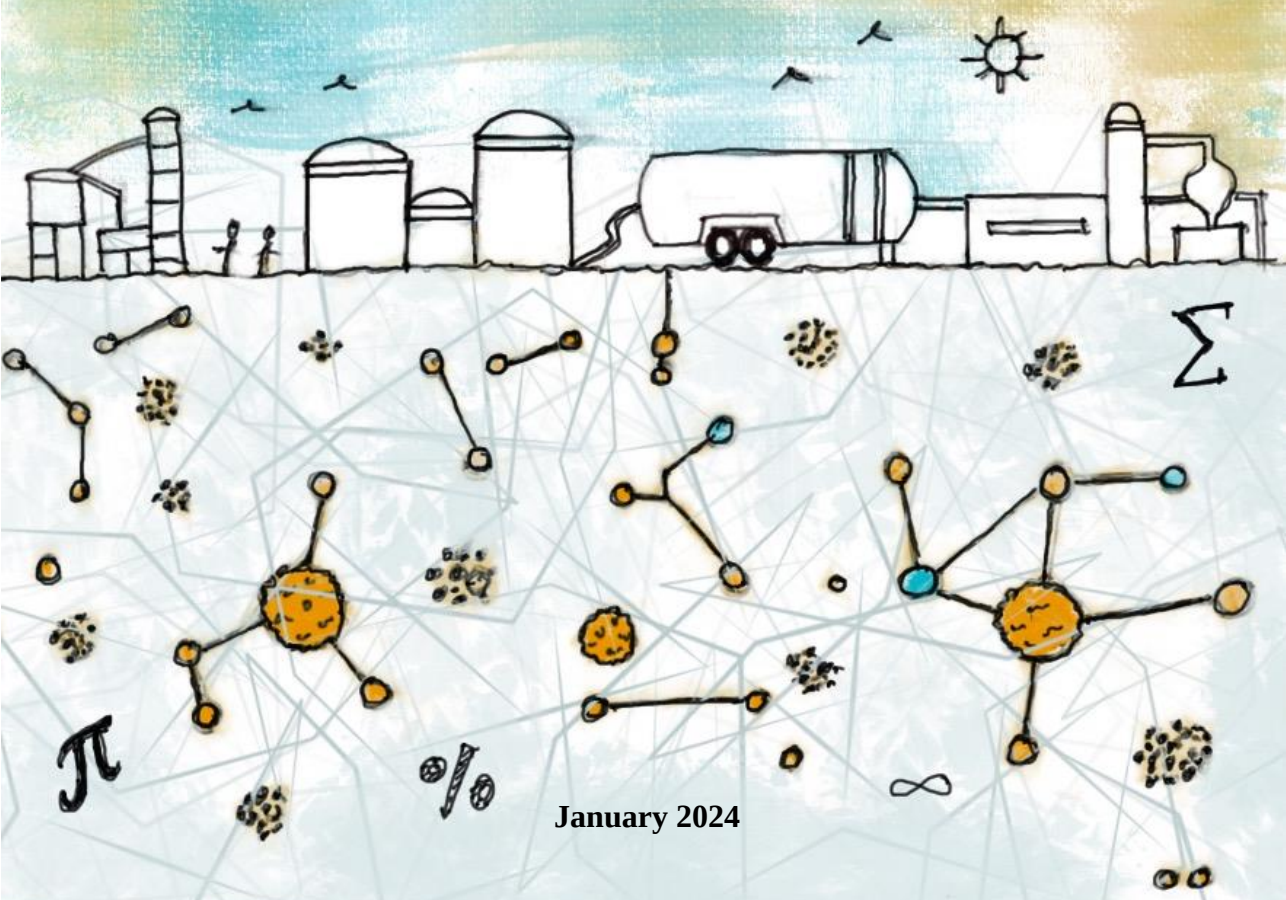

January 2024

Dynamic modelling of trace metal speciation in anaerobic digestion

An extended ADM1-based mechanistic model framework

Susan George

Bachelor of Technology in Civil Engineering

Master of Technology in Environmental Engineering and Management

A thesis submitted for the double degree of Doctor of Philosophy (Ph.D.) in "Biotechnology, Engineering and Chemical Technology" at Universidad Pablo de Olavide and in "Civil Systems Engineering" at University of Naples Federico II in January 2024

Dynamic modelling of trace metal speciation in anaerobic digestion

An extended ADM1-based mechanistic model framework

PhD Thesis

Susan George

Thesis Supervisors

Dr. Fernando Gonzalez Fermoso
Instituto de la Grasa, CSIC, Seville, Spain
Prof. Giovanni Esposito
University of Naples Federico II, Napoli, Italy
Prof. Luigi Frunzo
University of Naples Federico II, Napoli, Italy
Dr. Maria Rosaria Mattei
University of Naples Federico II, Napoli, Italy

This research was conducted within European Union's Horizon 2020 Marie Sklodowska-Curie grant (Nº 861088): M2ex "Exploiting metal-microbe applications to expand the circular economy"

Acknowledgements

When time flew fast during the three years of the PhD, knowledge and experience gained during these years are of great value. The circumstances and new faces I have met during these years have influenced and contributed to my growth, both personally and professionally. I take this opportunity to thank the people who have supported me for completion of this work.

I acknowledge European Union's Horizon 2020 Marie Skłodowska-Curie Innovative Training Network for the funding and the committee of the project M2ex "Exploiting metal-microbe applications to expand the circular economy" for providing me the opportunity to be a part of this European Joint Doctorate programme.

Being involved in a joint doctoral program to be guided by multiple supervisors is attractive and scary at the same time. Any communication gap could have made my journey complicated, but thanks to supervisors for finding the right balance. I express my sincere gratitude to all my supervisors, Dr. Fernando Gonzalez Fermoso, Prof. Luigi Frunzo, Dr. Maria Rosaria Mattei and Prof. Giovanni Esposito for their invaluable contributions in both academic and administrative matters. Thank you to all my supervisors for believing in me and letting me work independently enough, without giving me the feeling of being lost. This improved my self-confidence and accelerated the learning curve. The fruitful group meetings we had gave me a clear direction whereas the scheduled and informal meetings with each of you gave me clarity. Thanks to Fernando for being the support during the experimental phase of the PhD and Maria for being my support for modelling related doubts. Thank you, Maria, for the persistent encouragement and trust. I would like to acknowledge Prof. Esposito and Prof. Eric van Hullebusch for their thoughtful reviews and vital discussions that helped me to integrate the expert knowledge in the thesis. I would also like to thank Graciano Carpes and Eva Maria Rodriguez Gonzalez for providing the full-scale reactor data and for the support received during the four months of my industrial secondment at EMASESA Metropolitana, Seville.

My immense gratitude to the supervisors and my fellow early stage researchers involved in the Marie Skłodowska-Curie ITN M2ex project. Thanks to all the supervisors for organizing the training activities. Meeting the 14 ESRs from diverse backgrounds (both academically and culturally) has been the best part of this consortium. I am grateful to each of you for making my PhD days memorable. The fun we had after each training activities is worth more than a dime. I could always find someone within the international and multidisciplinary team of M2ex to answer my basic questions, whether it is chemistry, biology, mathematics or engineering. I thank each of you for your kindness and support: Ailen and Parvin for making my initial and final PhD days enjoyable, Julien for being my closest friend during these days, Balike for the sensible advises, Ahmed, Alexandra and Veronica for the chatty lunch breaks in UNINA. Thanks to Eric and Kris for giving me eventful memories in Spain. Neus, Rahul, Rafaello and Pau are acknowledged for their friendship and insightful conversations.

My research work has been carried out equally in two countries (Spain and Italy) where I don't speak the languages and this journey has not been easy. I express my sincere gratitude to the supervisors, colleagues and friends who have helped me with the translation and for the help received for dealing the bureaucracy. Thanks to all my colleagues at Instituto de la Grasa (IG-CSIC), Seville for making my stay there memorable. Thank you, Victor for the language lessons and for all the help at the administrative office. Antonio, Angeles and Juan are acknowledged for training and helping me during my experimental activities. I thank Ana for helping me with the travel and visa related matters. I would like to acknowledge Soraya, Maria, Javier and Elena for their support during my days at CSIC. I am also grateful to all my colleagues at University of Naples Federico II, Italy. Thank you, Vincenzo, Bikash and Fabiana for welcoming and helping me during the times of need.

Finally, I express my sincere gratitude to my family. I am extremely grateful to my husband, Allen for his constant motivation, support and coding lessons. Your dedication and commitment have always inspired me. I am happy that we decided to do our PhD journey together as it kept us busy and close while we were miles away chasing our dreams. I am immensely obliged to my mom Beena, my dad George, my brothers Joseph & Varghese, my grandmother and my in-laws for their persistent encouragement and love. Thanks to each of you for making this possible.

ABSTRACT

In attempts to improve methane yield from anaerobic digestors, the influence of trace metals is extensively studied and recognized. Trace metals (TM) like Fe, Co and Ni are components of enzymes and co-factors involved in different anaerobic digestion pathways. Lack of trace metals can cause hinderance to related enzymatic reactions and relevant digestion pathways. Moreover, excess of TMs can result in toxicity. Hence, optimal lability of metals in the media is significant and it depends on their chemical speciation. Metal speciation is driven by operational conditions like pH, redox potential, hydraulic retention time and is influenced by thermodynamics and kinetics of chemical processes. Due to analytical limitations in quantifying bioavailable fraction of trace metals in an anaerobic digestion system, a mathematical model-based approach will facilitate better understanding of the system, and optimising a reliable and precise trace metal dosing strategy for practical applications. This thesis aims to develop a dynamic mechanistic model for trace metal speciation in anaerobic digestion.

Major processes and factors influencing speciation of trace metals in anaerobic digestion have been identified and mathematically defined. Significance of considering ionic strength and ion pairing while modelling trace metal speciation has been extensively studied. It has been observed that anaerobic digestion performance increases with increase in ionic strength and ion pairing due to decrease in precipitation and increase in metal labile fractions. In addition to precipitation process, ionic strength also influences TM adsorption and hence ionic strength is an important operational parameter controlling the system.

The thesis presents the complete model framework where major processes are defined. The model includes metal uptake, precipitation, adsorption, inorganic complexation, organic complexation with metabolites and strong chelating agents. Influence of reactor conditions such as pH, temperature and ionic strength on these processes are included in the model along with other significant mechanisms such as metal release and dose response. Numerical simulations have been performed under different scenarios to check adaptability and capability of the model. Experiments have been conducted for calibration and application of the model in a lab scale reactor. The model reasonably predicted trace metal effects like metal deprivation in an anaerobic digestor as being observed during the experimental study.

The thesis further discussed the application of the model to optimise trace metal dosing strategies such as mode of dosing, dosing frequency, concentration of dosing, dosing form and time of dosing. Model results have been verified with existing observations from experimental studies and the dose response function has been modified to explicitly capture differential response of microbes to different trace metals. Best ways to dose trace metals to anaerobic digesters for improving methane yield have been analysed. Model results showed that repeated pulse dosing is the best mode to dose TM in comparison with other modes of dosing such as continuous, single pulse, preloading and in-situ loading. Low TM concentration at high dosing frequency is preferable over high dosage at low frequency. Trace

metals should be supplemented at the earliest time possible after metal deficits at optimum concentration levels. An excess of metal supplementation can result in toxicity. Preferred dosing form depends on reactor configuration. Easily dissociable metal forms like metal chlorides are ideal in continuous reactors whereas strong metal chelates like ethylenediamine tetraaceticacid (EDTA) complexes are advisable for reactors with high retention times like batch or semi-continuous reactors.

Applicability of the model in a full-scale reactor context has been studied using real full-scale reactor data and potential applications of the model including optimising metal dosing and co-digestion to improve methane yield have been tested. In the case of iron as an additive to reduce H_2S concentration, high dosage of iron will not only result in reduction of methane yield due to inhibition of Fe but will also add to extra costs due to adding excess of $FeCl_3$ for H_2S removal. The model has suggested that ideal dosage of iron for removal of H_2S from biogas is to maintain iron to sulphide ratio around 1. Results from trace metal speciation model for co-digestion indicate that substrate characteristics such as sulphide content and trace metal concentration influence co-digestion. In case of metal deprivation, co-digestion can be performed using co-substrates rich in trace metals to overcome metal limitation. However, optimum mixing ratio should be maintained to ensure sufficient metal bioavailability.

The mechanistic model framework presented in the thesis for defining trace metal speciation during anaerobic digestion has been tested and verified under various application domains such as predicting metal deprivation, optimising dosing strategies and full-scale application during co-digestion. Due to experimental limitations in quantifying bioavailable metal concentrations, the model framework after additional calibration and validation can be used as a predictive tool to understand trace metal bioavailability and develop a reliable dosing strategy applicable on each individual case.

Spanish

En un intento por mejorar el rendimiento de metano de los digestores anaeróbicos, se estudia y reconoce ampliamente la influencia de los metales traza. Los metales traza como Fe, Co y Ni son componentes de enzimas y cofactores involucrados en diferentes vías de digestión anaeróbica. La falta de metales traza puede obstaculizar las reacciones enzimáticas relacionadas y las vías de digestión relevantes. Además, el exceso de TM puede provocar toxicidad. Por tanto, la labilidad óptima de los metales en el medio es significativa y depende de la especiación química de los metales. La especiación del metal está impulsada por condiciones operativas como el pH, el potencial redox, el tiempo de retención hidráulica y está influenciada por la termodinámica y la cinética de los procesos químicos. Debido a las limitaciones analíticas en la cuantificación de la fracción biodisponible de metales traza en un sistema de digestión anaeróbica, un enfoque basado en modelos matemáticos facilitará una mejor comprensión del sistema y optimizará una estrategia de dosificación de metales traza confiable y precisa para aplicaciones prácticas. Esta tesis tiene como objetivo desarrollar un modelo mecanicista dinámico para la especiación de trazas de metales en digestión anaeróbica.

Se identifican y definen matemáticamente los principales procesos y factores que influyen en la especiación de metales traza en la digestión anaeróbica. Se estudia ampliamente la importancia de considerar la fuerza iónica y el emparejamiento iónico al modelar la especiación de metales traza. Se ha observado que el rendimiento de la digestión anaeróbica aumenta con el aumento de la fuerza iónica y el par iónico debido a la disminución de la precipitación y el aumento de las fracciones lábiles de metales. Además del proceso de precipitación, la fuerza iónica también influye en la adsorción de TM y, por lo tanto, la fuerza iónica es un parámetro operativo importante que controla el sistema.

La tesis presenta el marco modelo completo donde se definen los principales procesos. El modelo incluye absorción de metales, precipitación, adsorción, complejación inorgánica, complejación orgánica con metabolitos y agentes quelantes fuertes. La influencia de las condiciones del reactor, como el pH, la temperatura y la fuerza iónica, en estos procesos se incluye en el modelo junto con otros mecanismos importantes, como la liberación de metal y la respuesta a la dosis. Se realizan numerosas simulaciones en diferentes escenarios para comprobar la adaptabilidad y capacidad del modelo. Se realizan experimentos para la calibración y aplicación del modelo en un reactor a escala de laboratorio. El modelo predijo razonablemente los efectos de los metales traza, como la privación de metales en un digestor anaeróbico, que se observan durante la comparación con los datos experimentales.

La tesis discutió además la aplicación del modelo para optimizar las mejores estrategias de dosificación de trazas de metales, como el modo de dosificación, la frecuencia de dosificación, la concentración de dosificación, la forma de dosificación y el tiempo de dosificación. Los resultados del modelo se verifican con observaciones existentes de estudios experimentales y la función dosis-respuesta se ha modificado para capturar explícitamente la

respuesta diferencial de los microbios a diferentes metales traza. Se analizan las mejores formas de dosificar metales traza en digestores anaeróbicos para mejorar el rendimiento de metano. Los resultados del modelo mostraron que la dosificación por pulsos repetidos es el mejor modo de dosificar TM en comparación con otros modos de dosificación, como la carga continua, de pulso único, la precarga y la carga in situ. Es preferible una concentración baja de TM con una frecuencia de dosificación alta a una dosis alta con una frecuencia baja. Los metales traza deben complementarse lo antes posible después del déficit de metales en niveles de concentración óptimos. Un exceso de suplementos metálicos puede provocar toxicidad. La forma de dosificación preferida depende de la configuración del reactor. Las formas metálicas fácilmente disociables, como los cloruros metálicos, son ideales en reactores continuos, mientras que los quelatos metálicos fuertes, como los complejos de EDTA, son recomendables para reactores con tiempos de retención altos, como los reactores discontinuos o semicontinuos.

Se estudia la aplicabilidad del modelo en el contexto de un reactor a gran escala utilizando datos reales de reactores a gran escala y se prueban las aplicaciones potenciales del modelo, incluida la optimización de la dosificación de metales y la codigestión para mejorar el rendimiento de metano. Las dosis altas de hierro no sólo darán como resultado una reducción del rendimiento de metano debido a la inhibición del Fe, sino que tampoco son útiles para la eliminación de H2S del biogás. Por lo tanto, la dosis ideal de hierro para la eliminación de H2S del biogás es mantener la proporción de hierro a sulfuro alrededor de 1. Los resultados del modelo de especiación de metales traza para la codigestión indican que las características del sustrato, como el contenido de sulfuro y la concentración de metales traza, influyen en la codigestión. En caso de privación de metales, la codigestión se puede realizar utilizando cosustratos ricos en trazas de metales para superar la limitación de metales. Sin embargo, se debe mantener una proporción de mezcla óptima para garantizar una biodisponibilidad suficiente del metal.

El marco del modelo mecanicista presentado en la tesis para definir la especiación de trazas de metales durante la digestión anaeróbica se ha probado y verificado en varios dominios de aplicación, como la predicción de la privación de metales, la optimización de las estrategias de dosificación y la aplicación a gran escala durante la codigestión. Debido a las limitaciones experimentales en la cuantificación de las concentraciones de metales biodisponibles, el marco del modelo después de la calibración y validación adicionales se puede utilizar como una herramienta predictiva para comprender la biodisponibilidad de los metales traza y desarrollar una estrategia de dosificación confiable aplicable en cada caso individual.

Italian

Nell'ambito di ricerca relativo all'incremento delle rese di metano dagli impianti di digestione anaerobica, l'influenza dei metalli in tracce (TMs) è largamente riconosciuta. Metalli in tracce quali Fe, Co e Ni costituiscono componenti di enzimi e cofattori essenziali in quanto coinvolti in differenti percorsi metabolici della digestione anaerobica. La carenza di tali componenti può causare limitazioni alle relative reazioni enzimatiche ed ai relativi percorsi metabolici. D'altro canto, l'eccesso di TMs può condurre a significativi fenomeni di tossicità. Pertanto, la labilità ottimale dei metalli nelle matrici liquide sottoposte a digestione anaerobica è una caratteristica significativa e dipende dalla speciazione chimica dei metalli. La speciazione dei metalli è condizionata da molteplici condizioni operative quali pH, potenziale redox, tempo di ritenzione idraulica, ed è influenzata dalla termodinamica e dalla cinetica dei processi chimici. A causa delle limitazioni analitiche nella quantificazione della frazione biodisponibile dei metalli in tracce in un qualunque sistema di digestione anaerobica, un approccio basato su modelli matematici può condurre ad una migliore comprensione del sistema ed all'individuazione di una strategia ottimale di dosaggio dei metalli in tracce che sia affidabile e precisa in numerose applicazioni pratiche. L'obiettivo del presente lavoro di tesi è, quindi, di sviluppare un modello meccanicistico dinamico per la speciazione dei metalli in tracce nella digestione anaerobica.

In primo luogo, sono stati identificati e definiti dal punto di vista matematico i principali processi e fattori che influenzano la speciazione dei metalli in tracce nella digestione anaerobica. Particolare attenzione è stata rivolta al ruolo fondamentale della forza ionica e dell'accoppiamento ionico per la modellazione matematica della speciazione dei metalli in tracce nella digestione anaerobica. È stato osservato che le prestazioni del processo di digestione migliorano con l'aumento della forza ionica e dell'accoppiamento ionico a causa della diminuzione della precipitazione e dell'incremento delle frazioni labili. Oltre al processo di precipitazione, la forza ionica influenza anche l'adsorbimento dei TMs, e quindi costituisce un fondamentale parametro operativo di processo in grado di controllare l'intero sistema.

Nel lavoro di tesi viene presentato lo schema completo del modello matematico nel quale vengono definiti ed evidenziati i principali processi considerati. Il modello include l'assorbimento, la precipitazione, l'adsorbimento, la complessazione inorganica e la complessazione organica dei metalli con metaboliti e agenti chelanti forti. L'influenza delle più significative condizioni operative dei reattori, pH, temperatura e forza ionica, su tali processi viene inclusa nel modello matematico insieme ad altri meccanismi quali il rilascio di metalli e la cosiddetta risposta alla dose. Vengono presentate numerose simulazioni numeriche in diversi scenari per verificare l'effettiva adattabilità e attendibilità dei risultati del modello matematico proposto. Al fine di poter calibrare e verificare l'effettiva applicabilità del modello, sono stati, inoltre, condotti specifici esperimenti di digestione anaerobica in un reattore in scala di laboratorio. Dal confronto con i dati sperimentali ottenuti,

il modello è stato in grado di prevedere ragionevolmente gli effetti dovuti a diverse somministrazioni di metalli in tracce, come la privazione di metalli in un digestore anaerobico.

La tesi approfondisce ulteriormente l'applicazione del modello per l'ottimizzazione delle migliori strategie di dosaggio dei metalli in tracce, quali la modalità, la frequenza, la concentrazione, la forma ed il tempo di dosaggio. I risultati del modello sono stati verificati con osservazioni provenienti da studi sperimentali esistenti e la funzione di risposta alla dose è stata modificata per catturare esplicitamente la risposta differenziata dei microrganismi a diversi metalli in tracce. Sono stati analizzati i metodi migliori per il dosaggio di metalli in tracce nei digestori anaerobici per il miglioramento della resa di metano. I risultati del modello hanno mostrato che la metodologia a impulsi ripetuti è migliore rispetto alle altre modalità di dosaggio, continuo, a impulso singolo, con precarico e con caricamento in situ, per la somministrazione di TM in digestione anaerobica. Infatti, una bassa concentrazione di TM ad alta frequenza di dosaggio è preferibile rispetto ad un dosaggio elevato a bassa frequenza. Successivamente ad una fase di limitazione, i metalli in tracce dovrebbero essere integrati il prima possibile per ripristinare i livelli di concentrazione ottimali. D'altro canto, un eccesso di somministrazione di metalli può condurre al manifestarsi di fenomeni di tossicità. La miglior forma di dosaggio, in termini di specie chimica, dipende inoltre dalla configurazione del reattore. Forme metalliche facilmente dissociabili, come i cloruri metallici, risultano particolarmente efficaci nei reattori continui, mentre risultano consigliabili chelati metallici forti come i complessi EDTA nel caso di reattori con tempi di ritenzione elevati, reattori batch o semicontinui.

L'effettiva applicabilità del modello matematico è stata ulteriormente studiata utilizzando dati di reattori operanti in scala reale, e le potenziali applicazioni del modello, tra cui l'ottimizzazione del dosaggio dei metalli e la co-digestione per il miglioramento della resa di metano, sono state testate con ulteriori set di simulazioni numeriche. Un elevato dosaggio di ferro, ad esempio, non solo comporta una riduzione della resa di metano a causa dell'insorgere di fenomeni di inibizione da Fe, ma risulta allo stesso tempo eccessivo per la rimozione di H_2S dal biogas. Infatti, al fine di ottenere la rimozione di H_2S dal biogas, è stato osservato che il dosaggio ideale di ferro è quello ottenuto mantenendo il rapporto ferro/solfuro attorno a 1. I risultati del modello di speciazione dei metalli in tracce per la co-digestione hanno indicato che specifiche caratteristiche del substrato, quali il contenuto di solfuro e la concentrazione di metalli in tracce, sono in grado di influenzare notevolmente l'evoluzione del processo di co-digestione. Nel caso di basse concentrazioni di metalli, la co-digestione può essere condotta utilizzando co-substrati ricchi di metalli in tracce per evitare fenomeni di limitazione. Tuttavia, è necessario mantenere un rapporto di miscelazione ottimale per garantire una sufficiente biodisponibilità dei metalli.

La struttura complessiva del modello meccanicistico presentato nel presente elaborato di tesi per la definizione del ruolo cruciale della speciazione dei metalli in tracce durante la

digestione anaerobica è stata, quindi, testata e verificata in vari contesti applicativi, quali la prevenzione alla limitazione di metalli, l'ottimizzazione delle strategie di dosaggio e l'applicazione su vasta scala durante la co-digestione. A causa delle limitazioni sperimentali nella quantificazione delle concentrazioni di metalli biodisponibili, il modello matematico proposto, a valle di una più approfondita fase di calibrazione e di validazione dello stesso, può essere efficacemente utilizzato quale strumento predittivo per comprendere l'effettiva biodisponibilità dei metalli in tracce e sviluppare una strategia di dosaggio affidabile e applicabile ad ogni singolo contesto applicativo.

TABLE OF CONTENTS

CHAPTER 1

General Introduction

1.1. RESEARCH BACKGROUND

1.1.1. Anaerobic digestion

Anaerobic Digestion (AD) is the process of fermentation where degradation of organic material produces biogas, mainly methane and carbon dioxide. On daily basis, anaerobic digestion process occurs in environments like marshes, sediments, landfills, and stomachs of ruminants where redox potential is low (absence of oxygen) and organic material is available (Henze, 2008). AD is a widely exploited process in wastewater treatment plants for removal of sludge and treatment of wastes such as food wastes and agricultural residues due to its advantages like low operational costs, applicability at any scale (scalability of the process), less sludge production (excess sludge reduction), and potential energy production from biogas instead of high-grade energy being consumed in aerobic process (Appels et al., 2011, 2008; Khalid et al., 2011).

Anaerobic digestion follows a multistep process where organic polymers are degraded to methane (CH_4), ammonia (NH_3), hydrogen sulphide (H_2S), carbon dioxide (CO_2) and water (H_2O) through a combination of series and parallel reactions. The process involves four sequential stages – hydrolysis, acidogenesis, acetogenesis and methanogenesis. These processes are mediated by bacteria and archaea broadly grouped as hydrolytic and fermentative bacteria, acetogenic bacteria, homo-acetogenic bacteria, hydrogenotrophic and aceticlastic methanogens (Gujer and Zehnder, 1983).

Hydrolysis is the first step of anaerobic digestion process where large particulate/dissolved complex organic polymers are degraded into smaller dissolved polymers for bacteria to uptake. It is mostly reported as a surface phenomenon where exo-enzymes (secreted by fermentative bacteria) carry out the degradation of complex polymers. This process hydrolyses proteins into amino acids, polysaccharides to sugars and lipids into long chain fatty acids (LCFA). Hydrolysis is the rate limiting step in most cases, especially for substrates with high suspended solids to chemical oxygen demand ratio (SS/ COD) (Henze, 2008). Pre-treatment is carried out in such cases to make the process efficient.

Products of hydrolysis are the substrates of acidogenesis process. Proteins, sugars and LCFA diffuse through the cell walls of acidogenic bacteria where they are anaerobically oxidised or fermented (Mata-Alvarez et al., 2000). The process results in production of organic compounds such as volatile fatty acids, VFAs (acetate, propionate, butyrate), CO_2, H_2, ammonia, ethanol and lactic acids. Reactor medium conditions determine end products of acidogenesis. For example, acetate will be the main product if H_2 is removed by hydrogen consuming organisms like methanogens. However, more reduced products like propionate, butyrate, lactate and alcohol will be the main products if hydrogen is accumulated due to retardation of methanogenic bacteria which occurs in overloaded reactors or perturbed reactors such as acidifying reactors designed for recovery of those products (Appels et al., 2008). Due to rapid kinetic rate of acidogenesis process, pH drop is observed in overloaded

reactors resulting in accumulation of VFAs and inhibition of methanogenesis leading to further pH drop and VFAs accumulation.

Acetogenesis process involves conversion of short chain fatty acids into acetate, hydrogen and carbon dioxide by acetogenic bacteria (Gujer and Zehnder, 1983). Reduction of organic compounds like propionate, butyrate and ethanol into acetate is thermodynamically unfavourable as Gibbs free energy change, ΔG of those hydrogen producing reactions are positive (Henze, 2008). However, methanogenic and sulphate reducing bacteria consume hydrogen thereby maintaining low hydrogen partial pressure making those reactions happen. Hence, the syntrophic associations between hydrogen producing acetogenic and hydrogen consuming (hydrogenotrophic) methanogenic bacteria are significant in maintaining a stable operating environment (Schink, 2002). Due to faster growth rate of hydrogenotrophic bacteria (doubles in 4-12 hours), these associations remain stable under various conditions.

Methanogenesis is the final stage of anaerobic digestion where methanogenic archaea converts decarboxylate acetate into methane, and carbon dioxide into CH_4 using H_2 as electron donor (Gujer and Zehnder, 1983). This stage is the only step where its possible to release influent COD into gases that leave the reactor. Methanogens can be acetate converting aceticlastic methanogens or hydrogen utilising hydrogenotrophic methanogens. 70% of methane produced in most cases is by aceticlastic methanogens. Long start up period for reactors with unadapted seed material is due to extreme low growth rate of aceticlastic methanogens. Hence, its preferable to use high concentrations of sludge. There are two species of aceticlastic methanogens - Methanosarcina spp. and Methanosaeta spp (Ferry, 1999). Methanosarcina spp. has high growth rate and low substrate affinity but can convert substrates like acetate, H_2/CO_2, methylamines, methanol and formate. Methanosaeta spp. on the other hand is the most common acetotrophic species and has low growth rate with high substrate affinity and can use only acetate as the substrate.

1.1.2. Relation between metal speciation, bioavailability and lability

Speciation, originally used in biological context, where organisms are categorised evolutionarily to distinct biological species was adapted into chemistry to distinguish chemical forms of a substance. According to International Union for Pure and Applied Chemistry (IUPAC), chemical species is “the specific form of an element defined as to isotopic composition, electronic or oxidation state, and/or complex or molecular structure” (Templeton et al., 2000) and speciation is defined as “the distribution of an element amongst defined chemical species in a system”. Various forms or species through which a trace metal (TM) exists in a system is trace metal speciation. It is important to understand chemical speciation of a trace metal as TM behaviour is determined by its chemical form. For example, trivalent chromium is cationic, has low solubility and is beneficial whereas hexavalent chromium is anionic and toxic (Katz, 1991). Hence, information on total concentration of metal is not enough for understanding response of microbes to trace metals.

Though bioavailable metal is the metal form that can easily pass through cell membrane of an organism, it does not mean they are always removed from solution by the organism. For instance, some bacteria are known to tolerate high metal stress by binding the metals with proteins or extracellular polymeric substances (EPS) and reduce metal uptake (Mathivanan et al., 2021). Thus, a metal although available won't indicate that they are up taken by the organisms. In Marcato et al. (2009), bioavailability is defined as the "degree to which elements are available for interaction with biological systems". According to Siegel (2002), "bioavailability is the amount or concentration of a chemical that can be absorbed by an organism thereby creating the potential for toxicity or the necessary concentration for survival".

Speciation effects are widely explored in aquatic toxicology and free metals are in general reported to be more bioavailable (free ion model (Morel and Hering, 1993)) than other forms although there are exceptions. For example, in surface waters, hydroxycomplex $Cu(OH)_2$ and $CuOH^+$ were found to be toxic to *Selenastrum capricornutum* although their toxicity level is lower than Cu^{2+}, implying hydroxy complexes are bioavailable. Moreover, unlike aquatic media anaerobic digestion systems are quite complex, heterogeneous and dynamic. A term lability was used later on to assess bioavailability. In comparison to inert metal complexes, metals falling in labile fraction are more bioavailable. It essentially includes free metal ions, metal hydroxy complexes, metal complexes with inorganic ligands and metal complexes with organic ligands having fast dissociation rate.

1.1.3. Trace metal influence on AD

Growth of microorganisms depend on optimal environmental conditions (pH, redox potential, temperature) and availability of substrates (COD), macronutrients (P, N_2) and micronutrients (metals, halogens). Sub-optimal conditions of any of these factors can hinder metabolic activity of all or a specific group of microorganisms involved in the digestion process. Of all the microorganisms involved, methanogens are reported to be the most sensitive group to perturbations (Roussel, 2013).

Different groups of microorganisms perform various metabolic pathways and it involves numerous enzymatic reactions. Functional microorganisms produce many of such enzymes and it requires substrates, cofactors, activators and trace elements. Metallo enzymes or metal dependent enzymes are involved in anaerobic processes, methanogenesis being the most trace metal enriched enzymes involving metabolic pathway (Staicu et al., 2019; Thanh et al., 2016). Although exact requirement of trace metal depends on various factors such as substrate and microbial diversity, most abundantly required trace metal is Fe, followed by elements such as Ni, Co, Cu, Mn and Zn (Fermoso et al., 2009). V, Mo, Se and W are other trace elements that are required; however, their requirement is low compared to the previously mentioned TMs (Oleszkiewicz and Sharma, 1990; Roussel, 2013).

Fe serves as a redox carrier and terminal electron acceptor in an AD system and is an important structural component of majority of co-enzymes present in anerobic digestion

processes. Dosing Fe has been discovered to be useful in AD for reducing hydrogen sulphide (H_2S) formation, increasing propionate conversion rate, accelerating hydrolysis and acidogenesis, and reducing VFA accumulation (Choong et al., 2016). Methanogenic archea uses Ni due its presence in the cofactor F430. Co is present in cofactor vitamin B12 which is used by methanogenic bacteria during methanol degradation. Cu is used for transference of electrons while Mn exists in co-factors, and Zn is found to exist in several enzymes as single structural atom. Mo and W are found associated with 'pterin' cofactor ('molybdopterin' or 'tungstopterin'). Se and V are also essential for methanogenesis. This thesis considers modelling the effect of most abundant and influential TMs – Fe, Co and Ni.

1.1.4. Trace metal speciation in AD

Kinetics and equilibrium of processes affecting chemical speciation depend on the conditions (temperature, pH etc) and composition (sludge characteristics, existing metal concentration) of anaerobic digester. Metal species can be organic or inorganic compounds that can exist in the system in soluble or particulate form. They include free ions, aqueous metal complexes, metal chelates, molecules, precipitates, colloids or adsorbed species.

Trace metal influence on anaerobic digestion varies under different conditions due to variation in metal bioavailability existing under different conditions. Bioavailability of a metal is affected by its chemical speciation, which is driven by equilibrium and kinetics of processes influencing metal speciation (Thanh et al., 2016; Yekta et al., 2017). Understanding processes influencing metal speciation is therefore significant to study trace metal effects on AD. Physicochemical processes, metal uptake and biochemical processes influence metal speciation. Most influential processes controlling metal speciation in an anaerobic digestion system are the physicochemical processes - precipitation, complexation and adsorption processes (Zheng et al., 2021).

1.1.4.1. Precipitation

The main inorganic anions responsible for trace metal precipitation in anaerobic systems are carbonate, phosphate and sulphide. TM (Me) precipitates majorly found in AD systems are MeS, $Me_3(PO_4)_2$ and $MeCO_3$ (Callander and Barford, 1983; Fermoso et al., 2009; Maharaj et al., 2018). Sulphide forms the most thermodynamically stable metal precipitate in AD systems and hence metal speciation is controlled by sulphide followed by phosphate and carbonate (van der Veen et al., 2007). Metal carbonates and metal hydroxides have low solubility products and their tendency to precipitate TMs in AD systems is low. A few analytical studies using X-ray diffraction spectroscopy and acid volatile sulphide analysis also reported presence of metal sulphide precipitates like FeS, NiS, CoS and ZnS in anaerobic systems (Fang and Liu, 1995; Kaksonen et al., 2003; van der Veen et al., 2007). Moreover, secondary sludge contains $FePO_4$ when iron is added for phosphorous removal. In aerobic conditions, iron is oxidised to Fe(III) which are highly reactive and get precipitated as $FePO_4$. When it enters anaerobic digester, ferric phosphates dissolves to convert Fe(III) to Fe (II)

which react with sulphides to from FeS or with phosphates to form ferrous phosphates under high phosphorous conditions (Roussel, 2013).

1.1.4.2. Adsorption on precipitate, biomass and EPS

In addition to precipitation, trace metal speciation in inorganic fraction can occur due to chemisorption on mineral supports, primarily sulphide precipitates (Jong and Parry, 2004; van der Veen et al., 2007). Van Hullebusch et al. (2006) and Watson et al. (1995) reported Co and Ni adsorption on FeS precipitate. Additionally, trace metals can get adsorbed on bacterial cell walls and microbial products. Dead cells and extra cellular polymeric surfaces can adsorb trace metals due to presence of functional groups like carboxyl, sufyhydrl, hydroxyl and phosphoryl groups present on their surfaces contributing to fraction of TMs existing in solid phase. (Artola et al., 1997; Van Hullebusch et al., 2006). Functional groups present on cell surface act as binding site for metals and can be fully understood by a metal-organic complexation mechanism such as metal binding by ion exchange between protons and metals as well as surface complexation mechanism described in Chapter 3.

1.1.4.3. Inorganic complexes

Aqueous complexes can be broadly classified in three groups: ion pairs, inorganic complexes and organic complexes. Free metal ion in solution is principally an aquo complex, i.e. metal ion associated with water molecules, where water itself is the ligand. When other ligands replace water molecules around the central metal atom to share non-bonding pair of electrons, it forms complexes. When reaction between a metal and ligand is electrostatic where some water of hydration is retained, the product is named as ion pair or outer sphere complex. However, when the reaction occurs at several coordination sites, it is called chelation and such multidentate ligands are called chelating agents. In this work, the term complex is used in general to describe all dissolved metal ligand associations, involving both ion pairs and chelates.

Most influential reactive inorganic ligands commonly found in anaerobic digestion systems are HS^-, CO_3^{2-}, PO_4^{3-}, OH^-, Cl^-. Different complexes that can be formed associated with these ligands are listed in Chapter 2 and Chapter 3. Presence of sulphides is not only important for precipitate formation but they also form strong dissolved sulphide complexes. Besides sulphides, phosphates and carbonates are the other significant inorganic ligands present in anaerobic reactor. Carbonate is commonly present at high concentrations in microbial or reactor media and is important as it forms strong complexes with metals like Ni (II) (Jansen, 2004). Metals bound with sulphides and carbonates such as $Fe(HS)^+$ and $Fe(HCO_3)^+$ have stronger binding resulting in reduced reactivity whereas hydroxide or halogen bounded metals are weakly bound and more reactive (Fermoso et al., 2009). Though complexes with other predominant ligands such as OH^-, Cl^- are weakly bound, they influence metal precipitation as formation of these metal complexes reduces the availability of free metals for participation in precipitation process which is described in detail in Chapter 2.

1.1.4.4. Organic complexes

Organic complexes influencing trace metal speciation can be of three origins – ligands produced by microbes (biogenic ligands), soluble organic matter and strong anthropogenic chelating agents like EDTA, nitrilotriacetic acid (NTA) etc.

Soluble organic matter

Soluble organic matter constitutes a large fraction of volume in anaerobic digesters. It can be humic substances and other biodegradation products such as VFAs, amino acids (AAs) etc. Intermediary organic substrates produced during AD can act as chelating agents and influence TM speciation. AAs have strong affinity to form complexes with TMs than with major cations such as Ca^{2+}, Mg^{2+}. Gonzalez-Gil et al. (2003) reported increase in metal bioavailability due to production of soluble complexes of Ni and Co with amino acids in yeast extract. According to Shakeri Yekta et al. (2014), inclusion of TM complexation with thiols represented by amino acid (cysteine) improved thermodynamic model predictions.

Organic matter contains functional groups that interact with metals to form metal organic chelates and hence interaction of metals with organic matter can be considered as a reaction between metals and functional groups such as carboxyl or hydroxyl functional groups (Fletcher and Beckett, 1987). Metals bind with deprotonated functional groups following an acid-base reaction and hence is highly dependent on pH. This indicate that protons are the major competing ions to organics functional group. Under anaerobic conditions (at neutral/basic pH), metal organic complexation is favoured due to decrease in proton competition.

Metals associated with carbohydrates and protein like substances are more labile than metals complexed with humic substances as dissociation rate constant of metals complexed with humic substances are low. Information on ligand concentrations and stability constants are needed for modelling and this knowledge is lacking in anaerobic systems especially with regards to larger molecules such as humic and fulvic substances. It is complicated to study complexation of metals with large molecules such as humic acids that has large number of functional groups/binding sites. Hence interaction of TMs with simpler organic molecules such as VFAs and AAs can be studied based on complexation. TM interaction with large organic molecules (both soluble and insoluble) can be associated with adsorption which is often described as a surface complexation process between metals and functional groups/binding sites present on adsorbent surface (see Chapter 3 for further details).

Biogenic ligands

Microorganisms can produce two forms metal chelating agents – transport ligands that are produced to facilitate movement of essential TMs across cell membrane and buffering/detoxifying ligands that are produced to defend them against metal toxicity (Morel and Hering, 1993). These biogenic chelating ligands can be considered as soluble microbial

products (SMPs). They contain different compounds such as proteins, siderophores, nucleic acids, exocellular enzymes, and SMPs affinity with TMs can range from that of simple amino acids to strong chelates depending on the SMP compounds released.

Strong anthropogenic chelating agents

Unlike organic compounds such as humic substances, trace metals from strong complexes with artificial chelating agents such as NTA, EDTA and ethylenediamine-N,N′-disuccinic acid (EDDS). Metal concentrations can be maintained at levels below solubility products of metal precipitates if metal chelate complexes have higher stability constants (Callander & Barford, 1983). Synthetic chelating agents like EDTA (Bartacek et al., 2012; Cai et al., 2019; Vintiloiu et al., 2013; Zhong et al., 2019), NTA (Hu et al., 2008; Tsapekos et al., 2018) and EDDS (Thanh et al., 2017a,b; Zhang et al., 2015) are often supplemented to biogas reactors to increase metal bioavailability. Zhang et al. (2021) reported an increase in formation of methane when nickel was supplemented as chelator-Ni (23.34% for EDDS-Ni, 31.26% for NTA-Ni and 16.07% for EDTA-Ni) instead of supplementation in Ni (II) form. These chelating agents can also enter anaerobic digesters from sewage sludge as they are reported to exist in waste streams.

1.1.5. Metal uptake

In addition to complexation and adsorption of TMs on microbial ligands, microorganisms can influence TM speciation by depleting TM concentrations through uptake. TM complexes that are sufficiently lipid soluble diffuses through the lipid bilayer membrane of the microorganism. Passive diffusion rate is slow in most cases due to very low solubility of TMs and their complexes in lipids. TM uptake in most cases occurs in two steps where metals, M are first bound to a membrane uptake site, L followed by delivery into the cell, M_{cell} by transfer through the cell membrane as expressed in the Eq. (1.1).

$$M + L \leftrightarrows ML \rightarrow M_{cell} \tag{1.1}$$

Metal uptake ρ under steady state can be kinetically described using Michaelis-Menten equation (Eq. 1.2) where maximum uptake rate ρ_{max} and half saturation constant K_M depends on uptake site concentration, L_T and reaction rate constants, k_L (forward reaction rate constant of metal binding with uptake site), k_{-L} (reverse reaction rate constant of metal binding with uptake site) and k_{in} (metal transfer rate through the cell membrane) as represented in Eq. (1.3) and Eq. (1.4).

$$\rho = \frac{[M]}{K_M + [M]} \rho_{max} \tag{1.2}$$

$$\rho_{max} = L_T \, k_{in} \tag{1.3}$$

$$K_M = \frac{k_{-L} + k_{in}}{k_L} \tag{1.4}$$

1.1.6. Methods to determine TM speciation

1.1.6.1. Analytical methods applied in AD

Analytical techniques to determine speciation depend on its physical state. Different methods are available to quantify particulate and dissolved speciation of metals. Particulate metal speciation in AD systems is most commonly studied using fractionation technique in combination with spectroscopic techniques such as X-ray fluorescence spectroscopy, energy dispersive X-ray spectroscopy or X-ray absorption spectroscopy as well as microscopic techniques such as transmission electron microscopy, scanning electron microscopy or confocal laser scanning microscopy.

Fractionation procedures differentiate chemical species into separate fractions based on their response to different extraction steps. Extraction steps are designed to categorize analytes according to their physical or chemical properties like solubility, reactivity etc. A few extraction techniques using a series of chemical reagents are applied for metal fractionation of anaerobic solid samples such as sediments, soils, and sludges. Bioavailability of metals decreases after each extraction step in such chemical extraction procedures.

Different single and sequential extraction procedures are developed of which the widely used schemes for anaerobic sludges are modified Tessier method (Tessier et al., 1979) and revised Commission of the European Communities Bureau of Reference (BCR) scheme (Hullebusch et al., 2005; van Hullebusch et al., 2016). Modified Tessier method has four fractions namely, F1 (exchangeable), F2 (carbonates), F3 (organic matter and sulphides), F4 (residual) whereas sequential fractions extracted in revised BCR extraction scheme are identified as F1 (exchangeable + water and acid soluble), F2 (iron and manganese oxides), F3 (organic matter and sulphides), F4 (residual). According to Roussel (2013), phosphate and carbonate precipitates, weakly bound metal compounds and adsorbed metals are extracted in exchangeable fraction. Reducible fraction consists of metal oxide precipitates and metals incorporated within Fe and Mn oxides whereas oxidizable fraction consists of metal organic complexes and metal sulphide precipitates. Strongly bound metal compounds remain in residual fraction.

Bioavailability decreases with each extraction step during sequential extraction and hence is a good technique to understand bioavailability (Filgueiras et al., 2002; Osuna et al., 2003). In addition to water soluble fraction, exchangeable metal fraction is also reported to be bioavailable (Fuentes et al., 2008). However, sequential extraction methods are incomplete in understanding metal speciation both quantitatively and qualitatively. Hence, a combination with other techniques helps in providing more information. For instance, spectroscopic techniques give information on structural properties and elemental composition whereas microscopic techniques help in localization.

Dissolved metal speciation analysis is carried out using various techniques such as, voltammetry, ion exchange resins, electrochemical methods, ion selective electrodes,

capillary electrophoresis and chromatography (Sauvé and Parker, 2005). The methods involve a combination of separation process and a detector for quantification. Characteristics of bioreactor medium in anaerobic digesters and low metal concentrations limit the applicability of these techniques in AD context. However, techniques such as DGT and AdSV were reported to be applicable to AD systems (Jansen, 2004).

1.1.6.2. Model approaches

Different concentrations of trace metals are reported for optimum dosing in various studies. Inconsistency in the reported values is due to the difference in biochemical environment existing for different systems caused by variation in factors like operational conditions, feedstock characteristics and reactor configuration. Variation in biochemical environment is reflected in speciation and bioavailability of the metal which in turn is responsible for driving trace metal effects on AD. Hence, total metal concentration is a bad indicator for understanding metal effects. There are no instrumentation technologies available to date to quantify whole metal speciation or the trace level concentration of bioavailable metals. A mathematical model-based approach will hence provide missing information based on reliable and quantifiable data that can be given to the model as input.

Geochemical equilibrium models

Geochemical equilibrium softwares are universally and routinely used to estimate speciation in soils and environmental chemistry. A few of such software programs commonly in use today include GEOCHEM-PC (Parker et al., 1995), MINEQL+ (Schecher and McAvoy, 1992) and MINTEQA2 (Allison and Brown, 1995). Use of these models involve identifying stability constants to define thermodynamic database, specifying components and their concentrations along with other parameters (such as pH, temperature, ionic strength), performing computations and analysis of output results to study speciation of species of interest. Based on the input list of components, computer algorithm generates a list of output species and gives information on complexes, dissolved species, solubility, precipitates and adsorption.

These programs have also been used to define metal speciation during anaerobic digestion. Roussel (2013) used Phreeqc software to simulate fate of metals in anaerobically digested sludge. The model presented in the study failed to capture presence of Ni and Cu in exchangeable and reducible fractions as observed during the experiment. The study reported several differences between model and experimental results for metals like Co, Cu, Zn, Ni, Mn due to lack of consideration of metal dynamics and definition of processes including secondary reactions, metal adsorption and organic complexation processes. Yekta et al. (2017) performed a thermodynamic model-based study to investigate trace metal solubility in full scale continuous anaerobic reactor and reported good agreement of model results with measured values for aqueous metal concentrations.

Geochemical equilibrium softwares are therefore found to be useful for understanding trace metal speciation in anaerobic digesters. However, such models are not stand-alone and need backing from experimental results for complete understanding of metal speciation. Moreover, although the models help in determining main chemical reactions in the system, simulations are performed at equilibrium and kinetics of reactions are ignored. Additionally, geochemical equilibrium programs do not consider biological reactions taking place in an anerobic digestion system. This points to the need for a mechanistic dynamic model for defining metal speciation in AD systems.

Kinetic models

Though there are many models ranging from simple empirical models to complex dynamic models for describing anaerobic digestion processes, Anaerobic Digestion Model 1, ADM1 proposed by International Water Association, IWA is the most widely applied model (Batstone et al., 2002). ADM1 consists of process definitions for the key biological steps during anaerobic digestion. It represents physico-chemistry to some extent in terms of six acid-base reactions and three liquid gas transfer processes. pH is solved using a charge balance approach.

The biochemical module in ADM1 involves the principal intracellular and extracellular process reactions occurring in the AD system. The intracellular processes defined are acidogenesis, acetogenesis and methanogenesis, whereas disintegration and hydrolysis are the two important extracellular biochemical processes. The disintegration product of complex organic matter are particulate substrate of carbohydrate, protein and lipid. Moreover, the disintegration step is a collection of lysis, non-biological decay and physical breakdown. Hydrolysis step involves degradation of disintegration products to sugars, amino acids and long chain fatty acids. The two extracellular steps are described as first order kinetics based on concentration of substrate. The intracellular processes are described by kinetic rate expressions on substrate uptake limited by inhibition functions for pH and accumulation of intermediate products such as ammonia, hydrogen and inorganic nitrogen. Substrate uptake is described based on Monod-Type kinetics and is linked to biomass growth through yield coefficients. The decay of the biomass is considered through a first order kinetics and the decayed biomass end up as complex organics that will undergo disintegration and hydrolysis.

Numerous modifications have been made to ADM1 with respect to extending biochemical and physicochemical modules (Mo et al., 2023). The model lacked inaccuracy in describing complete physico-chemistry and hence incorporation of ion activity, ion pairing and mineral precipitation have been made (Kazadi Mbamba et al., 2015; Solon et al., 2015). Phosphorous and sulfur transformations have been added along with their interactions with Fe (Flores-Alsina et al., 2016). With respect to biochemical module, several improvements have been made such as to consider anaerobic co-digestion by modifying extracellular processes, syntrophic acetate oxidation etc. (Mo et al., 2023).

Owing to limited attention in defining physicochemical processes in biochemical reference models like ASMs and ADM1, IWA task group recently published a framework, generalised Physicochemical Chemical Model, PCM for wastewater treatment processes (Batstone and Flores-Alsina, 2022). It gives information regarding model approaches and reference implementation for defining physicochemical processes. Model representations for aqueous phase chemistry, mineral precipitation, gas-liquid transfer and chemical oxidation-reduction processes are defined in the model.

Original ADM1 considered simple acid-base equilibria. PCM incorporated new inorganic components and more acid-base equilibrium reactions such as incorporation of equilibria amongst inorganic phosphorous components. Due to considerable effects of ionic strength and ion pairing in defining physico-chemistry of the system, ion pairing reactions are added in PCM. Moreover, ion activity corrections are added by expressing it as the product of molar concentration and activity coefficient to consider ionic strength effects. Liquid-solid reactions or precipitation reactions were not included in ADM1. PCM considered major precipitation reactions such as struvite precipitation, carbonate and phosphate precipitation reactions with cations such as Ca, Mg and Fe. With respect to gas-liquid transfer processes, in addition to formation of CH_4, CO_2, and H_2, PCM emphasized the need to consider H_2S and NH_3 gas formation under necessary conditions. Gas stripping process in ADM1 is liquid film controlled. However, PCM highlighted that it can be gas film controlled for gases with high solubility. Though abiotic chemical oxidation-reduction processes have limited impact on biology of the system, PCM considers oxidation-reduction in cases of representing speciation behaviour and precipitation under different oxidation states.

A few model studies to understand trace metal speciation during anaerobic digestion are available (Frunzo et al., 2019; Maharaj et al., 2018, 2019, 2021). Maharaj et al. (2018) extended ADM1 model to include trace metal precipitation processes. The model was then extended to include complexation of TMs with VFAs and EDTA. A similar study was reported by Frunzo et al. (2019). Maharaj et al. (2021) proposed a comprehensive framework for TM speciation in AD. However, these models neglected influence of ionic strength during precipitation and adsorption. Moreover, other major processes that can influence TM speciation including ion pairing reactions and complexation with amino acids were not considered. The models are also not yet applied and verified with real data.

1.2. RESEARCH OBJECTIVES

The aim of this thesis is to propose a mechanistic model approach to define the effects of trace metals in an anaerobic digestion system. Major objectives of the thesis are as follows.

1. To develop ADM1 based mechanistic model to study trace metal speciation effects during anaerobic digestion.
2. To test application of the developed model in metal deprivation conditions using experimental datasets generated during the study.
3. To check capability of the model to design trace metal dosing strategies during anaerobic digestion.
4. To check the applicability of the model in a full-scale reactor context using real full-scale reactor data and test potential applications such as influence of metal dosing and co-digestion to improve methane yield.

1.3. RESEARCH APPROACH AND THESIS STRUCTURE

Research method followed in the thesis is shown in Fig. 1.1. Gaps and opportunities for trace metal speciation model in anaerobic digesters are recognised and existing model approaches are reviewed in Chapter 1. Based on evident knowledge from literature and expert knowledge, processes and factors influencing metal speciation that need to be modelled are identified in Chapter 1. Chapter 2 addressed one of the limitations in existing model framework concerning ionic strength influence on TM precipitation. The chapter discussed three different model approaches to define aqueous phase chemistry in anaerobic digestors – (i) existing TM speciation model framework (ii) with ionic activity correction and (iii) with ionic activity correction and ion pairing. Since bioavailability of a trace metal and its effects on AD relies on accurate description of metal speciation, this chapter showed the significance of considering non-ideal aqueous phase chemistry (ionic strength correction and ion pairing) in modelling trace metal dynamics. The model presented in Chapter 2 is further improved to incorporate the missing processes to give a complete model framework in Chapter 3. The complete model framework presented in Chapter 3 include all major processes affecting metal speciation – uptake, precipitation, complexation and adsoprtion of metals along with metal release and dose response with conisderation of factors like ionic strength, pH and temperature. Chapter 3 also dicussed lab scale experimental study performed to calibrate and verify the model for its application to predict metal deprivation in an anaerobic system. Chapter 4 discussed application of the model to design trace metal dosing strategies such as mode of dosing, dosing frequency, concentration of dosing, dosing form and time of dosing. Model results have been verified with existing observations from experimental studies and the dose response function has been modified to explicitly capture differential response of microbes to different trace metals. Chapter 5 presented application of the trace metal speciation model in the context of a full-scale reactor. Model based analysis has been performed to optimise metal addition of iron, the most common trace metal supplemented in chemical form to a full-scale reactor. Influence of trace metals during co-digestion has been

analysed and effect of optimising mixing ratio of substrates to maintain sufficient metal concentration has been studied.

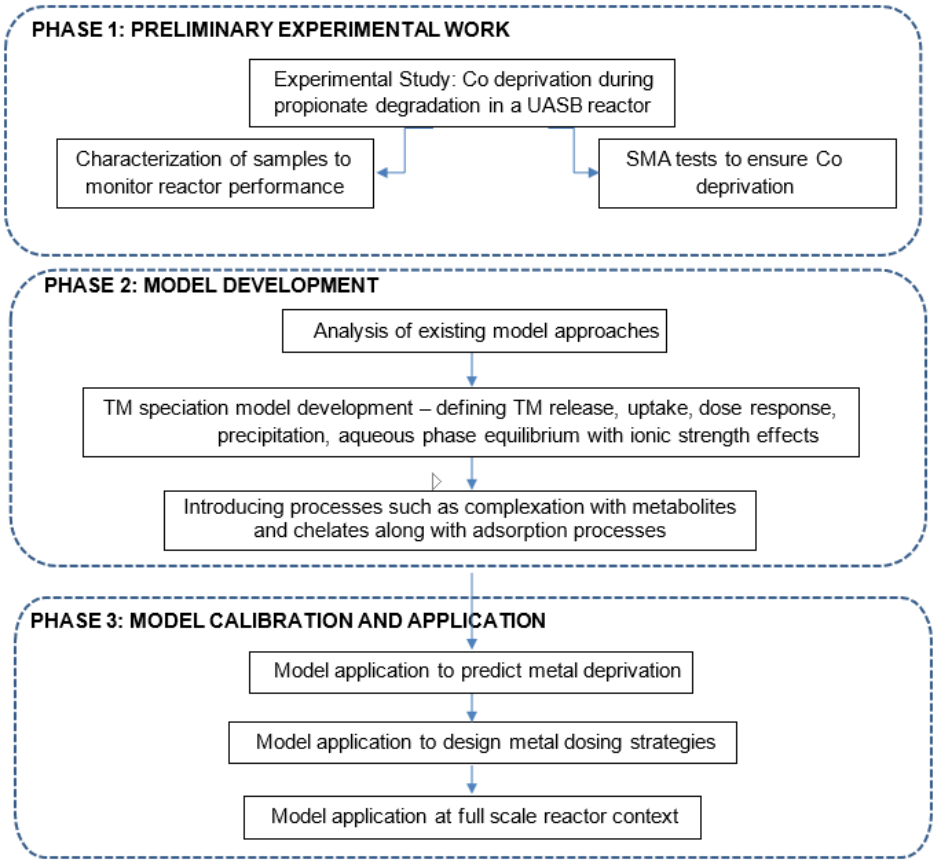

Figure 1.1 – Overview of thesis developmental stages.

1.4. REFERENCES

Allison, J.D., Brown, D.S., 1995. MINTEQA2/PRODEFA2—A Geochemical Speciation Model and Interactive Preprocessor, in: Chemical Equilibrium and Reaction Models. John Wiley & Sons, Ltd, pp. 241–252. https://doi.org/10.2136/sssaspecpub42.c12

Appels, L., Baeyens, J., Degrève, J., Dewil, R., 2008. Principles and potential of the anaerobic digestion of waste-activated sludge. Prog. Energy Combust. Sci. 34, 755–781. https://doi.org/10.1016/j.pecs.2008.06.002

Appels, L., Lauwers, J., Degrève, J., Helsen, L., Lievens, B., Willems, K., Van Impe, J., Dewil, R., 2011. Anaerobic digestion in global bio-energy production: Potential and research challenges. Renew. Sustain. Energy Rev. 15, 4295–4301. https://doi.org/10.1016/j.rser.2011.07.121

Artola, A., Balaguer, M.D., Rigola, M., 1997. Heavy metal binding to anaerobic sludge. Water Res. 31, 997–1004. https://doi.org/10.1016/S0043-1354(96)00345-4

Batstone, D., Flores-Alsina, X. (Eds.), 2022. Generalised Physicochemical Model (PCM) for Wastewater Processes. IWA Publishing. https://doi.org/10.2166/9781780409832

Batstone, D.J., Keller, J., Angelidaki, I., Kalyuzhnyi, S.V., Pavlostathis, S.G., Rozzi, A., Sanders, W.T., Siegrist, H., Vavilin, V.A., 2002. The IWA Anaerobic Digestion Model No 1 (ADM1). Water Sci. Technol. 45, 65–73. https://doi.org/10.2166/WST.2002.0292

Callander, I.J., Barford, J.P., 1983. Precipitation, chelation, and the availability of metals as nutrients in anaerobic digestion. I. Methodology. Biotechnol. Bioeng. 25, 1947–1957. https://doi.org/10.1002/BIT.260250805

Chen, S., Dong, B., Dai, X., Wang, H., Li, N., Yang, D., 2019. Effects of thermal hydrolysis on the metabolism of amino acids in sewage sludge in anaerobic digestion. Waste Manag. 88, 309–318. https://doi.org/10.1016/J.WASMAN.2019.03.060

Choudhury, A., Shelford, T., Felton, G., Gooch, C., Lansing, S., 2019. Evaluation of Hydrogen Sulfide Scrubbing Systems for Anaerobic Digesters on Two U.S. Dairy Farms. Energies 12, 4605. https://doi.org/10.3390/en12244605

Deublein, D., Steinhauser, A., 2011. Biogas from Waste and Renewable Resources: An Introduction. John Wiley & Sons.

Díaz, I., Ramos, I., Fdz-Polanco, M., 2015. Economic analysis of microaerobic removal of H2S from biogas in full-scale sludge digesters. Bioresour. Technol. 192, 280–286. https://doi.org/10.1016/j.biortech.2015.05.048

Dykstra, C.M., Pavlostathis, S.G., 2021. Hydrogen sulfide affects the performance of a methanogenic bioelectrochemical system used for biogas upgrading. Water Res. 200, 117268. https://doi.org/10.1016/j.watres.2021.117268

Erdirencelebi, D., Kucukhemek, M., 2018. Control of hydrogen sulphide in full-scale anaerobic digesters using iron (III) chloride: performance, origin and effects. Water SA 44. https://doi.org/10.4314/wsa.v44i2.04

Fang, H.H.P., Liu, Y., 1995. X-ray analysis of anaerobic granules. Biotechnol. Tech. 9, 513–518. https://doi.org/10.1007/BF00159568

Fermoso, F.G., Bartacek, J., Jansen, S., Lens, P.N.L., 2009. Metal supplementation to UASB bioreactors: from cell-metal interactions to full-scale application. Sci. Total Environ. 407, 3652–3667. https://doi.org/10.1016/J.SCITOTENV.2008.10.043

Ferry, J.G., 1999. Enzymology of one-carbon metabolism in methanogenic pathways. FEMS Microbiol. Rev. 23, 13–38. https://doi.org/10.1111/j.1574-6976.1999.tb00390.x

Filgueiras, A.V., Lavilla, I., Bendicho, C., 2002. Chemical sequential extraction for metal partitioning in environmental solid samples. J. Environ. Monit. 4, 823–857. https://doi.org/10.1039/b207574c

Firer, D., Friedler, E., Lahav, O., 2008. Control of sulfide in sewer systems by dosage of iron salts: Comparison between theoretical and experimental results, and practical implications. Sci. Total Environ. 392, 145–156. https://doi.org/10.1016/j.scitotenv.2007.11.008

Fletcher, P., Beckett, P.H.T., 1987. The chemistry of heavy metals in digested sewage sludge—II. Heavy metal complexation with soluble organic matter. Water Res. 21, 1163–1172. https://doi.org/10.1016/0043-1354(87)90167-9

Flores-Alsina, X., Solon, K., Kazadi Mbamba, C., Tait, S., Gernaey, K.V., Jeppsson, U., Batstone, D.J., 2016. Modelling phosphorus (P), sulfur (S) and iron (Fe) interactions for dynamic simulations of anaerobic digestion processes. Water Res. 95, 370–382. https://doi.org/10.1016/j.watres.2016.03.012

Frunzo, L., Fermoso, F.G., Luongo, V., Mattei, M.R., Esposito, G., 2019. ADM1-based mechanistic model for the role of trace elements in anaerobic digestion processes. J. Environ. Manage. 241, 587–602. https://doi.org/10.1016/j.jenvman.2018.11.058

Fuentes, A., Lloréns, M., Sáez, J., Isabel Aguilar, M., Ortuño, J.F., Meseguer, V.F., 2008. Comparative study of six different sludges by sequential speciation of heavy metals. Bioresour. Technol. 99, 517–525. https://doi.org/10.1016/j.biortech.2007.01.025

George, S., Mattei, M.R., Frunzo, L., Esposito, G., van Hullebusch, E.D., Fermoso, F.G., 2023. Dynamic modelling the effects of ionic strength and ion complexation on trace metal speciation during anaerobic digestion. J. Environ. Manage. 343, 118144. https://doi.org/10.1016/j.jenvman.2023.118144

Ghimire, A., Gyawali, R., Lens, P.N.L., Lohani, S.P., 2021. Chapter 11 - Technologies for removal of hydrogen sulfide (H2S) from biogas, in: Aryal, N., Mørck Ottosen, L.D., Wegener Kofoed, M.V., Pant, D. (Eds.), Emerging Technologies and Biological Systems for Biogas Upgrading. Academic Press, pp. 295–320. https://doi.org/10.1016/B978-0-12-822808-1.00011-8

Glass, J.B., Orphan, V.J., 2012. Trace metal requirements for microbial enzymes involved in the production and consumption of methane and nitrous oxide. Front. Microbiol. 3. https://doi.org/10.3389/fmicb.2012.00061

Gujer, W., Zehnder, A.J.B., 1983. Conversion Processes in Anaerobic Digestion. Water Sci. Technol. 15, 127–167. https://doi.org/10.2166/wst.1983.0164

Habagil, M., Keucken, A., Horváth, I.S., 2020. Biogas production from food residues—the role of trace metals and co-digestion with primary sludge. Environ. - MDPI 7. https://doi.org/10.3390/environments7060042

Henze, M., 2008. Biological wastewater treatment : principles, modelling and design. IWA Pub.

Hullebusch, E.D.V., Utomo, S., Zandvoort, M.H., Piet, P.N., 2005. Comparison of three sequential extraction procedures to describe metal fractionation in anaerobic granular sludges. Talanta 65, 549–558. https://doi.org/10.1016/J.TALANTA.2004.07.024

Jansen, S., 2004. Speciation and bioavailability of cobalt and nickel in anaerobic wastewater treatment.

Jong, T., Parry, D.L., 2004. Adsorption of Pb(II), Cu(II), Cd(II), Zn(II), Ni(II), Fe(II), and As(V) on bacterially produced metal sulfides. J. Colloid Interface Sci. 275, 61–71. https://doi.org/10.1016/j.jcis.2004.01.046

Kaksonen, A.H., Riekkola-Vanhanen, M.L., Puhakka, J.A., 2003. Optimization of metal sulphide precipitation in fluidized-bed treatment of acidic wastewater. Water Res. 37, 255–266. https://doi.org/10.1016/S0043-1354(02)00267-1

Katz, S.A., 1991. The analytical biochemistry of chromium. Environ. Health Perspect. 92, 13–16. https://doi.org/10.1289/ehp.919213

Kazadi Mbamba, C., Tait, S., Flores-Alsina, X., Batstone, D.J., 2015. A systematic study of multiple minerals precipitation modelling in wastewater treatment. Water Res. 85, 359–370. https://doi.org/10.1016/j.watres.2015.08.041

Khalid, A., Arshad, M., Anjum, M., Mahmood, T., Dawson, L., 2011. The anaerobic digestion of solid organic waste. Waste Manag. 31, 1737–1744. https://doi.org/10.1016/j.wasman.2011.03.021

Lens, P., LW Hulshoff, P., 2020. Environmental Technologies to Treat Sulfur Pollution: Principles and Engineering. IWA Publishing. https://doi.org/10.2166/9781789060966

Maharaj, B.C., Mattei, M.R., Frunzo, L., van Hullebusch, E.D., Esposito, G., 2018. ADM1 based mathematical model of trace element precipitation/dissolution in anaerobic digestion processes. Bioresour. Technol. 267, 666–676. https://doi.org/10.1016/j.biortech.2018.06.099

Marcato, C.-E., Pinelli, E., Cecchi, M., Winterton, P., Guiresse, M., 2009. Bioavailability of Cu and Zn in raw and anaerobically digested pig slurry. Ecotoxicol. Environ. Saf. 72, 1538–1544. https://doi.org/10.1016/j.ecoenv.2008.12.010

Mata-Alvarez, J., Macé, S., Llabrés, P., 2000. Anaerobic digestion of organic solid wastes. An overview of research achievements and perspectives. Bioresour. Technol. 74, 3–16. https://doi.org/10.1016/S0960-8524(00)00023-7

Mathivanan, K., Chandirika, J.U., Vinothkanna, A., Yin, H., Liu, X., Meng, D., 2021. Bacterial adaptive strategies to cope with metal toxicity in the contaminated environment – A review. Ecotoxicol. Environ. Saf. 226, 112863. https://doi.org/10.1016/j.ecoenv.2021.112863

Mo, R., Guo, W., Batstone, D., Makinia, J., Li, Y., 2023. Modifications to the anaerobic digestion model no. 1 (ADM1) for enhanced understanding and application of the anaerobic treatment processes – A comprehensive review. Water Res. 244, 120504. https://doi.org/10.1016/j.watres.2023.120504

Montecchio, D., Astals, S., Di Castro, V., Gallipoli, A., Gianico, A., Pagliaccia, P., Piemonte, V., Rossetti, S., Tonanzi, B., Braguglia, C.M., 2019. Anaerobic co-digestion of food waste and waste activated sludge: ADM1 modelling and microbial analysis to gain insights into the two substrates' synergistic effects. Waste Manag. 97, 27–37. https://doi.org/10.1016/j.wasman.2019.07.036

Morel, F., Hering, J., 1993. Principles and applications of aquatic chemistry.

Nguyen, L.N., Kumar, J., Vu, M.T., Mohammed, J.A.H., Pathak, N., Commault, A.S., Sutherland, D., Zdarta, J., Tyagi, V.K., Nghiem, L.D., 2021. Biomethane production from anaerobic co-digestion at wastewater treatment plants: A critical review on development and innovations in biogas upgrading techniques. Sci. Total Environ. 765, 142753. https://doi.org/10.1016/j.scitotenv.2020.142753

Oleszkiewicz, J.A., Sharma, V.K., 1990. Stimulation and Inhibition of Anaerobic Processes by Heavy MetalsmA Review.

Osuna, M.B., Zandvoort, M.H., Iza, J.M., Lettinga, G., Lens, P.N.L., 2003. Effects of trace element addition on volatile fatty acid conversions in anaerobic granular sludge reactors. Environ. Technol. U. K. 24, 573–587. https://doi.org/10.1080/09593330309385592

Ozyildiz, G., Zengin, G.E., Güven, D., Cokgor, E., Özdemir, Ö., Hauduc, H., Takács, I., Insel, G., 2023. Restructuring anaerobic hydrolysis kinetics in plant-wide models for accurate prediction of biogas production. Water Res. 245, 120620. https://doi.org/10.1016/j.watres.2023.120620

Parker, D.R., Norvell, W.A., Chaney, R.L., 1995. GEOCHEM-PC—A Chemical Speciation Program for IBM and Compatible Personal Computers, in: Chemical Equilibrium and Reaction Models. John Wiley & Sons, Ltd, pp. 253–269. https://doi.org/10.2136/sssaspecpub42.c13

Roussel, J., 2013. Metal behaviour in anaerobic sludge digesters supplemented with trace nutrients.

Sauvé, S., Parker, D.R., 2005. Chemical Speciation of Trace Elements in Soil Solution, in: Chemical Processes in Soils. John Wiley & Sons, Ltd, pp. 655–688. https://doi.org/10.2136/sssabookser8.c14

Schecher, W.D., McAvoy, D.C., 1992. MINEQL+: A software environment for chemical equilibrium modeling. Comput. Environ. Urban Syst. 16, 65–76. https://doi.org/10.1016/0198-9715(92)90053-T

Scherer, P., Sahm, H., 1981. Effect of trace elenments and vitamins on the growth of Methanosarcina barkeri. Acta Biotechnol. 1, 57–65; ISSN: 1618-2863.

Schink, B., 2002. Synergistic interactions in the microbial world. Antonie Van Leeuwenhoek 81, 257–261. https://doi.org/10.1023/A:1020579004534

Siegel, F.R., 2002. Environmental Geochemistry of Potentially Toxic Metals. Springer, Berlin, Heidelberg. https://doi.org/10.1007/978-3-662-04739-2

Solon, K., Flores-Alsina, X., Mbamba, C.K., Volcke, E.I.P., Tait, S., Batstone, D., Gernaey, K.V., Jeppsson, U., 2015. Effects of ionic strength and ion pairing on (plant-wide) modelling of anaerobic digestion. Water Res. 70, 235–245. https://doi.org/10.1016/j.watres.2014.11.035

Song, X., Luo, W., Hai, F.I., Price, W.E., Guo, W., Ngo, H.H., Nghiem, L.D., 2018. Resource recovery from wastewater by anaerobic membrane bioreactors: Opportunities and challenges. Bioresour. Technol. 270, 669–677. https://doi.org/10.1016/j.biortech.2018.09.001

Staicu, L.C., Simon, S., Guibaud, G., Yekta, S.S., Calli, B., Bartacek, J., Fermoso, F.G., Van Hullebusch, E.D., Van Hullebusch, E., Collins, G., Roussel, J., Mucha, A.P., Esposito, G., 2019. Chapter 2 Biogeochemistry of trace elements in anaerobic digesters from the book Trace Elements in Anaerobic Biotechnologies.

Templeton, D.M., Ariese, F., Cornelis, R., Danielsson, L.-G., Muntau, H., Leeuwen, H.P. van, Lobinski, R., 2000. Guidelines for terms related to chemical speciation and fractionation of elements. Definitions, structural aspects, and methodological approaches (IUPAC Recommendations 2000). Pure Appl. Chem. 72, 1453–1470. https://doi.org/10.1351/pac200072081453

Tessier, A., Campbell, P.G.C., Bisson, M., 1979. Sequential extraction procedure for the speciation of particulate trace metals. Anal. Chem. 51, 844–851. https://doi.org/10.1021/ac50043a017

Thanh, P.M., Ketheesan, B., Yan, Z., Stuckey, D., 2016. Trace metal speciation and bioavailability in anaerobic digestion: A review. Biotechnol. Adv. 34, 122–136. https://doi.org/10.1016/j.biotechadv.2015.12.006

van der Veen, A., Fermoso, F.G., Lens, P.N.L., 2007. Bonding Form Analysis of Metals and Sulfur Fractionation in Methanol-Grown Anaerobic Granular Sludge. Eng. Life Sci. 7, 480–489. https://doi.org/10.1002/ELSC.200720208

Van Hullebusch, E.D., Gieteling, J., Zhang, M., Zandvoort, M.H., Daele, W.V., Defrancq, J., Lens, P.N.L., 2006. Cobalt sorption onto anaerobic granular sludge: Isotherm and spatial localization analysis. J. Biotechnol. 121, 227–240. https://doi.org/10.1016/J.JBIOTEC.2005.07.011

van Hullebusch, E.D., Guibaud, G., Simon, S., Lenz, M., Yekta, S.S., Fermoso, F.G., Jain, R., Duester, L., Roussel, J., Guillon, E., Skyllberg, U., Almeida, C.M.R., Pechaud, Y., Garuti, M., Frunzo, L., Esposito, G., Carliell-Marquet, C., Ortner, M., Collins, G., 2016. Methodological approaches for fractionation and speciation to estimate trace element bioavailability in engineered anaerobic digestion ecosystems: An overview. Crit. Rev. Environ. Sci. Technol. 46, 1324–1366. https://doi.org/10.1080/10643389.2016.1235943

Vu, H.P., Nguyen, L.N., Wang, Q., Ngo, H.H., Liu, Q., Zhang, X., Nghiem, L.D., 2022. Hydrogen sulphide management in anaerobic digestion: A critical review on input control, process regulation, and post-treatment. Bioresour. Technol. 346, 126634. https://doi.org/10.1016/j.biortech.2021.126634

Watson, J.H.P., Ellwood, D.C., Deng, Q., Mikhalovsky, S., Haytert, C.E., Evanst, J., 1995. HEAVY METAL ADSORPTION ON BACTERIALLY PRODUCED FeS, Minerals Engineering.

Yekta, S.S., Skyllberg, U., Danielsson, Å., Björn, A., Svensson, B.H., 2017. Chemical speciation of sulfur and metals in biogas reactors – Implications for cobalt and nickel bio-uptake processes. J. Hazard. Mater. 324, 110–116. https://doi.org/10.1016/J.JHAZMAT.2015.12.058

Zheng, X., Wu, K., Sun, P., Zhouyang, S., Wang, Y., Wang, H., Zheng, Y., Li, Q., 2021. Effects of substrate types on the transformation of heavy metal speciation and bioavailability in an anaerobic digestion system. J. Environ. Sci. 101, 361–372. https://doi.org/10.1016/j.jes.2020.08.032

CHAPTER 2

Dynamic Modelling the Effects of Ionic Strength and Ion Complexation on Trace Metal Speciation during Anaerobic Digestion

ABSTRACT: Dosing trace metals into anaerobic digestors is proven to improve biogas production rate and yield by stimulating microorganisms involved in the metabolic pathways. Trace metal effects are governed by metal speciation and bioavailability. Though chemical equilibrium speciation models are well-established and widely used to understand metal speciation, the development of kinetic models considering biological and physicochemical processes has recently gained attention. This work proposes a dynamic model for metal speciation during anaerobic digestion which is based on a system of ordinary differential equations aimed to describe the kinetics of biological, precipitation/dissolution, gas transfer processes and, a system of algebraic differential equations to define fast ion complexation processes. The model also considers ion activity corrections to define effects of ionic strength. Results from this study shows the inaccuracy in predicting trace metal effects on anaerobic digestion by typical metal speciation models and the significance of considering non-ideal aqueous phase chemistry (ionic strength and ion pairing/complexation) to define speciation and metal labile fractions. Model results show a decrease in metal precipitation and increase in metal dissolved fraction and methane production yield with increase in ionic strength. Capability of the model to dynamically predict trace metal effects on anaerobic digestion under different conditions, like changing dosing conditions and initial iron to sulphide ratio, was also tested and verified. Dosing iron increases methane production and decreases hydrogen sulphide production. However, when iron to sulphide ratio is greater than 1, methane production decreases due to increase in dissolved iron which reaches inhibitory concentration levels.

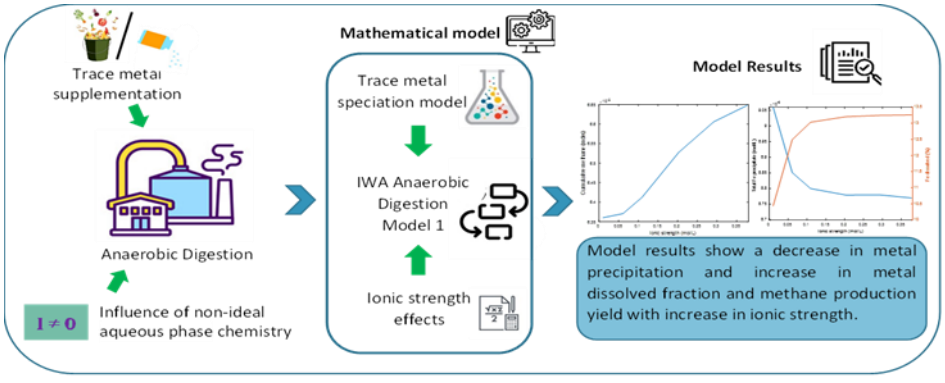

2.1. INTRODUCTION

Anaerobic digestion (AD) is proven to be one of the most economical and effective biotechnologies for the treatment and energy recovery from organic waste (Wu et al., 2022). Immense efforts are made worldwide to improve biogas yields during AD. Supplementing trace metals (TMs) to enhance AD performance is one such proven technique (Choong et al., 2016; Feng et al., 2010; Thanh et al., 2016). Trace metals are required at optimum concentrations in an AD system as they play an essential role in composition of enzymes and cofactors involved in AD pathways. They also significantly affect the microbial activity and abundance of microbes, thereby influencing the pathway of degradation in AD. Optimum bioavailability of TMs is important for enhancing biogas production. Lack of bioavailable TMs results in acidification of the reactors whereas an excess concentration results in toxicity (Bartacek et al., 2008; Fermoso et al., 2008). The effect of trace metal on microorganisms largely depends on the speciation of each metal. Speciation depends on many factors, such as operating conditions or chemical equilibrium and precipitation. Therefore, it is difficult to predict the effect of trace metal supplementation in an AD system. Precipitation of metal-sulphide for example is considered to be one of the critical processes in anaerobic digestion (van der Veen et al., 2007). Zheng et al. (2022) reported dissolution/precipitation, complexation, adsorption, bioaccumulation and participation in microbial activities as the major mechanics controlling metal migration in an anaerobic digestion system. Although numerous experimental efforts are made to quantify TM speciation in an AD system, a mathematical model-based approach will facilitate a reliable and precise TM dosing strategy applicable on each individual case.

Geochemical models like Visual MINTEQ and PHREEQC are widely used models to understand chemical speciation in different environmental systems. However, such models are not stand alone and are more useful as complementary outputs along with experimental results. Also, the results of these models are based on equilibrium state and do not consider biological reactions and kinetic influence on final speciation. Most extensively used biological model for anaerobic digestion is the benchmark model Anaerobic Digestion Model 1 (ADM1) developed by the International Water Association (IWA) task group on anaerobic digestion (Batstone et al., 2002). Since the model lacked consideration of major physicochemical processes occurring during anaerobic digestion, numerous ADM1 modification attempts are now available in the literature. For example, Flores-Alsina et al. (2016) extended ADM 1 to model interactions of phosphorous, sulphur and iron during anaerobic digestion and validated multiple mineral precipitation reactions.

Recently, few ADM1 based modelling studies have been carried out to study trace metal effects in anaerobic digestion, linking physicochemical processes with the biological model (Frunzo et al., 2019; Maharaj et al., 2018, 2019, 2021). ADM1 based mathematical models were developed to predict precipitation and complexation reactions in anaerobic digestion(Maharaj et al., 2018, 2019). Frunzo et al. (2019) proposed a mechanistic model considering major biochemical and physiochemical processes affecting bioavailability of

TMs. Lately, a more comprehensive model considering adsorption–desorption reactions of TMs with biomass, inerts and mineral precipitates, as well as TM precipitation/dissolution, complexation reactions and biodegradation processes has been published (Maharaj et al., 2021). However, reactor media in all these models were considered to behave ideally and ionic strength effects on chemical equilibrium were not considered.

Most attempts on anaerobic digestion modelling consider ideal physicochemical behaviour (ionic strength equal to zero). However, anaerobic digesters have total dissolved solids concentration in the range 5000-10,000 mg/L and ionic strength ranges from 0.025 to 1 mol/L (Batstone et al., 2012; Musvoto et al., 2000). Therefore, it is not negligible and is important to consider ion pairing/complexes when total dissolved solids concentration is more than 1,000 mg/L (Musvoto et al., 2000). According to Solon et al. (2015) the influence of ionic strength on pH is significant for media with ionic strength greater than 0.2 mol/L. Moreover, ionic strength effect on precipitation is significant even at lower ionic strengths ($I < 0.2$ mol/L) (Tait et al., 2012).

Few publications in the recent past presented various approaches to account for non-ideal aqueous phase chemistry in anaerobic digestion modelling (Huber et al., 2017; Lizarralde et al., 2015; Patón et al., 2018; Solon et al., 2015). Solon et al. (2015) presented a framework for modelling ion pairing and ionic strength effects and Huber et al. (2017) coupled ADM1 with PHREEQC. Patón et al. (2018) presented a model where only ionic strength is considered and observed a 5% error between ideal and non-ideal behaviour modelling in free ammonia, biogas composition and hydrogen sulphide inhibition in anaerobic digestor scenarios of low ionic strengths. Non-ideal modelling conditions showed considerable influence on pH, concentration of inhibitors (i.e. TMs, NH_3), and liquid-gas transfer (i.e. H_2S, CO_2) in high solids anaerobic digestors (Pastor-Poquet et al., 2019). Compared to alkali earth metals like Ca^{2+}/Mg^{2+}, trace metals form more ion pairs/complexes (Callander & Barford, 1983). Hence it is important to consider complexation while modelling trace metal speciation.

Increase in ionic strength decreases activity of ions. Moreover, ion pairing/complexation reduces concentration of free ions in solution. Thus, thermodynamic driving force for solid-liquid precipitation decreases. Saturation index and solubility of salts increases with ionic strength (Tait et al., 2009). Hence, saturated solution contains lower concentration of solid precipitate. Few precipitation models under non-ideal behaviour have been published (Hauduc et al., 2015; Kazadi Mbamba et al., 2015, 2019; Y. Zhang et al., 2015). It is important to define TM speciation precisely to study TM effects in AD as such effects depend greatly on bioavailable TM, which are controlled by TM speciation.

Despite its significance, this impact of ionic strength and ion pairing/complexation on physicochemical modelling has been neglected and anaerobic digestors were over simplified to ideal solution in previous literature modelling. Hence, the main novelty of this work is to develop a non-ideal aqueous phase model framework for defining trace metal speciation processes during anaerobic digestion. To the best of our knowledge, this model represents

the only attempt to track trace metals dynamics in anaerobic digestion systems as affected by ionic strength by using an ADM1 approach. The main objectives of the paper are (1) to show effects of ionic strength and ion pairing/complexation on modelling of trace metal precipitation in anaerobic digestion, (2) to determine its influence on speciation and bioavailability of trace metals in anaerobic digestion, (3) to develop a more compatible ADM1 based dynamic model for defining biochemical/physicochemical processes under non-ideal conditions to study trace metal dynamics in anaerobic digestion and their influence on biogas production yield and rate. Existing physicochemical framework for defining trace metal dynamics in anaerobic digestors has been improved and effects were studied and verified under different test scenarios.

2.2. METHODOLOGY

ADM1 model is modified to capture trace metal precipitation while considering ionic strength of the medium. The three-phase (solid, liquid, gas) model developed in this study is defined in terms of 52 dynamic state variables (concentration of substrates, products, biomass, gases, precipitates, cations, anions) and consists of four process types: (1) 19 biochemical processes, (2) 13 chemical precipitation reactions, (3) 96 aqueous phase reactions (ion pairing and acid base reactions), (4) four gas transfer processes. Processes defined in the model are schematically represented in Fig. 2.1.

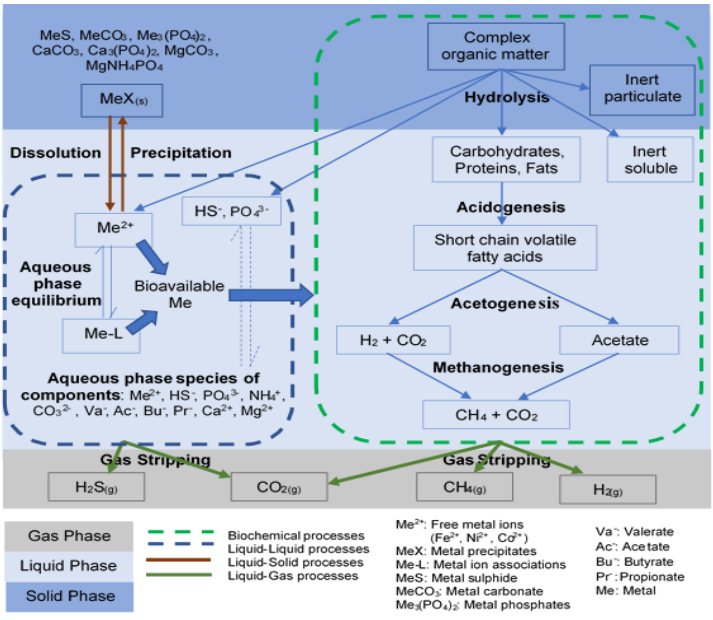

Figure 2.1 - Trace metal speciation processes in the model during anaerobic digestion

Aqueous phase reactions are very fast, reach equilibrium quickly (Barat et al., 2011) and thus are modelled based on chemical equilibrium. Liquid to solid phase reactions (precipitation),

gas transfer and biochemical reactions are slower and are modelled kinetically using process rates. Defining aqueous phase processes as equilibrium reactions reduced the number of differential equations to be defined for aqueous phase from 96 to 16. Stoichiometry and kinetic rates of all kinetic reactions are represented in a Gujer matrix (see Appendix 2.1). Aqueous phase reactions are formulated as non-linear algebraic equations as further explained in Section 2.2.3.2. Dynamics of the model components are formulated as ordinary differential equations and are modelled based on mass conservation principle for soluble, particulate and gaseous components as described in ADM1.

2.2.1. Biochemical module

The main biological pathways in anaerobic digestion including disintegration, hydrolysis, acidogenesis, acetogenesis and methanogenesis are kinetically modelled according to IWA Anaerobic Digestion Model 1. Stoichiometry of the disintegration process is modified to include release of trace metals, sulphur (HS^-) and phosphorous (PO_4^{3-}) from organic matter. Uptake of the trace metals by microbes is added in the acetate and hydrogen uptake stoichiometry since TM effects on anaerobic digestion predominantly occur during methanogenesis (Thanh et al., 2016). Moreover, the study aims at modelling influence of physicochemical reactions on TM speciation effects and modelling metal effects on each metabolic pathway is outside the scope of this work. Stimulation and inhibition effect of trace metals on metabolic activity is considered using an additional limiting factor, I_{Me} (Eq. (2.1)) in the inhibition expressions as proposed by Maharaj et al. (2018). Bioavailable form of trace metal used in dose response function I_{Me} is the total dissolved concentration Me_{tot} including free ions Me^{2+} and ion associations Me-L as represented in Fig. 2.1. Me_{tot} (dissolved Me) is solved from mass balance equation for each metal ion.

$$I_{Me} = \frac{c_1\, Me_{tot} + c_2}{Me_{tot}^2 + c_3\, Me_{tot} + c_4}, \tag{2.1}$$

where c_1, c_2, c_3 and c_4 are constants to adjust desirable optimum trace metal concentration.

2.2.2. Model Variants

Based on the approaches to model the physiochemical module, 3 model variants are presented. Model 1 considers ideal aqueous phase chemistry and is modelled according to the physiochemical framework proposed by Maharaj et al. (2018). It includes a charge balance equation and kinetic rate expressions for acid base reactions, precipitation/dissolution and gas transfer processes. Further detailed description can be also found in Frunzo et al. (2019). Model 2 and Model 3 are based on non-ideal aqueous phase chemistry. Model 2 neglects ion pairing whereas Model 3 considers ion pairing in precipitation reaction modelling. Physicochemical framework used for non-ideal aqueous phase chemistry is based on Solon et al. (2015) as described in Section 2.2.3.

2.2.3. Improved physiochemical module for modelling trace metal dynamics in anaerobic digesters

Physicochemical reactions are formulated in two parts: (1) kinetic rate expressions for precipitation/dissolution and gas transfer processes, (2) non-linear algebraic equations for aqueous phase reactions. Soluble or dissolved form (Me_{tot}) of a metal exists in the system mainly as free ions (Me^{2+}) and associated form (Me-L) such as weak acid-base and ion pairs. Precipitation is driven only by the free ion concentration and is not dependent on the total metal ion concentration. The aqueous-phase chemistry model solves for the activity of free metal ion species (Me^{2+}) that participate in precipitation/dissolution.

2.2.3.1. Precipitation and Gas transfer processes

Kinetics of precipitation processes are modelled as reversible processes based on saturation index (SI) according to Koutsoukos et al. (1980). Ion activity product (IAP) of a general precipitation-dissolution reaction represented in the form of Eq. (2.2) is as expressed in Eq. (2.3).

$$xM^{\nu+} + yN^{\nu-} \leftrightarrows M_xN_y \tag{2.2}$$

$$IAP = (A_{M^{\nu+}})^x (A_{N^{\nu-}})^y , \tag{2.3}$$

where $\nu+$ and $\nu-$ denote valences and x and y denote the stoichiometric coefficients. $A_{M^{\nu+}}$ and $A_{N^{\nu-}}$ are the activities of cations and anions. The model checks the value of SI (ratio of IAP to solubility product (K_{sp})) at each time step. When SI is greater than 1, precipitation reaction occurs as presented in Eq. (2.4) and dissolution rate will be zero. If SI is less than 1, precipitation rate is zero and dissolution rate as expressed in Eq. (2.5) is activated.

$$\rho_{prec} = k_r' (IAP^{1/\nu} - {K_{sp}}^{1/\nu})^n, \tag{2.4}$$

$$\rho_{diss} = -k_r' (IAP^{1/\nu} - {K_{sp}}^{1/\nu})^n \frac{1}{1 + (K/S_{M_xN_y})}, \tag{2.5}$$

where k_r' is the precipitation rate constant, ν is the sum of cations and anions and n is the order of the reaction. $S_{M_xN_y}$ is the precipitate concentration and K is the hyperbolic inhibition constant. Liquid-Gas transfer kinetics are modelled as presented in ADM1 (Eq. (2.6)). Carbon dioxide, hydrogen, methane and hydrogen sulphide gases are the components considered in gaseous phase and are considered as dynamic state variables in the model in addition to the liquid and solid-state components.

$$\rho_T = k_{La}(S_{liq} - K_H P_{gas}), \tag{2.6}$$

where k_{La} is the overall mass transfer coefficient, K_H is the Henry's law coefficient, S_{liq} is the dissolved gas and P_{gas} is the gas phase partial pressure.

2.2.3.2. Modelling aqueous phase reactions (weak acid-base reactions and ion pairing)

This module consists of ionic strength correction based on Davies equation and modelling aqueous phase equilibrium reactions. Model 3 considers 96 aqueous phase reaction species (ion pairing and acid base reaction species) expressed as 17 components, where component S_j is the fully dissociated form of species S_i. In Model 2, aqueous phase reaction species include only acid base reactions species and ion pairing is excluded.

Aqueous phase reactions in the system are modelled in terms of chemical activity of species instead of molar concentration to account for non-ideal physicochemical behavior. Chemical activity A_i of species is the product of species concentration S_i and activity coefficient γ_i. Chemical activity and ionic strength *I* of the medium is calculated based on Eq. (2.7) and Eq. (2.8), respectively, where z_i denotes ion valency. Activity coefficient is calculated based on Davies equation (Eq. (2.9)) which holds true for ionic strengths up to 0.5 mol/L (Stumm & Morgan, 1996), where A' is a temperature dependent parameter. Note that the sum in equation (2.8) is extended to the number of all charged chemical species.

$$A_i = S_i \ \gamma_i, \tag{2.7}$$

$$I = \tfrac{1}{2}\Sigma S_i z_i^2, \tag{2.8}$$

$$\log \gamma_i = -A' z_i^2 \left(\frac{\sqrt{I}}{1+\sqrt{I}} - 0.3I\right). \tag{2.9}$$

Aqueous phase reactions occur fast, reach equilibrium instantaneously and hence can be calculated algebraically (DAEs) at each iteration. Equilibrium of aqueous phase system is represented in terms of a set of species and components. 17 unique components are chosen to represent all possible species including equilibrium complexes and acid/base species. Aqueous phase reactions are formulated as set of nonlinear algebraic equations based on component conservation principle. It includes one law of mass action for each species (Eq. (2.10)) and 1M contribution balance for each component (Eq. (2.11)), where k_i and $\nu_{i,j}$ represent equilibrium coefficient and stoichiometric coefficient for each respective aqueous phase reaction. $S_{j,tot}$ is the total dissolved concentration and is obtained from the mass balance equation for each component. A_j is the activity of jth iterative species, N_c and N_s are the number of components and species respectively. Stoichiometry matrix of the component-species in aqueous phase reactions and an example of solving aqueous phase reaction are given in Appendix 2.1. Charge balance equation (Eq. (2.12)) is used to complete the set of

algebraic equations and monitor pH of the system where $S_{cat,tot}$ and $S_{an,tot}$ represent total concentrations of cationic and anionic charges respectively.

$$A_i = k_i \prod_{j=1}^{N_c} A_j^{\nu_{i,j}} \tag{2.10}$$

$$S_{j,tot} = S_j + \sum_{i=1}^{N_s} \nu_{i,j} S_i = \frac{A_j}{\gamma_j} + \sum_{i=1}^{N_s} \nu_{i,j} \frac{A_i}{\gamma_i} \tag{2.11}$$

$$S_{cat,tot} - S_{an,tot} = 0 \tag{2.12}$$

2.2.4. Model implementation

The equations defined in the model are implemented in an original MATLAB code. Ordinary differential equations in the model are solved by ode15s solver of MATLAB platform. Aqueous phase reactions are solved by multi-dimensional Newton Raphson method to deal algebraic interdependencies. It is combined with simulated annealing algorithm to improve system robustness and make the system less dependent on initial guess. Formulating the liquid-liquid processes as a set of Algebraic Equations (AEs) instead of Ordinary Differential Equations (ODEs) reduces the model stiffness and increases computational efficiency and speed. Iterations to solve the Differential Algebraic Equations (DAEs) converge when absolute tolerance is less than 10^{-12}. Ordinary differential equations (biochemical, precipitation and gas transfer) and algebraic equations (aqueous phase reactions) are sequentially solved in iteration. Total concentrations of ions used in aqueous phase model are solutions of ODEs governing mass balance of components while concentrations of ionic species in kinetic rates of the mass balance equations are solutions of algebraic equations defined for aqueous phase equilibrium

Simulated annealing algorithm converges to find the best initial guess for activity of ions (variables) based on random initial guess and initial total concentration. Newton-Raphson method then uses initial total concentration for the components as inputs based on the calculated initial guess and an initial aqueous speciation is calculated using equilibrium ion associations and acid/base reactions. Kinetic rate equations for biochemical, gas transfer and precipitation reactions are then solved using aqueous species concentrations from the solution of aqueous speciation model in the current time step. System is re-equilibrated in the next time step using the new total component concentrations solved from kinetic rates. This sequential iteration continues until user defined conditions like maximum time duration are met.

2.2.5. Model scenarios

The model is tested under different scenarios to check its capability to simulate the process dynamics under different chemical environments of variable ionic strength, initial sulphur concentrations and iron dose. Optimum initial trace metal concentrations and pH around 6.5 is maintained for all the simulations. More information on the initial conditions and model

parameters used for modelling different scenarios can be found in Appendix 2.1. In the first scenario, simulations are performed with three model variants for different ionic strengths ranging from 0.01M – 0.4M. Changes in ionic strength are made by varying cationic (K^+) and anionic load (Cl^-). Since pH plays a significant role in influencing physicochemical corrections on ADM1 state variables (Solon et al., 2015), concentrations of K^+ and Cl^- are varied at same levels to keep pH unchanged while varying the ionic strength. Two cases - (i) without iron dosing and (ii) with iron dosing are tested in the second scenario to study the influence of TM dosing on digestor performance and sulphur speciation. Initial iron to sulphur ratio (Fe/S) is varied in the third scenario to highlight its effects on iron speciation and methane production.

2.3. RESULTS AND DISCUSSION

2.3.1. Effects of ionic strength and ion pairing/complexation in modelling TM speciation

Capability of the model to simulate the process and predict its performances under different ionic strengths is verified with Scenario 1. Fig 2.2. shows the influence of ionic strength and ion pairing in modelling trace metal precipitation to study TM effects on AD. Model 1 (no ion activity corrections) with ideal aqueous phase chemistry does not capture effects of varying ionic strength and hence cumulative methane prediction is the same for all ionic strengths. Model 2 (with ion activity corrections) and Model 3 (with ion activity corrections and ion pairing) can capture ionic strength variation as they are modelled using physicochemical framework considering non-ideal aqueous phase chemistry ($I \neq 0$). Also, cumulative methane production predicted from all three model approaches is different with predictions from Model 3>Model 2>Model 1. This suggests the relevance of considering ionic strength correction and ion pairing in modelling TM effects on anaerobic digestion.

TM speciation results of the simulations from the first scenario (variable ionic strength) obtained from the three model variants is given in Table 2.1. pH predicted from Model 1 is different from Models 2 and 3 owing to activity corrections. Even though pH and ionic strength predictions at the end of the simulation period obtained from Model 2 and Model 3 are the same, speciation and cumulative methane production are different for the 3 model variants for all ionic strengths considered. Even at low ionic strengths ($I = 0.01$ M), cumulative methane production predicted from Model 1 (0.003134 M) is lower than that predicted from Model 2 (0.00547 M) and Model 3 (0.00636 M). This is because dissolved metal fraction that contributes to lability and bioavailability of ions reduces in the order Model 3>Model 2>Model 1. At $I = 0.01$ M, dissolved percentage of iron in the system predicted by Model 3 is 10.43% followed by Model 2 (0.867%) and Model 1 (0.079%). This trend holds true for all the ionic strengths tested.

Dissolved metal fraction is lowest in Model 1 due to highest precipitation levels. When effect of ionic strength is introduced in Model 2, ion activity corrections reduce free metal ion participation in precipitation. Activity coefficient is altered by intermolecular interactions

between the solvent and solute and is primarily dependent on ionic strength of the solution and charge of the ions (Stumm & Morgan, 1996). Hence lability of metals increases due to increase in free metal fraction. When ion pairing is taken into consideration (Model 3) availability of free ions in aqueous phase decreases due to formation of ion pairs, thus reducing precipitation. Furthermore, for a specific charge activity corrections of unpaired metal ions are larger than paired metal ions due to electrostatic interactions, thereby reducing precipitation. Hence, labile metal fraction (free metal ions and ion pairing species) increases causing an increase in cumulative methane production. This difference in TM speciation observed with three different physicochemical model approaches at ionic strength equal to 0.2 M is shown in Fig 2.3.

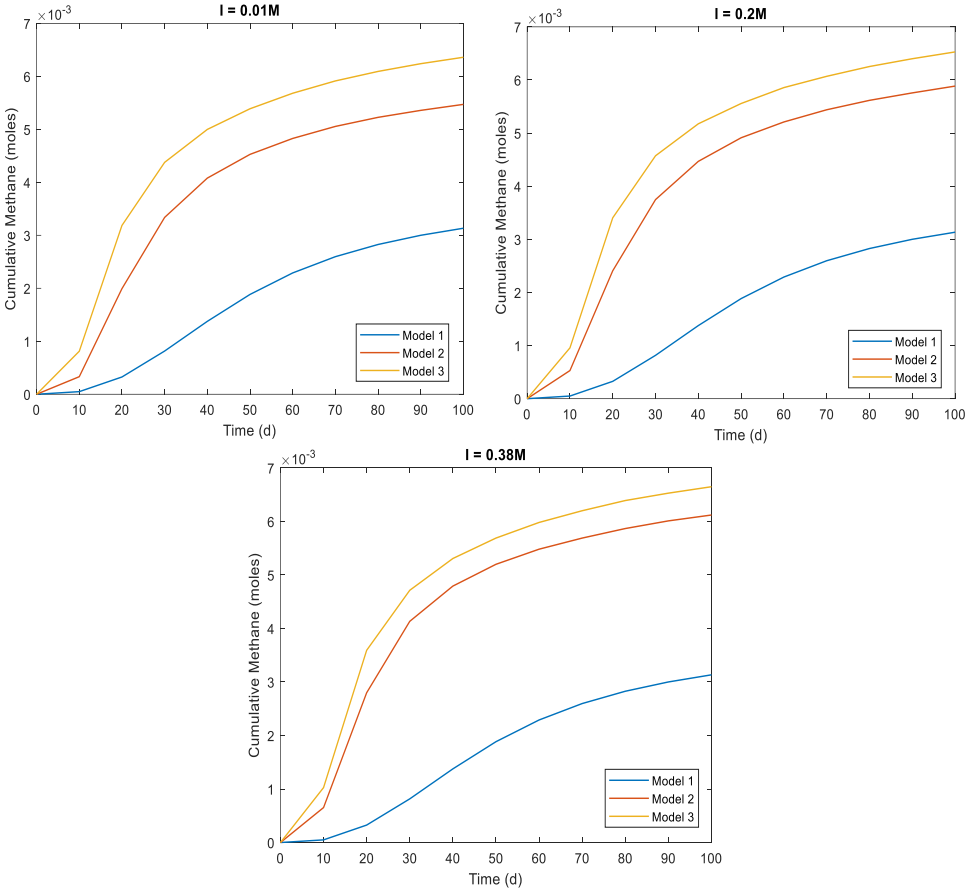

Figure 2.2 - Influence of ionic strength and ion pairing in modelling TM effects on AD performance

Table 2.1- Model results obtained at the end of simulations for variable ionic strengths with three different physicochemical modelling approaches

	$K^+ = Cl^- = 0.01M$			$K^+ = Cl^- = 0.05M$			$K^+ = Cl^- = 0.1M$		
	Model 1	Model 2	Model 3	Model 1	Model 2	Model 3	Model 1	Model 2	Model 3
pH	6.819	6.563	6.530	6.81	6.488	6.489	6.819	6.476	6.483
I	-	0.012	0.010	-	0.061	0.061	-	0.110	0.110
Methane (moles)	0.003134	0.0054709	0.0063601	0.003134	0.0055918	0.0063705	0.0031336	0.0056749	0.0064124
FeS	1.11×10^{-5}	0.00001	0.00000906	1.11×10^{-5}	9.98×10^{-6}	8.85×10^{-6}	1.109×10^{-5}	0.0000099	0.0000088
NiS	5.11×10^{-6}	0.0000051	0.00000511	5.11×10^{-6}	5.11×10^{-6}	5.11×10^{-6}	5.109×10^{-6}	0.0000051	0.0000051
CoS	5.01×10^{-6}	0.0000051	0.00000511	5.01×10^{-6}	5.11×10^{-6}	5.11×10^{-6}	5.010×10^{-6}	0.0000051	0.0000051
$Fe_3(PO_4)_2$	1.03×10^{-10}	4.30×10^{-11}	1.31×10^{-12}	1.0×10^{-10}	3.00×10^{-11}	1.01×10^{-12}	1.032×10^{-10}	2.29×10^{-11}	1.00×10^{-12}
$Ni_3(PO_4)_2$	3.44×10^{-13}	1.00×10^{-12}	1.00×10^{-12}	3.4×10^{-13}	1.00×10^{-12}	1.00×10^{-12}	3.443×10^{-13}	1.00×10^{-12}	1.00×10^{-12}
$Co_3(PO_4)_2$	8.26×10^{-12}	1.7×10^{-12}	1.00×10^{-12}	8.2×10^{-12}	1.00×10^{-12}	1.00×10^{-12}	8.255×10^{-12}	1.00×10^{-12}	1.00×10^{-12}
$FeCO_3$	0	1.00×10^{-12}	1.00×10^{-12}	0	1.00×10^{-12}	1.00×10^{-12}	0	1.00×10^{-12}	1.00×10^{-12}
$NiCO_3$	0	1.00×10^{-12}	1.00×10^{-12}	0	1.00×10^{-12}	1.00×10^{-12}	0	1.00×10^{-12}	1.00×10^{-12}
$CoCO_3$	0	1.00×10^{-12}	1.00×10^{-12}	0	1.00×10^{-12}	1.00×10^{-12}	0	1.00×10^{-12}	1.00×10^{-12}
$CaCO_3$	0	1.52×10^{-14}	1.69×10^{-14}	0	1.67×10^{-14}	1.77×10^{-14}	0	1.70×10^{-14}	1.75×10^{-14}
$Ca_3(PO_4)_2$	2.14×10^{-5}	0.0005387	0.0004 6939	2.14×10^{-5}	0.0003765	0.0003114	2.137×10^{-5}	0.0002666	0.0002086
$MgCO_3$	0	6.53×10^{-13}	6.46×10^{-13}	0	6.36×10^{-13}	6.34×10^{-13}	0	6.31×10^{-13}	6.3×10^{-13}
$MgNH_4PO_4$	9.60×10^{-10}	1.00×10^{-12}	1.00×10^{-12}	9.6×10^{-10}	1.00×10^{-12}	1.00×10^{-12}	9.60×10^{-10}	1.00×10^{-12}	1.00×10^{-12}
%Fe free	0.079	0.868	1.074	0.08	1.312	1.918	0.079	1.619	2.320
%Ni free	0.000442	0.0053734	0.006279	0.000442	0.011091	0.011454	0.0004421	0.013815	0.013917
%Co free	0.000884	0.012036	0.013942	0.000884	0.024781	0.025366	0.0008841	0.030834	0.030795
%Fe $_{\text{ion pairs}}$	-	-	9.360	-	-	10.57	-	-	10.71
%Ni $_{\text{ion pairs}}$	-	-	0.027	-	-	0.033	-	-	0.034
%Co $_{\text{ion pairs}}$	-	-	0.0364	-	-	0.042	-	-	0.044

Table 2.2 *(Continued)*

	$K^+ = Cl^- = 0.2M$			$K^+ = Cl^- = 0.3M$			$K^+ = Cl^- = 0.4M$		
	Model 1	Model 2	Model 3	Model 1	Model 2	Model 3	Model 1	Model 2	Model 3
pH	6.819	6.484	6.493	6.81	6.484	6.493	6.819	6.484	6.493
I	-	0.203	0.203	-	0.203	0.203	-	0.203	0.203
Methane (moles)	0.003 1336	0.0058 842	0.0065 276	0.003 133	0.005 8842	0.006 5276	0.003 1336	0.005 8842	0.006 5276
FeS	1.109 $\times 10^{-5}$	0.0000 099	8.779×10^{-6}	1.1×10^{-5}	0.000 0099	8.779×10^{-6}	1.109 $\times 10^{-5}$	0.000 0099	8.779×10^{-6}
NiS	5.109 $\times 10^{-6}$	0.0000 051	5.111×10^{-6}	5.1×10^{-6}	0.000 0051	5.111×10^{-6}	5.109 $\times 10^{-6}$	0.000 0051	5.111×10^{-6}
CoS	5.010 $\times 10^{-6}$	0.0000 051	5.109×10^{-6}	5.0×10^{-6}	0.000 0051	5.109×10^{-6}	5.010 $\times 10^{-6}$	0.000 0051	5.109×10^{-6}
$Fe_3(PO_4)_2$	1.03×10^{-10}	1.50×10^{-11}	1.00×10^{-12}	1.03×10^{-10}	1.50×10^{-11}	1.00×10^{-12}	1.032 $\times 10^{-10}$	1.50×10^{-11}	1.00×10^{-12}
$Ni_3(PO_4)_2$	3.44×10^{-13}	1.00×10^{-12}	1.00×10^{-12}	3.443 $\times 10^{-13}$	1.00×10^{-12}	1.00×10^{-12}	3.443 $\times 10^{-13}$	1.00×10^{-12}	1.00×10^{-12}
$Co_3(PO_4)_2$	8.26×10^{-12}	1.00×10^{-12}	1.00×10^{-12}	8.255 $\times 10^{-12}$	1.00×10^{-12}	1.00×10^{-12}	8.255 $\times 10^{-12}$	1.00×10^{-12}	1.00×10^{-12}
$FeCO_3$	0	1.00×10^{-12}	1.00×10^{-12}	0	1.00×10^{-12}	1.00×10^{-12}	0	1.00×10^{-12}	1.00×10^{-12}
$NiCO_3$	0	1.00×10^{-12}	1.00×10^{-12}	0	1.00×10^{-12}	1.00×10^{-12}	0	1.00×10^{-12}	1.00×10^{-12}
$CoCO_3$	0	1.00×10^{-12}	1.00×10^{-12}	0	1.00×10^{-12}	1.00×10^{-12}	0	1.00×10^{-12}	1.00×10^{-12}
$CaCO_3$	0	1.64×10^{-14}	1.584×10^{-14}	0	1.64×10^{-14}	1.584 $\times 10^{-14}$	0	1.64×10^{-14}	1.584 $\times 10^{-14}$
$Ca_3(PO_4)_2$	2.137 $\times 10^{-5}$	0.0001 239	0.0000 758	2.137 $\times 10^{-5}$	0.000 1239	0.000 0758	2.137 $\times 10^{-5}$	0.000 1239	0.000 0758
$MgCO_3$	0	6.26×10^{-13}	6.243×10^{-13}	0	6.26×10^{-13}	6.243 $\times 10^{-13}$	0	6.26×10^{-13}	6.243 $\times 10^{-13}$
$MgNH_4PO_4$	9.60×10^{-10}	1.00×10^{-12}	9.90×10^{-13}	9.60×10^{-10}	1.00×10^{-12}	9.90×10^{-13}	9.60×10^{-10}	1.00×10^{-12}	9.90×10^{-13}
%Fe free	0.079	2.245	2.692	0.079	2.245	2.692	0.079	2.245	2.692
%Ni free	0.000 4421	0.0158 36	0.0159 11	0.000 4421	0.015 836	0.015 911	0.000 4421	0.015 836	0.015 911
%Co free	0.000 8841	0.0353 15	0.0352	0.000 8841	0.035 315	0.035 2	0.000 8841	0.035 315	0.035 2
%Fe $_{\text{ion pairs}}$	-	-	10.51	-	-	10.51	-	-	10.51
%Ni $_{\text{ion pairs}}$	-	-	0.034	-	-	0.034	-	-	0.034
%Co $_{\text{ion pairs}}$	-	-	0.0438 29	-	-	0.043 829	-	-	0.043 829

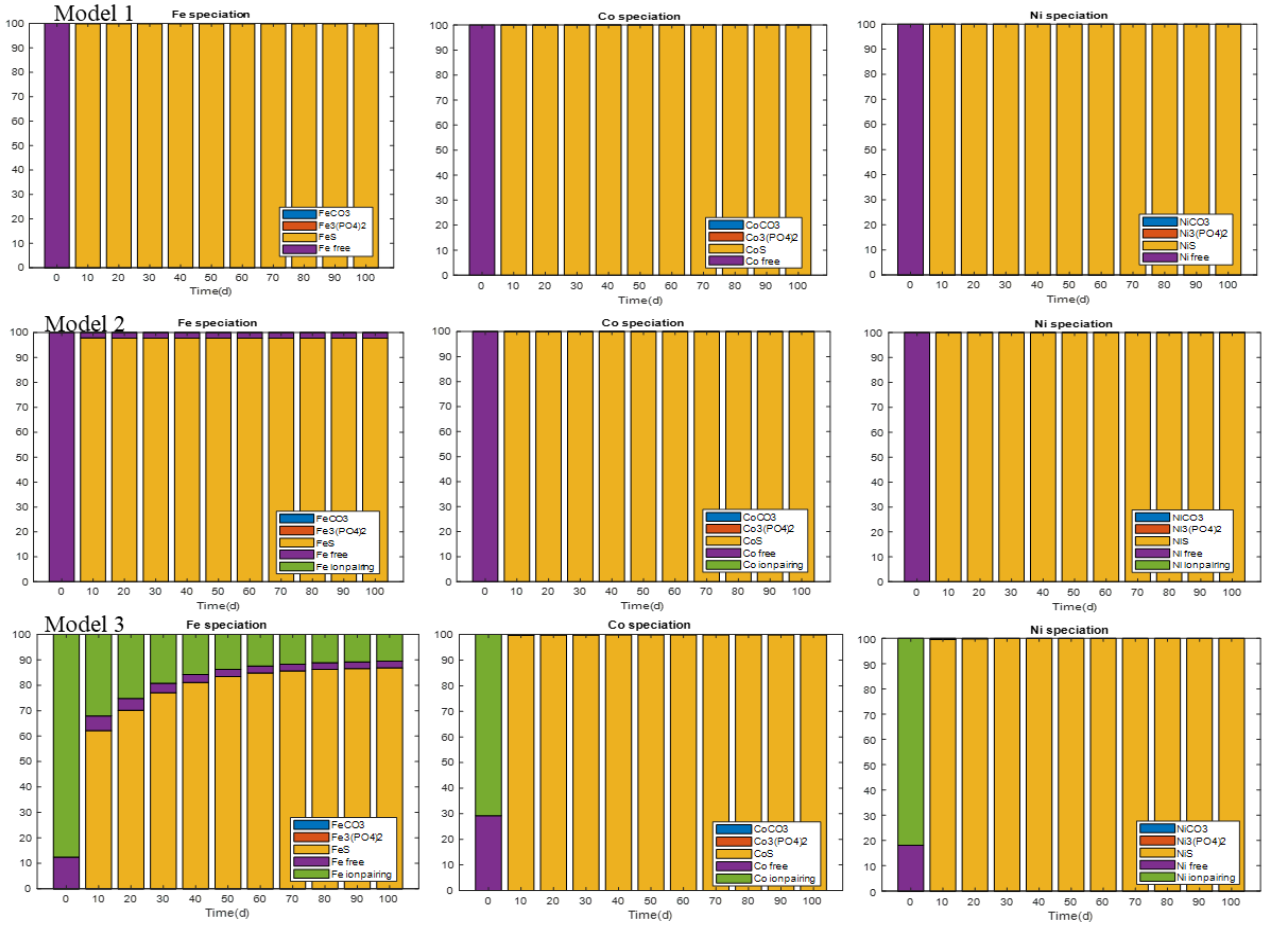

Figure 2.3 - Dynamic profiles of TM speciation for the three model variants

Tait et al. (2012) reported similar observation where concentration of free Ca and Mg ions were determined to study influence on thermodynamic driving force for solid liquid precipitation. They observed reduction in concentration of free ions and active component of those ions participating in the precipitation (ion activity) with increase in ionic strength. All subsequent scenarios are tested with Model 3 physicochemical approach considering ionic strength and ion pairing as it is found to be the best and correct approach to model TM effects based on the results obtained from first scenario. Effect of increasing ionic strength on TM speciation and digestor performance obtained from Model 3 are shown in Fig. 2.4. Increasing influent concentration of K^+ and Cl^- ions increases ionic strength and this reduces activity of free ions, thereby reducing precipitation. Thus, cumulative methane production increases due to more lability of trace metals. Ionic strengths tested in this study are considered based on reliability of Davis approach to ionic activity approximation. For higher ionic strengths, it is recommended to use other approximations like WATEQ Debye-Hückel to calculate activity coefficient (Reis, 2021).

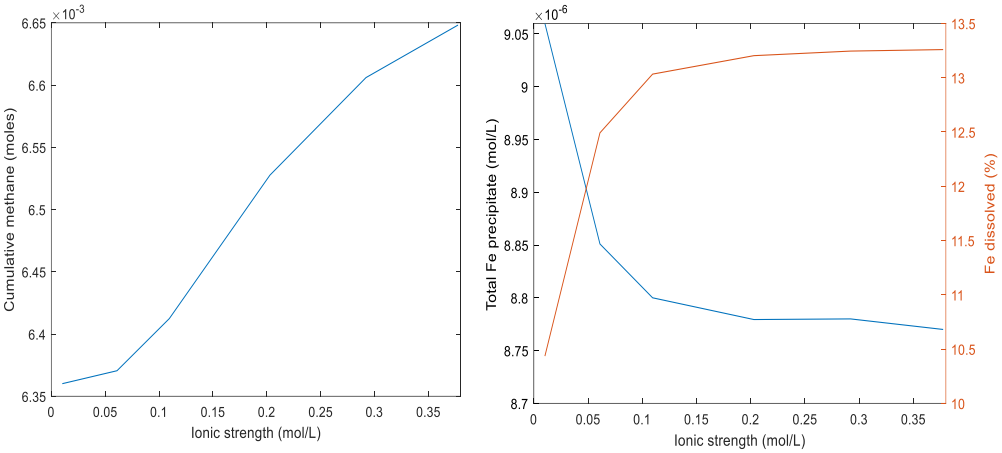

Figure 2.4 - Effect of ionic strength on TM speciation and AD performance

2.3.2. Trace metal dosing effects on anaerobic digestion

This scenario analyses influence of trace metal dosing on anaerobic digestion and simulation ability of the model to predict the kinetic behaviour. Fig. 2.5 depicts effects of iron dosing during anaerobic digestion. Initial TM concentration (Fe) is varied to see dosing effects. When iron is not dosed (Fe_{ini} = 0 µM), cumulative methane production is found to be 0.0055 M. Cumulative methane production increases to 0.0065 M when iron dosing is increased to 100 µM. This shows the stimulatory effects of trace metals on anaerobic digestion. However, if iron dosing is increased to 500 µM, methane production decreases due to inhibitory effects of trace metals (data not shown). If dosing is further increased, it reaches toxic concentration levels and methane production reduces further (0.0018 M) along with poor anaerobic digestor performance. Hence, it is important to dose trace metals at optimum concentrations. Bi et al. (2019) observed similar effects when iron and nickel were supplemented in high solid

anaerobic digestion of chicken manure where the TM dosing enhanced methane production and reduced volatile fatty acids, while W. Zhang et al. (2015) reported toxicity to methanogens when iron was supplemented excessively. Moreover, Thanh et al. (2017) reported precipitation of Fe^{2+} as FeS in presence of sulphide, thereby reducing bioavailability of Fe^{2+}. Nevertheless, TM dosing can help in improving biogas yield by reducing hydrogen sulphide concentrations in biogas (Liu et al., 2015). Fig. 2.5 shows that when iron is absent inorganic sulphur exists mostly as H_2S. However, when iron is dosed inorganic sulphur precipitates as metal sulphide and H_2S production decreases. Similar effects on influencing quantity and quality of biogas can be observed by dosing other trace metals like Co and Ni (data not shown).

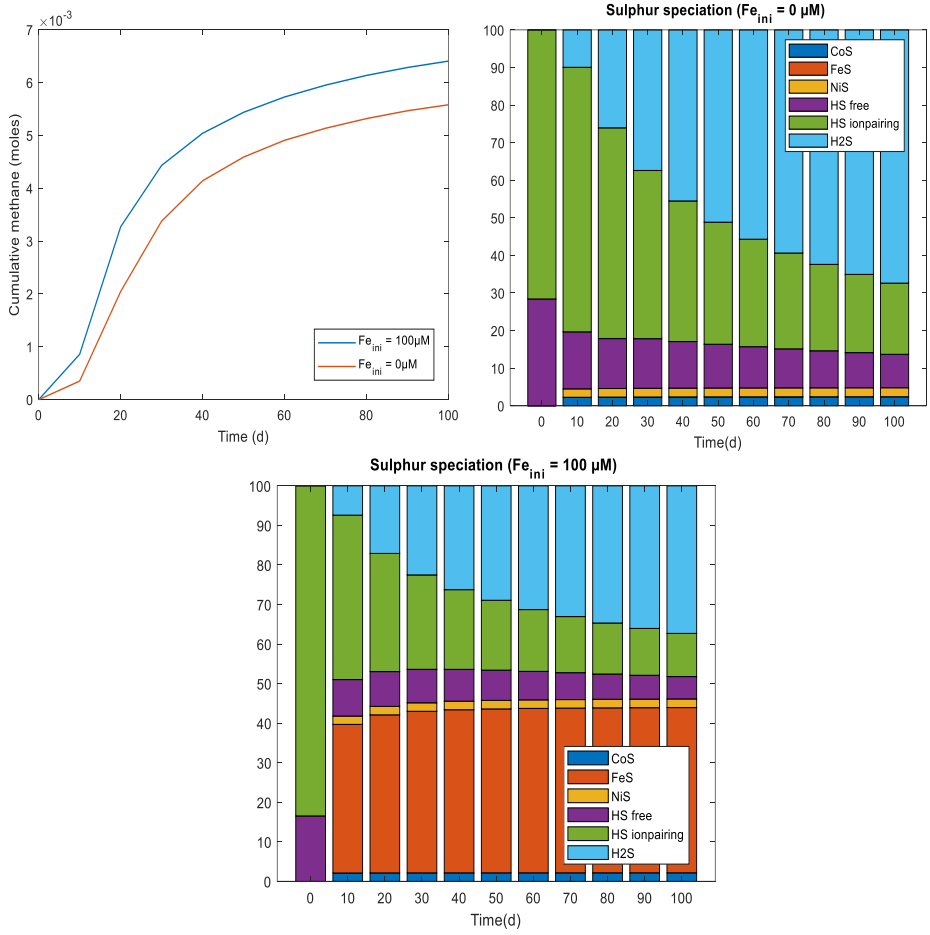

Figure 2.5 - Influence of TM(Fe) dosing on AD performance and sulphur speciation

2.3.3. Trace metal speciation model results

Metal speciation and thereby optimum bioavailability of trace metals for microorganisms is driven by numerous factors including operational conditions and chemical equilibrium. The model developed in this study is capable to predict dynamic metal speciation in anaerobic digestion. Physicochemical module of the model including precipitation and aqueous phase reactions is validated with Visual MINTEQ geochemical program (Gustafsson, 2018) (see Appendix 2.1).

In the current model, dosed trace metals supplemented in an anaerobic system are found to exist as free, complexed or precipitated. It is observed from the model results that majority of trace metal precipitated as sulphides-FeS, NiS and CoS (Fig. 2.3). Van der Veen et al. (2007) reported metal sulphides as the major form of precipitation reaction in an AD system. Kinetics of precipitation decrease in the order sulphides>phosphates>carbonates. Callander & Barford (1983) demonstrated quantitative assessment of metal precipitation with sulphides, phosphates, carbonates and its influence on metal availability in digestors. The key process controlling speciation and lability of a trace metal is found to be sulphide precipitation/dissolution as observed by Shakeri Yekta et al. (2014). Influence of inorganic sulphur in controlling chemical speciation of iron is studied by varying initial iron to sulphide (Fe/HS^-) ratio and is depicted in Fig. 2.6. More than 95% of iron precipitates as FeS when the ratio is less than 1. When Fe/HS^- ratio becomes greater than 1, sulphur is limited and metal starts precipitating as phosphates and carbonates similar to the trend presented by Roussel & Carliell-Marquet (2016). Nevertheless, dissolved metal fraction increases as concentration of phosphate and carbonate precipitates formed is very less. This causes inhibitory TM effects on anaerobic digestion followed by toxicity effects. Thus, anaerobic digestion performance and cumulative methane production decrease for $Fe/HS^- > 1$. Roussel & Carliell-Marquet (2016) reported precipitation of iron as pyrite until sulphide became limiting factor after which Fe precipitated as vivianite. They also observed complete precipitation of iron as vivianite in the absence of sulphide.

The model can be applied to study other effects like trace metal dosing under sub-optimal, optimal and starvation conditions, effects of pH on metal solubility, phosphate and carbonate influence on metal speciation etc. The improved physiochemical framework presented in this study can be extended to include other processes like TM adsorption and complexation reactions with chelates like EDTA to further define metal speciation in anaerobic digestion. The proposed model needs to be calibrated and this demands ad hoc experiments to be performed.

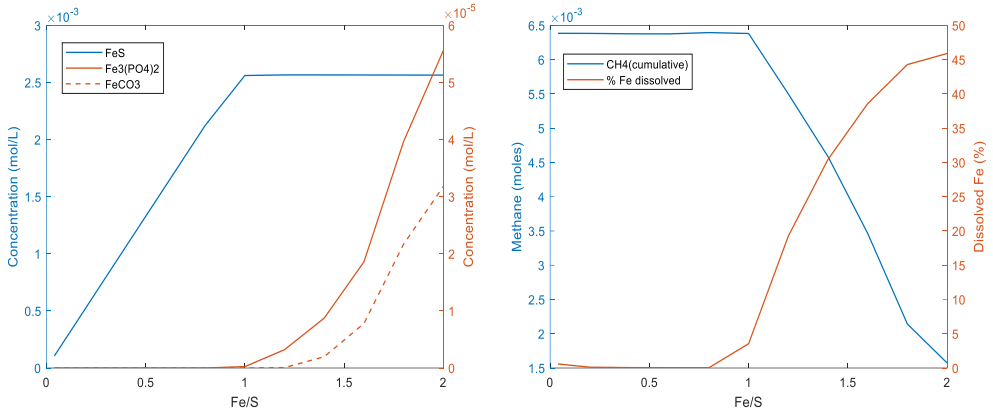

Figure 2.6 - Effect of initial Fe/S ratio on Fe speciation and cumulative methane production

2.4. CONCLUSIONS

A mathematical model to define trace metal speciation during anaerobic digestion as affected by ionic strength has been presented. Since bioavailability of a trace metal and its effects on AD relies on accurate description of metal speciation, effect of non-ideal aqueous phase chemistry (ionic strength correction and ion pairing) in modelling trace metal dynamics has been studied. The work discusses three different model approaches to define aqueous phase chemistry in anaerobic digestors and demonstrated the significance of including ion activity corrections and ion pairing in modelling TM speciation effects. Defining non-ideal aqueous phase chemistry has been found to influence trace metal effects on anaerobic digestion performance and methane production by changing the total dissolved and labile metal fraction. Increase in ionic strength and ion pairing leads to decrease in precipitation and increase in labile metal fraction resulting in improved methane production. Hence, it is highly recommended to consider physicochemical framework for non-ideal aqueous phase chemistry in modelling trace metal effects in AD.

2.5. REFERENCES

Barat, R., Montoya, T., Seco, A., & Ferrer, J. (2011). Modelling biological and chemically induced precipitation of calcium phosphate in enhanced biological phosphorus removal systems. *Water Research*, *45*(12), 3744–3752. https://doi.org/10.1016/J.WATRES.2011.04.028

Bartacek, J., Fermoso, F. G., Baldó-Urrutia, A. M., van Hullebusch, E. D., & Lens, P. N. L. (2008). Cobalt toxicity in anaerobic granular sludge: Influence of chemical speciation. *Journal of Industrial Microbiology and Biotechnology*, *35*(11), 1465–1474. https://doi.org/10.1007/s10295-008-0448-0

Batstone, D. J., Amerlinck, Y., Ekama, G., Goel, R., Grau, P., Johnson, B., Kaya, I., Steyer, J. P., Tait, S., Takaćs, I., Vanrolleghem, P. A., Brouckaert, C. J., & Volcke, E. (2012). Towards a generalized physicochemical framework. In *Water Science and Technology* (Vol. 66, Issue 6, pp. 1147–1161). https://doi.org/10.2166/wst.2012.300

Batstone, D. J., Keller, J., Angelidaki, I., Kalyuzhnyi, S. v., Pavlostathis, S. G., Rozzi, A., Sanders, W. T., Siegrist, H., & Vavilin, V. A. (2002). The IWA Anaerobic Digestion Model No 1 (ADM1). *Water Science and Technology*, *45*(10), 65–73. https://doi.org/10.2166/WST.2002.0292

Bi, S., Westerholm, M., Qiao, W., Mahdy, A., Xiong, L., Yin, D., Fan, R., Dach, J., & Dong, R. (2019). Enhanced methanogenic performance and metabolic pathway of high solid anaerobic digestion of chicken manure by Fe2+ and Ni2+ supplementation. *Waste Management*, *94*, 10–17. https://doi.org/10.1016/j.wasman.2019.05.036

Callander, I. J., & Barford, J. P. (1983). Precipitation, chelation, and the availability of metals as nutrients in anaerobic digestion. I. Methodology. *Biotechnology and Bioengineering*, *25*(8), 1947–1957. https://doi.org/10.1002/BIT.260250805

Choong, Y. Y., Norli, I., Abdullah, A. Z., & Yhaya, M. F. (2016). Impacts of trace element supplementation on the performance of anaerobic digestion process: A critical review. In *Bioresource Technology* (Vol. 209, pp. 369–379). Elsevier Ltd. https://doi.org/10.1016/j.biortech.2016.03.028

Feng, X. M., Karlsson, A., Svensson, B. H., & Bertilsson, S. (2010). Impact of trace element addition on biogas production from food industrial waste - Linking process to microbial communities. *FEMS Microbiology Ecology*, *74*(1), 226–240. https://doi.org/10.1111/j.1574-6941.2010.00932.x

Fermoso, F. G., Collins, G., Bartacek, J., O'Flaherty, V., & Lens, P. (2008). Acidification of methanol-fed anaerobic granular sludge bioreactors by cobalt deprivation: Induction and microbial community dynamics. *Biotechnology and Bioengineering*, *99*(1), 49–58. https://doi.org/10.1002/bit.21528

Flores-Alsina, X., Solon, K., Kazadi Mbamba, C., Tait, S., Gernaey, K. v., Jeppsson, U., & Batstone, D. J. (2016). Modelling phosphorus (P), sulfur (S) and iron (Fe) interactions for dynamic simulations of anaerobic digestion processes. *Water Research*, *95*, 370–382. https://doi.org/10.1016/j.watres.2016.03.012

Frunzo, L., Fermoso, F. G., Luongo, V., Mattei, M. R., & Esposito, G. (2019). ADM1-based mechanistic model for the role of trace elements in anaerobic digestion processes. *Journal of Environmental Management*, *241*, 587–602. https://doi.org/10.1016/j.jenvman.2018.11.058

Gustafsson, J. P. (2018). *Visual MINTEQ – Visual MINTEQ – a free equilibrium speciation model*. https://vminteq.lwr.kth.se/

Hauduc, H., Takács, I., Smith, S., Szabo, A., Murthy, S., Daigger, G. T., & Spérandio, M. (2015). A dynamic physicochemical model for chemical phosphorus removal. *Water Research*, *73*, 157–170. https://doi.org/10.1016/J.WATRES.2014.12.053

Huber, P., Neyret, C., & Fourest, E. (2017). *Implementation of the anaerobic digestion model (ADM1) in the PHREEQC chemistry engine*. https://doi.org/10.2166/wst.2017.282

Kazadi Mbamba, C., Lindblom, E., Flores-Alsina, X., Tait, S., Anderson, S., Saagi, R., Batstone, D. J., Gernaey, K. v., & Jeppsson, U. (2019). Plant-wide model-based analysis of iron dosage strategies for chemical phosphorus removal in wastewater treatment systems. *Water Research*, *155*, 12–25. https://doi.org/10.1016/J.WATRES.2019.01.048

Kazadi Mbamba, C., Tait, S., Flores-Alsina, X., & Batstone, D. J. (2015). A systematic study of multiple minerals precipitation modelling in wastewater treatment. *Water Research*, *85*, 359–370. https://doi.org/10.1016/j.watres.2015.08.041

Koutsoukos, P., Amjad, Z., Tomson, B., & Nancollas, G. H. (1980). Crystallization of Calcium Phosphates. A Constant Composition Study. *Journal of the American Chemical Society*, *102*(5), 1553–1557. https://doi.org/10.1021/JA00525A015

Liu, Y., Zhang, Y., & Ni, B. J. (2015). Evaluating enhanced sulfate reduction and optimized volatile fatty acids (VFA) composition in anaerobic reactor by Fe (III) addition. *Environmental Science & Technology*, *49*(4), 2123–2131. https://doi.org/10.1021/ES504200J

Lizarralde, I., Fernández-Arévalo, T., Brouckaert, C., Vanrolleghem, P., Ikumi, D. S., Ekama, G. A., Ayesa, E., & Grau, P. (2015). A new general methodology for incorporating physico-chemical transformations into multi-phase wastewater treatment process models. *Water Research*, *74*, 239–256. https://doi.org/10.1016/J.WATRES.2015.01.031

Maharaj, B. C., Mattei, M. R., Frunzo, L., Hullebusch, E. D. van, & Esposito, G. (2019). ADM1 based mathematical model of trace element complexation in anaerobic digestion processes. *Bioresource Technology*, *276*, 253–259. https://doi.org/10.1016/j.biortech.2018.12.064

Maharaj, B. C., Mattei, M. R., Frunzo, L., van Hullebusch, E. D., & Esposito, G. (2018). ADM1 based mathematical model of trace element precipitation/dissolution in anaerobic digestion processes. *Bioresource Technology*, *267*, 666–676. https://doi.org/10.1016/j.biortech.2018.06.099

Maharaj, B. C., Mattei, M. R., Frunzo, L., van Hullebusch, E. D., & Esposito, G. (2021). A general framework to model the fate of trace elements in anaerobic digestion environments. *Scientific Reports*, *11*(1). https://doi.org/10.1038/s41598-021-85403-2

Musvoto, E. v., Wentzel, M. C., Loewenthal, R. E., & Ekama, G. A. (2000). Integrated chemical-physical processes modelling - I. Development of a kinetic-based model for mixed weak acid/base systems. *Water Research*, *34*(6), 1857–1867. https://doi.org/10.1016/S0043-1354(99)00334-6

Pastor-Poquet, V., Papirio, S., Steyer, J. P., Trably, E., Escudié, R., & Esposito, G. (2019). Modelling non-ideal bio-physical-chemical effects on high-solids anaerobic digestion of the organic fraction of municipal solid waste. *Journal of Environmental Management*, *238*, 408–419. https://doi.org/10.1016/J.JENVMAN.2019.03.014

Patón, M., González-Cabaleiro, R., & Rodríguez, J. (2018). *Activity corrections are required for accurate anaerobic digestion modelling*. https://doi.org/10.2166/wst.2018.119

Reis, M. C. (2021). *Ion activity models: the Debye-Hückel equation and its extensions*. *7*, 9. https://doi.org/10.1007/s40828-020-00130-x

Roussel, J., & Carliell-Marquet, C. (2016). Significance of vivianite precipitation on the mobility of iron in anaerobically digested sludge. *Frontiers in Environmental Science*, *4*(SEP), 60. https://doi.org/10.3389/FENVS.2016.00060/BIBTEX

Shakeri Yekta, S., Lindmark, A., Skyllberg, U., Danielsson, Å., & Svensson, B. H. (2014). Importance of reduced sulfur for the equilibrium chemistry and kinetics of Fe(II), Co(II) and Ni(II) supplemented to semi-continuous stirred tank biogas reactors fed with stillage. *Journal of Hazardous Materials*, *269*, 83–88. https://doi.org/10.1016/J.JHAZMAT.2014.01.051

Solon, K., Flores-Alsina, X., Mbamba, C. K., Volcke, E. I. P., Tait, S., Batstone, D., Gernaey, K. v., & Jeppsson, U. (2015). Effects of ionic strength and ion pairing on (plant-wide) modelling of anaerobic digestion. *Water Research*, *70*, 235–245. https://doi.org/10.1016/j.watres.2014.11.035

Stumm, W., & Morgan, J. J. (1996). *Aquatic chemistry : chemical equilibria and rates in natural waters* (3rd ed.). Wiley.

Tait, S., Clarke, W. P., Keller, J., & Batstone, D. J. (2009). Removal of sulfate from high-strength wastewater by crystallisation. *Water Research*, *43*(3), 762–772. https://doi.org/10.1016/J.WATRES.2008.11.008

Tait, S., Solon, K., Volcke, E. I. P., & Batstone, D. J. (2012). A Unified Approach to Modelling Wastewater Chemistry: Model Corrections. *Procs. 3rd IWA/WEF Wastewater Treatment Modelling Seminar (WWTmod2012), Mont-St-Anne, Quebec, Feb 26–28 (2012)*. https://scholar.google.com/scholar_lookup?title=A%20unified%20approach%20to%20modelling%20wastewater%20chemistry%3A%20model%20corrections&publication_year=2012&author=S.%20Tait&author=K.%20Solon&author=E.I.P.%20Volcke&author=D.J.%20Batstone

Thanh, P. M., Ketheesan, B., Yan, Z., & Stuckey, D. (2016). Trace metal speciation and bioavailability in anaerobic digestion: A review. In *Biotechnology Advances* (Vol. 34, Issue 2, pp. 122–136). Elsevier Inc. https://doi.org/10.1016/j.biotechadv.2015.12.006

Thanh, P. M., Ketheesan, B., Yan, Z., & Stuckey, D. (2017). Effect of Ethylenediamine-N,N′-disuccinic acid (EDDS) on the speciation and bioavailability of Fe2+ in the presence of sulfide in anaerobic digestion. *Bioresource Technology*, *229*, 169–179. https://doi.org/10.1016/J.BIORTECH.2016.12.113

van der Veen, A., Fermoso, F. G., & Lens, P. N. L. (2007). Bonding Form Analysis of Metals and Sulfur Fractionation in Methanol-Grown Anaerobic Granular Sludge. *Engineering in Life Sciences*, *7*(5), 480–489. https://doi.org/10.1002/ELSC.200720208

Wu, Q., Zou, D., Zheng, X., Liu, F., Li, L., & Xiao, Z. (2022). Effects of antibiotics on anaerobic digestion of sewage sludge: Performance of anaerobic digestion and structure of the microbial community. *Science of The Total Environment*, 845, 157384. https://doi.org/10.1016/J.SCITOTENV.2022.157384

Zhang, W., Zhang, L., & Li, A. (2015). Enhanced anaerobic digestion of food waste by trace metal elements supplementation and reduced metals dosage by green chelating agent [S, S]-EDDS via improving metals bioavailability. *Water Research*, *84*, 266–277. https://doi.org/10.1016/J.WATRES.2015.07.010

Zhang, Y., Piccard, S., & Zhou, W. (2015). Improved ADM1 model for anaerobic digestion process considering physico-chemical reactions. *Bioresource Technology*, *196*, 279–289. https://doi.org/10.1016/j.biortech.2015.07.065

Zheng, X., Zou, D., Wu, Q., Wang, H., Li, S., Liu, F., & Xiao, Z. (2022). Review on fate and bioavailability of heavy metals during anaerobic digestion and composting of animal manure. *Waste Management*, 150, 75-89. https://doi.org/10.1016/j.wasman.2022.06.033

APPENDIX 2.1

Table 2A.1- Stoichiometry matrix for soluble components in biochemical processes

Component →	1	2	3	4	5	6
Process ↓	**S_{su}**	**S_{aa}**	**S_{fa}**	**S_{va}**	**S_{bu}**	**S_{pro}**
1 Disintegration						
2 Hydrolysis of carbohydrates	1					
3 Hydrolysis of proteins		1				
4 Hydrolysis of lipids	$1 - f_{fa,li}$		$f_{fa,li}$			
5 Uptake of sugars	-1				$(1 - Y_{su})f_{bu,su}$	$(1 - Y_{su})f_{pro,su}$
6 Uptake of amino acids		-1		$(1 - Y_{aa})f_{va,aa}$	$(1 - Y_{aa})f_{bu,aa}$	$(1 - Y_{aa})f_{pro,aa}$
7 Uptake of LCFA			-1			
8 Uptake of Valerate				-1		$(1 - Y_{c4})0.54$
9 Uptake of Butyrate					-1	
10 Uptake of propionate						-1
11 Uptake of acetate						
12 Uptake of Hydrogen						
13 Decay of X_{su}						
14 Decay of X_{aa}						
15 Decay of X_{fa}						
16 Decay of X_{c4}						
17 Decay of X_{pro}						
18 Decay of X_{ac}						
19 Decay of X_{H2}						

	Monosaccharides (kgCOD m^{-3})	Amino acids (kgCOD m^{-3})	LCFA (kgCOD m^{-3})	Total valerate (kgCOD m^{-3})	Total butyrate (kgCOD m^{-3})	Total propionate (kgCOD m^{-3})

Table 2A.1 *(Continued)*

Component → / Process ↓		7 S_{ac}	8 S_{H2}	9 S_{CH4}	10 S_{IC}	11 S_{IN}
1	Disintegration					
2	Hydrolysis of carbohydrates					
3	Hydrolysis of proteins					
4	Hydrolysis of lipids					
5	Uptake of sugars	$(1-Y_{su})f_{ac,su}$	$(1-Y_{su})f_{H2,su}$		$-\sum_{i=1-9,11-29} C_l v_{i,5}$	$-(Y_{su})N_{bac}$
6	Uptake of amino acids	$(1-Y_{aa})f_{ac,aa}$	$(1-Y_{aa})f_{H2,aa}$		$-\sum_{i=1-9,11-29} C_l v_{i,5}$	$N_{aa}-(Y_{aa})N_{bac}$
7	Uptake of LCFA	$(1-Y_{fa})0.7$	$(1-Y_{fa})0.3$			$-(Y_{fa})N_{bac}$
8	Uptake of Valerate	$(1-Y_{c4})0.31$	$(1-Y_{c4})0.15$			$-(Y_{c4})N_{bac}$
9	Uptake of Butyrate	$(1-Y_{c4})0.8$	$(1-Y_{c4})0.2$			$-(Y_{c4})N_{bac}$
10	Uptake of propionate	$(1-Y_{pro})0.57$	$(1-Y_{pro})0.43$		$-\sum_{i=1-9,11-29} C_l v_{i,5}$	$-(Y_{pro})N_{bac}$
11	Uptake of acetate	-1		$(1-Y_{ac})$	$-\sum_{i=1-9,11-29} C_l v_{i,5}$	$-(Y_{ac})N_{bac}$
12	Uptake of Hydrogen		-1	$(1-Y_{h2})$	$-\sum_{i=1-9,11-29} C_l v_{i,5}$	$-(Y_{h2})N_{bac}$
13	Decay of X_{su}					
14	Decay of X_{aa}					
15	Decay of X_{fa}					
16	Decay of X_{c4}					
17	Decay of X_{pro}					
18	Decay of X_{ac}					
19	Decay of X_{H2}					
		Total acetate (kgCOD m^{-3})	Hydrogen (kgCOD m^{-3})	Methane (kgCOD m^{-3})	Inorganic carbon (kmole m^{-3})	Inorganic nitrogen (kmole m^{-3})

Table 2A.1 *(Continued)*

	Component →	12	13	14	15	16	17
	Process ↓	**S_I**	**S_{Ni2+}**	**S_{Co2+}**	**S_{Fe2+}**	**S_{IP}**	**S_{IS}**
1	Disintegration	$f_{sI,xc}$	$f_{Ni,xc}$	$f_{Co,xc}$	$f_{Fe,xc}$	$f_{P,xc}$	$f_{S,xc}$
2	Hydrolysis of carbohydrates						
3	Hydrolysis of proteins						
4	Hydrolysis of lipids						
5	Uptake of sugars						
6	Uptake of amino acids						
7	Uptake of LCFA						
8	Uptake of Valerate						
9	Uptake of Butyrate						
10	Uptake of propionate						
11	Uptake of acetate		$-(Y_{ac})Ni_{ac}$	$-(Y_{ac})Co_{ac}$	$-(Y_{ac})Fe_{ac}$		
12	Uptake of Hydrogen		$-(Y_{h2})Ni_{h2}$	$-(Y_{h2})Co_{h2}$	$-(Y_{h2})Fe_{h2}$		
13	Decay of X_{su}						
14	Decay of X_{aa}						
15	Decay of X_{fa}						
16	Decay of X_{c4}						
17	Decay of X_{pro}						
18	Decay of X_{ac}						
19	Decay of X_{H2}						
		Soluble Inerts (kgCOD m^{-3})	Total dissolved Nickel (kmole m^{-3})	Total dissolved Cobalt (kmole m^{-3})	Total dissolved Iron (kmole m^{-3})	Inorganic Phosphorous (kmole m^{-3})	Inorganic Sulfur (kmole m^{-3})

Table 2A.2 - Stoichiometry of particulate components and kinetic rate equations for biochemical processes

Component →		18	19	20	21	22	23	24	25
Process ↓		**X_c**	**X_{ch}**	**X_{pr}**	**X_{li}**	**X_{su}**	**X_{aa}**	**X_{fa}**	**X_{c4}**
1	Disintegration	-1	$f_{ch,xc}$	$f_{pr,xc}$	$f_{li,xc}$				
2	Hydrolysis of carbohydrates		-1						
3	Hydrolysis of proteins			-1					
4	Hydrolysis of lipids				-1				
5	Uptake of sugars					Y_{su}			
6	Uptake of amino acids						Y_{aa}		
7	Uptake of LCFA							Y_{fa}	
8	Uptake of Valerate								Y_{c4}
9	Uptake of Butyrate								Y_{c4}
10	Uptake of propionate								
11	Uptake of acetate								
12	Uptake of Hydrogen								
13	Decay of X_{su}	1				-1			
14	Decay of X_{aa}	1					-1		
15	Decay of X_{fa}	1						-1	
16	Decay of X_{c4}	1							-1
17	Decay of X_{pro}	1							
18	Decay of X_{ac}	1							
19	Decay of X_{H2}	1							

	Composites (kgCOD m^{-3})	Carbohydrates (kgCOD m^{-3})	Proteins (kgCOD m^{-3})	Lipids (kgCOD m^{-3})	Sugar degraders (kgCOD m^{-3})	A,mio acid degraders (kgCOD m^{-3})	LCFA degraders (kgCOD m^{-3})	Valerate and butyrate degraders (kgCOD m^{-3})

Table 2A.2 *(Continued)*

	Component →	26	27	28	29	**Kinetic rate**
	Process ↓	**X_{pro}**	**X_{ac}**	**X_{h2}**	**X_I**	**(ρ_{bio}, kg COD m^{-3} d^{-1})**
1	Disintegration				$f_{xI,xc}$	$k_{dis}.X_c$
2	Hydrolysis of carbohydrates					$k_{hyd,ch}.X_{ch}$
3	Hydrolysis of proteins					$k_{hyd,pr}.X_{pr}$
4	Hydrolysis of lipids					$k_{hyd,pr}.X_{li}$
5	Uptake of sugars					$k_{m,su} \cdot \frac{S_{su}}{K_s+S_{su}} \cdot X_{su} \cdot I_1$
6	Uptake of amino acids					$k_{m,aa} \cdot \frac{S_{aa}}{K_s+S_{aa}} \cdot X_{aa} \cdot I_1$
7	Uptake of LCFA					$k_{m,fa} \cdot \frac{S_{fa}}{K_s+S_{fa}} \cdot X_{fa} \cdot I_2$
8	Uptake of Valerate					$k_{m,c4} \cdot \frac{S_{va}}{K_{s,c4}+S_{va}} \cdot X_{c4} \cdot \frac{S_{va}}{S_{bu}+S_{va}} \cdot I_2$
9	Uptake of Butyrate					$k_{m,c4} \cdot \frac{S_{bu}}{K_{s,c4}+S_{bu}} \cdot X_{c4} \cdot \frac{S_{bu}}{S_{va}+S_{bu}} \cdot I_2$
10	Uptake of propionate	Y_{pro}				$k_{m,pro} \cdot \frac{S_{pro}}{K_{S,c4}+S_{pro}} \cdot X_{pro} \cdot I_2$
11	Uptake of acetate		Y_{ac}			$k_{m,ac} \cdot \frac{S_{ac}}{K_{S,ac}+S_{ac}} \cdot X_{ac} \cdot I_3$
12	Uptake of Hydrogen			Y_{h2}		$k_{m,H_2} \cdot \frac{S_{H_2}}{K_{S,H_2}+S_{H_2}} \cdot X_{H_2} \cdot I_1$
13	Decay of X_{su}					$k_{dec,X_{su}} \cdot X_{su}$
14	Decay of X_{aa}					$k_{dec,X_{aa}} \cdot X_{aa}$
15	Decay of X_{fa}					$k_{dec,X_{fa}} \cdot X_{fa}$
16	Decay of X_{c4}					$k_{dec,X_{c4}} \cdot X_{c4}$
17	Decay of X_{pro}	-1				$k_{dec,X_{pro}} \cdot X_{pro}$
18	Decay of X_{ac}		-1			$k_{dec,X_{ac}} \cdot X_{ac}$
19	Decay of X_{H2}			-1		$k_{dec,X_{H_2}} \cdot X_{H_2}$

Propionate degraders (kgCOD m^{-3})

Acetate degraders (kmole m^{-3})

Hydrogen degraders (kmole m^{-3})

Particulate Inerts (kgCOD m^{-3})

Inhibition factors:
$I_1 = I_{pH}\ I_{IN,lim}\ I_{Me}$
$I_2 = I_{pH}\ I_{IN,lim}\ I_{H2}\ I_{Me}$
$I_3 = I_{pH}\ I_{IN,lim}\ I_{NH3}\ I_{Me}$

Table 2A.3 - Stoichiometry and kinetic rate matrix for gas transfer processes

Component →	8	9	10	17	43	44	45	46	**Kinetic rate (ρ_T, kg COD m^{-3} d^{-1})**
Process ↓	S_{H2}	S_{CH4}	S_{IC}	S_{IS}	S_{H2} (gas)	S_{CH4} (gas)	S_{CO2} (gas)	S_{H2S} (gas)	
H_2 stripping	−1				1				$k_{La}(S_{H2} - 16\,K_{H,h2}P_{h2,gas})$
CH_4 stripping		−1				1			$k_{La}(S_{CH4} - 64\,K_{H,ch4}P_{ch4,gas})$
CO_2 stripping			−1				1		$k_{La}(S_{H2CO3} - K_{H,h2co3}\,P_{h2co3,gas})$
H_2S stripping				−1				1	$k_{La}(S_{H2S} - 64\,K_{H,h2s}P_{h2s,gas})$

Model Parameters

Model parameters for Biochemical and Gas transfer processes are obtained from IWA ADM1 model (Batstone et al., 2002) and Maharaj et al. (2018).

Additional parameters:
Henry's Law coefficient for H_2S ($K_{H,h2s}$) = 0.105 mol bar^{-1}
Gas-Liquid H_2S transfer coefficient = 40 d^{-1}
Dose response parameters in I_{Me} inhibition function

For Nickel, c1 = -551.155; c2 = 10.0024; c3 = 2020.015; c4 = 10.9415;
For Cobalt, c1 = -7.384; c2 = 1.066; c3 = 4.99; c4 = 1.30;
For Iron, c1 = 0.0033; c2 = 0.00000000057; c3 = 0.00316; c4 = 0.00000000104;

Model parameters for aqueous phase equilibrium model and precipitation/dissolution model are given in Table 2A.4 and Table 2A.6.

Aqueous phase equilibrium reactions

The model considers 96 aqueous phase reactions including ion pairing and acid base reactions. An example of law of mass action for the species $Ca(NH_3)_2^{2+}$ is given in Eq. (2A.1). Eq. (2A.2) gives an example 1M contribution balance for component Ca^{2+}

$$[Ca(NH_3)_2^{2+}] = (1/\gamma^4) \,.\, K_{Ca(NH3)2^{2+}} \,.\, \{Ca\} \,.\, (\{NH_4^+\}/\{H^+\})^2 \quad (2A.1)$$

$$Ca_{tot} = [Ca^{2+}] + [Ca(NH_3)_2^{2+}] + [Ca\text{-}Acetate^+] + [Ca\text{-}Butyrate^+] + [CaCO_3(aq)] + [CaH_2PO_4^+] + [CaHCO_3^+] + [CaHPO_4(aq)] + [CaNH_3^{2+}] + [CaOH^+] + [CaPO_4^-] + [Ca\text{-}Propionate^+] + [Ca\text{-}Propionate^+] + [Ca\text{-}Valerate^+] + [CaCl^+] \quad (2A.2)$$

Table 2A.4 - Model parameters and stoichiometry matrix of component-species in aqueous phase equilibrium model

Component → / **Species** ↓	**log K**	**delta Hr (kJ/mol)**	**$Acetate^{-1}$**	**$Butyrate^{-1}$**	**CO_3^{2-}**	**Ca^{2+}**	**Co^{2+}**	**H^+**	**NH_4^+**	**PO_4^{3-}**	**$Propionate^{-1}$**	**$Valerate^{-1}$**	**Cl^-**
$Ca(NH_3)_2^{2+}$	-18.59	0				1		-2	2				
$Ca\text{-}Acetate^+$	1.18	4	1			1							
$Ca\text{-}Butyrate^+$	0.94	3.3472		1		1							
$CaCO_3$ (aq)	3.22	16			1	1							
$CaH_2PO_4^+$	20.923	-6				1		2		1			
$CaHCO_3^+$	11.434	0			1	1		1					
$CaHPO_4$ (aq)	15.035	-3				1		1		1			
$CaNH_3^{2+}$	-9.04	0				1		-1	1				
$CaOH^+$	-12.697	64.11				1		-1					
$CaPO_4^-$	6.46	12.9704				1				1			
$Ca\text{-}Propionate^+$	0.93	3.3472				1					1		
$Ca\text{-}Valerate^+$	0.3	0				1						1	
$CaCl^+$	0.4	4				1							1
$Co\text{-}(Acetate)_2$ (aq)	0.7565	0	2				1						
$Co\text{-}(Butyrate)_2$ (aq)	0.7765	0		2			1						
$Co(NH_3)^{2+}$	-7.21	39					1	-1	1				
$Co(NH_3)_2^{2+}$	-14.99	0					1	-2	2				
$Co(NH_3)_3^{2+}$	-23.3	0					1	-3	3				
$Co(NH_3)_4^{2+}$	-31.91	0					1	-4	4				
$Co(NH_3)_5^{2+}$	-41.09	0					1	-5	5				

Table 2A.4 *(Continued)*

Component → / Species ↓	log K	delta Hr (kJ/mol)	$Acetate^{-1}$	$Butyrate^{-1}$	CO_3^{2-}	Co^{2+}	Fe^{2+}	H^+	HS^-	NH_4^+	PO_4^{3-}	$Propionate^{-1}$	Cl^-
$Co(OH)_2$ (aq)	-18.794	0				1		-2					
$Co(OH)_3^-$	-31.491	0				1		-3					
$Co_4(OH)_4^{4+}$	-30.488	0				4		-4					
Co-$Acetate^+$	1.38	0	1			1							
Co-$Butyrate^+$	0.591	0		1		1							
$CoCO_3$ (aq)	4.28	0			1	1							
$CoHCO_3^+$	12.22	0			1	1		1					
$CoHPO_4$ (aq)	15.43	0				1		1			1		
$CoHS^+$	5.2	0				1			1				
$CoOH^+$	-9.697	0				1		-1					
Co-$Propionate^+$	1.13	4.6				1						1	
$CoCl^+$	-0.35	2				1							1
$FeCl^+$	-0.2	0					1						1
$Fe(NH_3)_2^{2+}$	-16.24	89					1	-2		2			
$Fe(NH_3)_3^{2+}$	-25.05	133					1	-3		3			
$Fe(NH_3)_4^{2+}$	-34.23	177					1	-4		4			
$Fe(OH)_2$ (aq)	-20.494	119.62					1	-2					
$Fe(OH)^{3-}$	-30.991	126.43					1	-3					
Fe-$Acetate^+$	1.4	0	1				1						
$FeHCO_3^+$	11.429	0			1		1	1					
$FeHPO_4$ (aq)	15.975	0					1	1			1		
S^{2-}	-12.9	49.4						-1	1				

Table 2A.4 *(Continued)*

Component → / Species ↓	log K	delta Hr (kJ/mol)	Acetate^{-1}	Butyrate^{-1}	CO_3^{2-}	Fe^{2+}	H^+	HS^-	Mg^{2+}	NH_4^+	PO_4^{3-}	Propionate^{-1}	Valerate^{-1}
$FeHS^+$	5.62	0				1		1					
$FeNH_3^{2+}$	-7.84	44.1				1	-1			1			
$FeOH^+$	-9.397	55.81				1	-1						
$FeH_2PO_4^+$	22.273	0				1	2				1		
H_2CO_3* (aq)	16.681	-32			1		2						
$H_2PO_4^-$	19.573	-18					2				1		
H_2S (aq)	7.02	-22					1	1					
H_3PO_4	21.721	-10.5					3				1		
H-Acetate (aq)	4.757	0.41	1				1						
H-Butyrate (aq)	4.818	2.8		1			1						
HCO_3^-	10.329	-14.6			1		1						
HPO_4^{2-}	12.375	-15					1				1		
H-Propionate (aq)	4.874	0.75					1					1	
H-Valerate (aq)	4.843	2.8					1						1
$Mg(NH_3)_2^{2+}$	-18.29	99					-2		1	2			
$Mg_2CO_3^{2+}$	3.59	0			1				2				
Mg-Acetate$^+$	1.26	0	1						1				
Mg-Butyrate$^+$	0.96	0		1					1				
$MgCO_3$ (aq)	2.92	10			1				1				
$MgHCO_3^+$	11.34	-9.6			1		1		1		0		
$MgHPO_4$ (aq)	15.175	-3					1		1		1		
$MgOH^+$	-11.417	67.81					-1		1				
$MgPO_4^-$	4.654	12.9704							1		1		
Mg-Propionate$^+$	0.97	4.2677							1			1	
NH_3 (aq)	-9.244	52					-1			1			
OH^-	-13.997	55.81					-1						

Table 2A.4 *(Continued)*

Component → / Species ↓	log K	delta Hr (kJ/mol)	Acetate^{-1}	Butyrate^{-1}	CO_3^{2-}	H^+	HS^-	Mg^{2+}	NH_4^+	Ni^{2+}	PO_4^{3-}	Propionate^{-1}	Cl^-	K^+
$MgCl^+$	0.6	4						1					1	
Ni-$(Acetate)_2$ (aq)	2.4	10	2							1				
$Ni(NH_3)_2^{2+}$	-13.61	74				-2			2	1				
$Ni(NH_3)_3^{2+}$	-21.19	110				-3			3	1				
$Ni(NH_3)_4^{2+}$	-29.31	144				-4			4	1				
$Ni(NH_3)_5^{2+}$	-37.89	183.1				-5			5	1				
$Ni(NH_3)_6^{2+}$	-47.17	217.5				-6			6	1				
$Ni(OH)_2$ (aq)	-18.994	0				-2				1				
$Ni(OH)_3^-$	-29.991	0				-3				1				
Ni-$Acetate^+$	1.44	8.7	1							1				
Ni-$Butyrate^+$	0.691	0		1						1				
$NiCO_3$ (aq)	4.57	0			1					1				
$NiH_2PO_4^+$	20.5	0				2				1	1			
$NiHCO_3^+$	12.42	0			1	1				1				
$NiHPO_4$ (aq)	15.33	0				1				1	1			
$NiHS^+$	5.49	0					1			1				
$NiNH_3^{2+}$	-6.52	37				-1			1	1				
$NiOH^+$	-9.897	51.81				-1				1				
Ni-$Propionate^+$	1.19	4.6								1		1		
$NiCl^+$	-0.43	2								1			1	
K_2HPO_4	13.5	0				1					1			2
$K_2PO_4^-$	2.26	0									1			2
K-Acetate(aq)	-0.27	4	1											1
KCl(aq)	-0.3	-4												1
KH_2PO_4(aq)	19.873	0											1	1
$KHPO_4^-$	13.255	0				2					1			1
KOH(aq)	-13.757	55.81				1					1			1
KPO_4^{2-}	1.43	15				-1								1

Table 2A.5 - Stoichiometry matrix for precipitation/dissolution processes

Component →											30	31	32	33	34	35	36	37	38	39	40	41	42
(kmole m^{-3}) S: Activity of free Ion species ($S_{free} = S_{tot} - S\text{-}L$) X: Precipitates **Processes** ↓	S_{NH4}^{+}	S_{CO3}^{2-}	S_{PO4}^{3-}	S_{s}^{2-}	S_{Ca}^{2+}	S_{Mg}^{2+}	S_{Ni}^{2+}	S_{Co}^{2+}	S_{Fe}^{2+}		X_{CaCO3}	X_{MgCO3}	X_{NiCO3}	X_{CoCO3}	X_{FeCO3}	$X_{Ca3(PO4)2}$	$X_{Ni3(PO4)2}$	$X_{Co3(PO4)2}$	$X_{Fe3(PO4)2}$	X_{FeS}	X_{NiS}	X_{CoS}	$X_{MgNH4PO4}$
$CaCO_{3\,(s)}$ precipitation		−1			−1						1												
$CaCO_{3\,(s)}$ dissolution		1			1						-1												
$MgCO_{3(s)}$ precipitation		−1				−1						1											
$MgCO_{3(s)}$ dissolution		1				1						-1											
$NiCO_{3(s)}$ precipitation		−1					−1						1										
$NiCO_{3(s)}$ dissolution		1					1						-1										
$CoCO_{3(s)}$ precipitation		−1						−1						1									
$CoCO_{3(s)}$ dissolution		1						1						-1									
$FeCO_{3(s)}$ precipitation		−1							−1						1								
$FeCO_{3(s)}$ dissolution		1							1						-1								
$Ca_3(PO_4)_{2(s)}$ precipitation			$-2/3$		−1											1							
$Ca_3(PO_4)_{2(s)}$ dissolution			2/3		1											-1							
$Ni_3(PO_4)_{2\,(s)}$ precipitation			$-2/3$				−1										1						

Table 2A.5 *(Continued)*

Component →										30	31	32	33	34	35	36	37	38	39	40	41	42
(kmole m^{-3}) S: Activity of free Ion species ($S_{free} = S_{tot} - S\text{-}L$) X: Precipitates **Processes** ↓	S_{NH4}^{+}	S_{CO3}^{2-}	S_{PO4}^{3-}	S_s^{2-}	S_{Ca}^{2+}	S_{Mg}^{2+}	S_{Ni}^{2+}	S_{Co}^{2+}	S_{Fe}^{2+}	X_{CaCO3}	X_{MgCO3}	X_{NiCO3}	X_{CoCO3}	X_{FeCO3}	$X_{Ca3(PO4)2}$	$X_{Ni3(PO4)2}$	$X_{Co3(PO4)2}$	$X_{Fe3(PO4)2}$	X_{FeS}	X_{NiS}	X_{CoS}	$X_{MgNH4PO4}$
$Ni_3(PO_4)_2$ (s) dissolution			2/3				1									-1							
$Co_3(PO_4)_2$ (s) precipitation			$-2/3$					−1									1						
$Co_3(PO_4)_2$ (s) dissolution			2/3					1									-1						
$Fe_3(PO_4)_{2(s)}$ precipitation			$-2/3$						−1									1					
$Fe_3(PO_4)_{2(s)}$ dissolution			2/3						1									-1					
FeS (s) precipitation				−1			−1												1				
FeS (s) dissolution				1			1												-1				
NiS (s) precipitation				−1				−1												1			
NiS (s) dissolution				1				1												-1			
CoS (s) precipitation				−1					−1												1		
CoS (s) dissolution				1					1												-1		
$MgNH_4PO_{4(S)}$ precipitation	−1		−1			−1																	1
$MgNH_4PO_{4(S)}$ dissolution	1		1			1																	-1

Table 2A.6 - Kinetic rate equations and model parameters for precipitation/dissolution processes

Process	log K_{sp}	delta Hr (kJ/mol)	k'_r	Kinetic rate ($\rho_{prec/diss}$, kmol m^{-3} d^{-1})
$CaCO_{3\,(s)}$ precipitation	-8.48	-8	10^7	$k'_{r,CaCO_3}\left[\left(S_{Ca^{2+}}S_{CO_3^{2-}}\right)^{1/2} - K_{sp,CaCO_3}{}^{1/2}\right]^2 \frac{1+sin(SI_{CaCO_3})}{2}$
$CaCO_{3\,(s)}$ dissolution	-8.48	-8	10^7	$k'_{r,CaCO_3}\frac{1}{1+(K/X_{CaCO_3})}\left[\left(S_{Ca^{2+}}S_{CO_3^{2-}}\right)^{1/2} - K_{sp,CaCO_3}{}^{1/2}\right]^2 \frac{1-sin(SI_{CaCO_3})}{2}$
$MgCO_{3(s)}$ precipitation	-7.46	-20	10^5	$k'_{r,MgCO_3}\left[\left(S_{Mg^{2+}}S_{CO_3^{2-}}\right)^{1/2} - K'_{sp,MgCO_3}{}^{1/2}\right]^2 \frac{1+sin(SI_{MgCO_3})}{2}$
$MgCO_{3(s)}$ dissolution	-7.46	-20	10^5	$k'_{r,MgCO_3}\frac{1}{1+(K/X_{MgCO_3})}\left[\left(S_{Mg^{2+}}S_{CO_3^{2-}}\right)^{1/2} - K_{sp,MgCO_3}{}^{1/2}\right]^2 \frac{1-sin(SI_{MgCO_3})}{2}$
$NiCO_{3(s)}$ precipitation	-11.2	-41.589	10^3	$k'_{r,NiCO_3}\left[\left(S_{Ni^{2+}}S_{CO_3^{2-}}\right)^{1/2} - K'_{sp,NiCO_3}{}^{1/2}\right]^2 \frac{1+sin(SI_{NiCO_3})}{2}$
$NiCO_{3(s)}$ dissolution	-11.2	-41.589	10^3	$k'_{r,NiCO_3}\frac{1}{1+(K/X_{NiCO_3})}\left[\left(S_{Ni^{2+}}S_{CO_3^{2-}}\right)^{1/2} - K_{sp,NiCO_3}{}^{1/2}\right]^2 \frac{1-sin(SI_{NiCO_3})}{2}$
$CoCO_{3(s)}$ precipitation	-11.2	-12.7612	10^3	$k'_{r,CoCO_3}\left[\left(S_{Co^{2+}}S_{CO_3^{2-}}\right)^{1/2} - K'_{sp,CoCO_3}{}^{1/2}\right]^2 \frac{1+sin(SI_{CoCO_3})}{2}$
$CoCO_{3(s)}$ dissolution	-11.2	-12.7612	10^3	$k'_{r,CoCO_3}\frac{1}{1+(K/X_{CoCO_3})}\left[\left(S_{Co^{2+}}S_{CO_3^{2-}}\right)^{1/2} - K_{sp,CoCO_3}{}^{1/2}\right]^2 \frac{1-sin(SI_{CoCO_3})}{2}$

Table 2A.6 *(Continued)*

Process	log K_{sp}	delta Hr (kJ/mol)	k'_r	Kinetic rate ($\rho_{prec/diss}$, kmol m^{-3} d^{-1})
$FeCO_{3(s)}$ precipitation	-10.59	-7.3	10^3	$k'_{r,FeCO_3}\left[\left(S_{Fe^{2+}}S_{CO_3^{2-}}\right)^{1/2} - K'_{sp,FeCO_3}{}^{1/2}\right]^2 \frac{1+sin(SI_{FeCO_3})}{2}$
$FeCO_{3(s)}$ dissolution	-10.59	-7.3	10^3	$k'_{r,FeCO_3}\frac{1}{1+(K/X_{FeCO_3})}\left[\left(S_{Fe^{2+}}S_{CO_3^{2-}}\right)^{1/2} - K_{sp,FeCO_3}{}^{1/2}\right]^2 \frac{1-sin(SI_{FeCO_3})}{2}$
$Ca_3(PO_4)_{2(s)}$ precipitation	-28.4	54	10^8	$k'_{r,Ca_3(PO_4)_2}\left[S_{Ca^{2+}}{}^{3/5}S_{PO_4^{3-}}{}^{2/5} - K_{sp,Ca_3(PO_4)_2}{}^{1/5}\right]^2 \frac{1+sin(SI_{Ca_3(PO_4)_2})}{2}$
$Ca_3(PO_4)_{2(s)}$ dissolution	-28.4	54	10^8	$k'_{r,Ca_3(PO_4)_2}\frac{1}{1+(K/X_{Ca_3(PO_4)_2})}\left[S_{Ca^{2+}}{}^{3/5}S_{PO_4^{3-}}{}^{2/5} - K'_{sp,Ca_3(PO_4)_2}{}^{1/5}\right]^2 \frac{1-sin(SI_{Ca_3(PO_4)_2})}{2}$
$Ni_3(PO_4)_{2\ (s)}$ precipitation	-31	0	10^5	$k'_{r,Ni_3(PO_4)_2}\left[S_{Ni^{2+}}{}^{3/5}S_{PO_4^{3-}}{}^{2/5} - K_{sp,Ni_3(PO_4)_2}{}^{1/5}\right]^2 \frac{1+sin(SI_{Ni_3(PO_4)_2})}{2}$
$Ni_3(PO_4)_{2\ (s)}$ dissolution	-31	0	10^5	$k'_{r,Ni_3(PO_4)_2}\frac{1}{1+(K/X_{Ni(PO_4)_2})}\left[S_{Ni^{2+}}{}^{3/5}S_{PO_4^{3-}}{}^{2/5} - K_{sp,Ni_3(PO_4)_2}{}^{1/5}\right]^2 \frac{1-sin(SI_{Ni_3(PO_4)_2})}{2}$
$Co_3(PO_4)_{2\ (s)}$ precipitation	-34	0	10^5	$k'_{r,Co_3(PO_4)_2}\left[S_{Co^{2+}}{}^{3/5}S_{PO_4^{3-}}{}^{2/5} - K_{sp,Co_3(PO_4)_2}{}^{1/5}\right]^2 \frac{1+sin(SI_{Co_3(PO_4)_2})}{2}$
$Co_3(PO_4)_{2\ (s)}$ dissolution	-34	0	10^5	$k'_{r,Co_3(PO_4)_2}\frac{1}{1+(K/X_{Co_3(PO_4)_2})}\left[S_{Co^{2+}}{}^{3/5}S_{PO_4^{3-}}{}^{2/5} - K_{sp,Co_3(PO_4)_2}{}^{1/5}\right]^2 \frac{1-sin(SI_{Co_3(PO_4)_2})}{2}$
$Fe_3(PO_4)_{2(s)}$ precipitation	-37.76	0	10^5	$k'_{r,Fe_3(PO_4)_2}\left[S_{Fe^{2+}}{}^{3/5}S_{PO_4^{3-}}{}^{2/5} - K_{sp,Fe_3(PO_4)_2}{}^{1/5}\right]^2 \frac{1+sin(SI_{Fe_3(PO_4)_2})}{2}$

Table 2A.6 *(Continued)*

Process	log K_{sp}	delta Hr (kJ/mol)	k'_r	Kinetic rate ($\rho_{prec/diss}$, kmol m^{-3} d^{-1})
$Fe_3(PO_4)_{2(s)}$ dissolution	-37.76	0	10^5	$k'_{r,Fe_3(PO_4)_2} \frac{1}{1 + (K/X_{Fe_3(PO_4)_2})} \left[S_{Fe^{2+}}{}^{3/5} S_{PO_4^{3-}}{}^{2/5} - K_{sp,Fe_3(PO_4)_2}{}^{1/5} \right]^2 \frac{1 - sin(SI_{Fe_3(PO_4)_2})}{2}$
FeS (s) precipitation	-18	-11	10^{12}	$k'_{r,FeS} \left[(S_{Fe^{2+}} S_{S^{2-}})^{1/2} - K_{sp,FeS}{}^{1/2} \right]^2 \frac{1 + sin(SI_{FeS})}{2}$
FeS (s) dissolution	-18	-11	10^{12}	$k'_{r,FeS} \frac{1}{1 + (K/X_{FeS})} \left[(S_{Fe^{2+}} S_{S^{2-}})^{1/2} - K_{sp,FeS}{}^{1/2} \right]^2 \frac{1 - sin(SI_{FeS})}{2}$
NiS (s) precipitation	-20.7	0	10^{10}	$k'_{r,NiS} \left[(S_{Ni^{2+}} S_{S^{2-}})^{1/2} - K_{sp,NiS}{}^{1/2} \right]^2 \frac{1 + sin(SI_{NiS})}{2}$
NiS (s) dissolution	-20.7	0	10^{10}	$k'_{r,NiS} \frac{1}{1 + (K/X_{NiS})} \left[(S_{Ni^{2+}} S_{S^{2-}})^{1/2} - K_{sp,NiS}{}^{1/2} \right]^2 \frac{1 - sin(SI_{NiS})}{2}$
CoS (s) precipitation	-20.3	0	10^{10}	$k'_{r,CoS} \left[(S_{Co^{2+}} S_{S^{2-}})^{1/2} - K_{sp,CoS}{}^{1/2} \right]^2 \frac{1 + sin(SI_{CoS})}{2}$
CoS (s) dissolution	-20.3	0	10^{10}	$k'_{r,CoS} \frac{1}{1 + (K/X_{CoS})} \left[(S_{Co^{2+}} S_{S^{2-}})^{1/2} - K_{sp,CoS}{}^{1/2} \right]^2 \frac{1 - sin(SI_{CoS})}{2}$
$MgNH_4PO_{4(S)}$ precipitation	-13.26	-22.6	10^8	$k'_{r,MgNH_4PO_4} \left[(S_{Mg^{2+}} S_{NH_4^+} S_{PO_4^{3-}})^{1/3} - K_{sp,MgNH_4PO_4}{}^{1/3} \right]^3 \frac{1 + sin(SI_{MgNH_4PO_4})}{2}$
$MgNH_4PO_{4(S)}$ dissolution	-13.26	-22.6	10^8	$k'_{r,MgNH_4PO_4} \frac{1}{1 + (K/X_{MgNH_4PO_4})} \left[(S_{Mg^{2+}} S_{NH_4^+} S_{PO_4^{3-}})^{1/3} - K_{sp,MgNH_4PO_4}{}^{1/3} \right]^3 \frac{-1 + sin(SI_{MgNH_4PO_4})}{2}$

Table 2A.7 - Validation of physiochemical model results with Visual MINTEQ outputs

INPUT											I		pH		Precipitates	
NH_4^+	CO_3^{2-}	PO_4^{3-}	Ca^{2+}	Mg^{2+}	Co^{2+}	Ni^{2+}	Fe^{2+}	HS^-	$Cation^+$	$Anion^-$	Model	MINTEQ	Model	MINTEQ	Model	MINTEQ
0	0	0.05	$2.5*10^{-6}$	$2.5*10^{-5}$	$5*10^{-7}$	$5*10^{-4}$	0.05	0	0	0	0.01629	0.0163	3.494	3.495	$Fe_3(PO_4)_2$: 10^{-2}	$Fe_3(PO_4)_2$: 10^{-2}
0	0	0.05	$2.5*10^{-6}$	$2.5*10^{-5}$	$5*10^{-7}$	$5*10^{-4}$	0.05	0	0.1	0.2	0.2297	0.2297	1.625	1.621	Nil	Nil
0	0.05	0	0.02	0.0025	$5*10^{-7}$	$5*10^{-4}$	$5*10^{-4}$	0	0	0	0.0137	0.0136	5.57	5.622	$NiCO_3$: 10^{-4} $FeCO_3$: 10^{-4}	$NiCO_3$: 10^{-4} $FeCO_3$: 10^{-4}
0	0.05	0	0.02	0.0025	$5*10^{-7}$	$5*10^{-4}$	$5*10^{-4}$	0	0.1	0.2	0.2055	0.2055	1.180	1.181	Nil	Nil
0	0	0	$2.5*10^{-6}$	$2.5*10^{-6}$	$5*10^{-6}$	$5*10^{-6}$	$5*10^{-6}$	0.05	0	0	$2.7*10^{-4}$	$2.68*10^{-4}$	3.614	3.614	NiS: $5*10^{-6}$ CoS: $5*10^{-6}$	NiS: $5*10^{-6}$ CoS: $4.99*10^{-6}$
0	0	0	$2.5*10^{-6}$	$2.5*10^{-6}$	$5*10^{-6}$	$5*10^{-6}$	$5*10^{-6}$	0.05	0.1	0.2	0.2427	0.2427	2.275	2.269	NiS: $5*10^{-4}$ CoS: $4.64*10^{-7}$	NiS: $4.99*10^{-4}$ CoS: $4.43*10^{-7}$
0.1	0.02	0.006	0.002	0.0025	10^{-7}	10^{-5}	10^{-4}	0.001	0.1	0.2	0.2233	0.2234	6.17	6.250	NiS: 10^{-5} CoS: 10^{-7} $Fe_3(PO_4)_2$: 10^{-5}	NiS: 10^{-5} CoS: 10^{-7} $Fe_3(PO_4)_2$: 10^{-5}
0.12	0.02	0.006	0.002	0.0025	10^{-7}	10^{-5}	10^{-4}	0.001	0.1	0.2	0.2257	0.2263	6.662	6.779	$MgNH_4PO_4$: 10^{-3} $Ca_3(PO_4)_2$: 10^{-4} $Fe_3(PO_4)_2$: 10^{-5}	$MgNH_4PO_4$: 10^{-3} $Ca_3(PO_4)_2$: 10^{-4} $Fe_3(PO_4)_2$: 10^{-5}

Table 2A.8 - Operational and initial conditions considered for numerical simulations

Parameter	Variable	Value			Unit
		Scenario 1: Variable Ionic Strength	Scenario 2: Effect of iron dosing	Scenario 3: Variable Fe/S	
Digester volume	V_{liq}	0.75	0.75	0.75	m^3
Headspace volume	V_{gas}	0.25	0.25	0.25	m^3
Influent flow rate	q_{in}	0	0	0	$m^3\ d^{-1}$
Temperature	T	308.15	308.15	308.15	K
Monosaccharides	S_{su}	0	0	0	kgCOD m^{-3}
Amino acids	S_{aa}	0	0	0	kgCOD m^{-3}
Long chain fatty acids	S_{fa}	0	0	0	kgCOD m^{-3}
Total Valerate	S_{va}	0	0	0	kgCOD m^{-3}
Total Butyrate	S_{bu}	0	0	0	kgCOD m^{-3}
Total Propionate	S_{pro}	0	0	0	kgCOD m^{-3}
Total Acetate	S_{ac}	0	0	0	kgCOD m^{-3}
Hydrogen	S_{h2}	0	0	0	kgCOD m^{-3}
Methane	S_{ch4}	0	0	0	kgCOD m^{-3}
Inorganic carbon	S_{IC}	0.0025	0.0025	0.0025	kmole m^{-3}
Inorganic nitrogen	S_{IN}	0.001	0.001	0.001	kmole m^{-3}
Soluble inerts	S_I	0	0	0	kgCOD m^{-3}
Composites	X_c	1	1	1	kgCOD m^{-3}
Carbohydrates	X_{ch}	0	0	0	kgCOD m^{-3}
Proteins	X_{pr}	0	0	0	kgCOD m^{-3}
Lipids	X_{li}	0	0	0	kgCOD m^{-3}
Sugar degraders	X_{su}	0.012	0.012	0.012	kgCOD m^{-3}
Amino acid degraders	X_{aa}	0.012	0.012	0.012	kgCOD m^{-3}
LCFA degraders	X_{fa}	0.012	0.012	0.012	kgCOD m^{-3}
Valerate and butyrate degraders	X_{c4}	0.012	0.012	0.012	kgCOD m^{-3}
Propionate degraders	X_{pro}	0.012	0.012	0.012	kgCOD m^{-3}
Acetate degraders	X_{ac}	0.012	0.012	0.012	kgCOD m^{-3}
Hydrogen degraders	X_{h2}	0.012	0.012	0.012	kgCOD m^{-3}
Particulate inerts	X_I	0	0	0	kgCOD m^{-3}
Total dissolved Calcium	S_{Ca}	0.002	0.002	0.002	kmole m^{-3}
Total dissolved Magnesium	S_{Mg}	0.0025	0.0025	0.0025	kmole m^{-3}

Table 2A.8 *(Continued)*

Parameter	Variable	Value			Unit
		Scenario 1: Variable Ionic Strength	Scenario 2: Effect of iron dosing	Scenario 3: Variable Fe/S	
Total dissolved Nickel	S_{Ni}	0.000005	0.000005	0.000005	kmole m^{-3}
Total dissolved Cobalt	S_{Co}	0.000005	0.000005	0.000005	kmole m^{-3}
Total dissolved Iron	S_{Fe}	0.00001	0, 0.0001	0.0001- 0.0045	kmole m^{-3}
Inorganic phosphorous	S_{po4}	0.006	0.006	0.006	kmole m^{-3}
Inorganic sulphur	S_{hs}	0.0002	0.0002	0.0025	kmole m^{-3}
Potassium	S_K	0,0.1,0.2,0.3,0.4,0.55	0.2	0	kmole m^{-3}
Chlorine	S_{Cl}	0,0.1,0.2,0.3,0.4,0.55	0.2	0	kmole m^{-3}
Precipitates	X_{prec}	0	0	0	kmole m^{-3}
Gases	S_{gases}	0	0	0	kgCOD m^{-3}

CHAPTER 3

Extended ADM1 Model to Study Trace Metal Speciation and its Effects on Anaerobic Digestion

ABSTRACT: Trace metals (TM) are often added to anaerobic digestors (AD) to improve digestor performance and methane yield. Though numerous experimental studies are done to study TM effects, a model based on ADM1 will help plant operators in case of metal deprivation as there are analytical limitations in quantifying metal speciation which controls TM effects on AD. This study developed a complete dynamic model based on ADM1 with least and unavoidable model input information to study TM speciation and its influence on AD. In addition to the biochemical and gas stripping processes described in ADM1, the model introduced new physicochemical processes with effects of operational conditions like pH, temperature and ionic strength. The biogeochemical processes influencing TM speciation include microbial uptake, precipitation (sulphides, phosphates, carbonates), adsorption (onto biomass, soluble inerts and precipitates), inorganic complexation and organic complexation (with EDTA, VFAs, amino acids (AAs)). The model was tested under different scenarios: variable EDTA concentration and dosing form, variable substrate and variable ionic strength. Complexation of TMs with EDTA and AAs influences metal bioavailability and methane yield. Supplementing EDTA reduces TM dosing and dosing EDTA as metal-EDTA complex is more effective than supplementing metals and EDTA separately. TM-AA complexation depends on substrates as amino acid compounds vary with substrates. Ionic strength influences TM adsorption and precipitation processes and hence is an important operational parameter controlling the system like pH and temperature. The model has been compared to experimental data obtained from this study and has been successfully applied to predict cobalt deprivation in an anaerobic digestor.

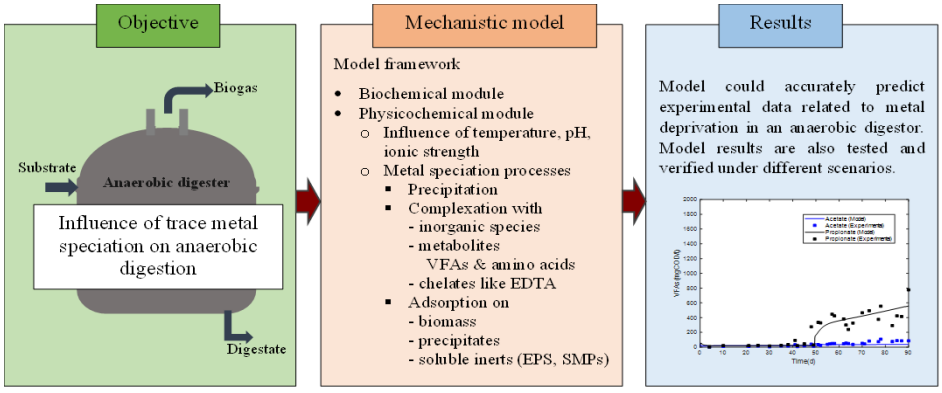

3.1. INTRODUCTION

Anaerobic digestion (AD) is the most economical and widely accepted technology considering its role in waste management and energy production at the same time. Supplementing trace metals (TMs) in anaerobic digesters fed with metal deprived substrates improves methane yield and the effects are linked to trace metal bioavailability for microorganisms involved in the digestion process. TM effects on microorganisms can be stimulatory, inhibitory or toxic. Hence, optimal concentration of labile metals in the media is significant (Fermoso et al., 2009). Speciation of trace metals like Co and Ni in anerobic media and its relation to bioavailability as well as biological effects has been reported (Jansen et al., 2005, 2007). Metal bioavailability and speciation are driven by operational conditions like hydraulic retention time, redox potential, pH (Thanh et al., 2016) and is influenced by thermodynamics and kinetics of chemical processes.

Most model approaches to study speciation of TMs in biogas reactors are thermodynamic equilibrium studies where speciation is modelled based on equilibrium constants and dynamics of biogeochemical processes are neglected (Aquino & Stuckey, 2007; Shakeri Yekta et al., 2014). A few kinetic model studies based on Anerobic Digestion Model 1 (ADM1) have been recently published (Frunzo et al., 2019; Maharaj et al., 2018, 2019, 2021). A general framework for trace metal speciation model in AD was proposed by Maharaj et al. (2021). However, these studies lack consideration of ionic strength effects on metal speciation. Moreover, the models neglected speciation of metals influenced by aqueous phase equilibrium. Since complexation of TMs with ligands in aqueous media reduces free metal concentration and metal speciation processes like precipitation depends on concentration of free metals, modelling trace metal speciation without modelling aqueous phase is not accurate. Recently, George et al. (2023) demonstrated the significance of considering ionic strength and ion pairing in dynamic modeling of precipitation of trace metals in AD. The model considered TM speciation being influenced by following processes: microbial uptake, precipitation, aqueous complexation by inorganic ligands and organic ligands like acetate, butyrate, valerate and propionate (volatile fatty acids, VFAs). However, trace metal effects on AD are also influenced by other chemical processes including adsorption and organic complexation with chelates like amino acids (AAs) and ethyleneaminetetraacetic acid (EDTA).

Amino acids and chelates like nitrilotriacetic acid (NTA), EDTA and ethylenediamine-N,N′-disuccinic acid (EDDS) form strong organic complexes with TMs. Gonzalez-Gil et al., (2003) reported increase in metal bioavailability due to production of soluble complexes of Ni and Co with amino acids in yeast extract. Metal concentrations can be maintained at levels below solubility products of metal precipitates if metal chelate complexes have higher stability constants (Callander & Barford, 1983). Synthetic chelating agents like EDTA (Bartacek et al., 2012; Cai et al., 2019; Vintiloiu et al., 2013; Zhong et al., 2019), NTA (Hu et al., 2008; Tsapekos et al., 2018) and EDDS (Thanh et al., 2017a,b; Zhang et al., 2015) are often

supplemented to biogas reactors to increase metal bioavailability. Zhang et al. (2021) reported an increase in formation of methane when nickel was supplemented as chelator-Ni (23.34% for EDDS-Ni, 31.26% for NTA-Ni and 16.07% for EDTA-Ni) instead of supplementation in Ni (II) form. According to Shakeri Yekta et al. (2014), inclusion of TM complexation with thiols represented by amino acid (cysteine) improved thermodynamic model predictions.

Adsorption of TMs is due surface functional groups like carboxyl, phosphate and hydroxyl groups present on surfaces of cell walls of biomass, microbial products and mineral precipitates like FeS (Stumm & Morgan, 1996; van Hullebusch et al., 2016). Microbial products generated by active biomass include mobile biogenic ligand sources like soluble microbial products (SMPs) and solid complexing ligands like extracellular polymeric substances (EPS) and inert (non-active/dead) biomass (Schwarz et al., 2007). Schwarz et al. (2007) developed a comprehensive biogeochemical framework with expanded sub models for adsorption to model metal speciation in sulfidic microbial systems. Adsorption process defined in previous TM speciation ADM1 models did not consider influence of functional groups and hence pH and ionic strength effects on adsorption were neglected.

No studies are reported so far to kinetically model all processes influencing trace metal speciation in AD, considering effects of operational conditions - pH, temperature and ionic strength. This paper aims to extend the ADM1 model framework to study TM effects on AD by defining physicochemical processes - precipitation (as sulphides, phosphates, carbonates), adsorption (on biomass, microbial products and precipitates), inorganic complexation and organic complexation with EDTA, VFAs, AAs. The study focuses (1) to develop a complete model framework for TM speciation in ADM1 that can be easily implemented with model input information adequately easy to be acquired by plant operators, (2) to model influence of trace metal adsorption and complexation with EDTA and amino acids, (3) to show effects of ionic strength on modelling adsorption and precipitation of TMs in AD and (4) to check model capability for predicting Co deprivation in an anaerobic digestor using experimental data generated from this study.

3.2. METHODOLOGY

3.2.1. Mathematical Model

ADM1 is extended to include effect of trace metals (Fe^{2+}, Ni^{2+}, Co^{2+}) on AD by modifying physicochemical and biochemical modules. Fe (II) is modelled instead of Fe (III) as iron is reported to be existing as Fe (II) in AD systems (Shakeri Yekta et al., 2014). Fig. 3.1 shows a schematic representation of processes defined in the developed model. Extensions made in biochemical module are according to Chapter 2. Bioavailable/labile metal fraction defined in the studies for the trace metal dose response function in biochemical module is revised to include dissolved metal and metal adsorbed on biomass and soluble inerts as depicted in Fig. 3.1. Modified physicochemical framework consists of: (1) kinetic precipitation model, (2) aqueous phase equilibrium model for inorganic complexation and organic complexation with

metabolites - VFAs and AAs, (3) kinetic model for EDTA complexation and (4) kinetic adsorption model. Precipitation processes are expressed as reversible reactions using saturation index as the driving force. Aqueous phase equilibrium model estimates pH, ionic strength and ion speciation by representing ion complexation reactions in terms of ion activities instead of concentrations. Further detailed description on modeling TM precipitation and non-ideal aqueous phase equilibrium can be found in Chapter 2. In addition to 13 precipitation reactions and 96 aqueous phase reactions presented in second chapter of the thesis (Appendix 2.1), the physicochemical framework in the modified model includes 34 TM complexation reactions with amino acids, 14 metal-EDTA complexation reactions and 23 TM adsorption reactions.

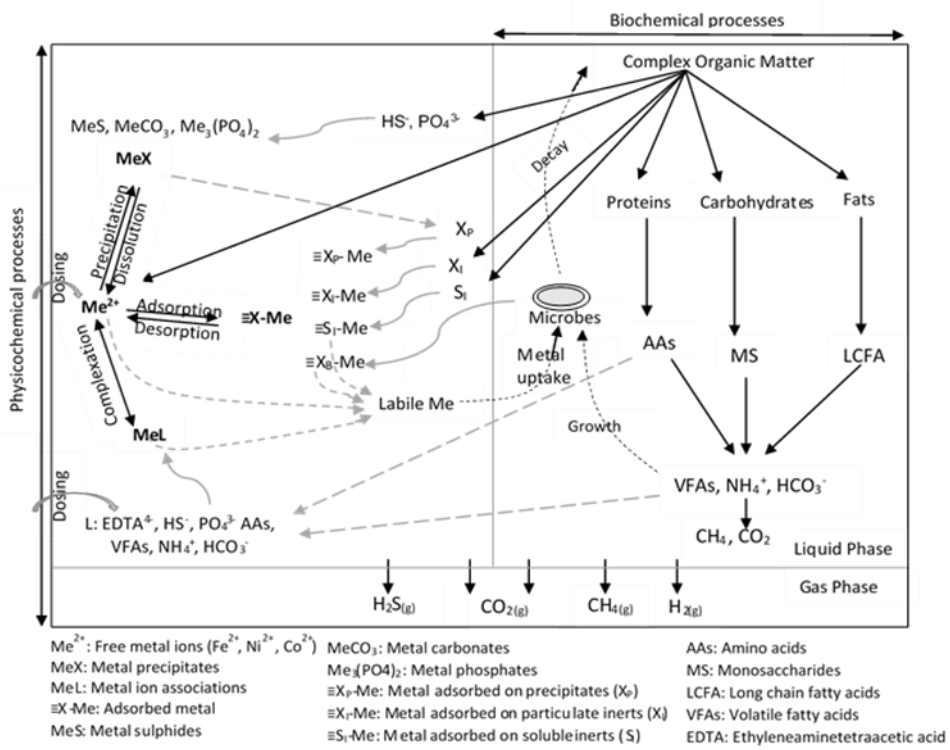

Figure 3.1- Schematic representation of extended ADM1 model to include TM effects

3.2.1.1. Organic complexation with amino acids

34 TM complexation reactions with three major amino acids identified in anaerobic digestors (Cysteine, Glutamate, Glycine) are incorporated to the aqueous phase equilibrium module. Total amino acid produced during biochemical reactions in AD is represented in form of the three compounds using percentage fractions of the compounds present in different substrates. Amino acid complexation reactions along with their stability constants and percentages of amino acid compounds are given in Appendix 3.1.

3.2.1.2. Organic complexation with EDTA

Willett & Rittmann (2003) observed differences in model predictions with equilibrium and kinetic approaches for modelling TM-EDTA complexation because of slow kinetics for dissociation of such complexes. Hence, unlike complexation of TMs with other compounds, EDTA complexation is modelled as kinetic reactions. TM complexation with EDTA presented in form of Eq. (3.1) is expressed as in Eq. (3.2).

$$Me^{2+} + EDTA^{4-} \leftrightarrows MeEDTA^{2-} \quad (3.1)$$

$$\rho_{comp} = k_1 A_{EDTA} A_{Me} - k_{-1} A_{MeEDTA} \quad (3.2)$$

where k_1 and k_{-1} are rate constants of formation and dissociation respectively. Rate constant for formation of metal-EDTA complex is the product of water loss rate constant k_{-w} and stability constant for outer-sphere complexes K_{OS} as given in Eq. (3.3). Constant K_{OS} depends on ionic strength of the medium and the charges of metal and ligand while k_{-w} depends on charge of the reacting metal. Dissociation rate constants can be related to rate constant of complex formation through Eq. (3.4), where K_{eq} is the equilibrium stability constant. Metal-EDTA complexation reactions along with parameter values used in the model are given in Appendix 3.1.

$$k_1 = K_{OS} * k_{-w} \quad (3.3)$$

$$K_{eq} = k_1 / k_{-1} \quad (3.4)$$

3.2.1.3. Adsorption of TMs

Metals can be adsorbed by active and inert biomass, soluble microbial products (SMPs), extracellular polymeric substances (EPS) and precipitates such as FeS. Metal adsorption on surfaces of these adsorbents are modelled by classifying them in four main categories based on their representation in ADM1. It includes adsorption on surfaces of biomass X, particulate inerts X_I (dead biomass), soluble inerts S_I (EPS and SMPs) and precipitate FeS. Generalized adsorption model (Yee & Fein, 2001) where metal adsorption behavior on biomass is independent of the microbial species involved is adopted in the study. According to the generalized model, adsorption on bacterial cell wall takes place due to negative surface charge formed from deprotonation of carboxyl, hydroxyl and phosphoryl functional groups present on the cell surface. Similarly, adsorption on soluble and particulate inerts are majorly due to surface complexation of metals with deprotonated carboxyl, phosphoryl and hydroxyl functional groups. Hydroxyl and sulfydryl functional groups are present on the surface of FeS precipitate and sulfydryl functional groups cause major metal adsorption on FeS (Davis & Kent, 2018). Surface characteristics of adsorbents along with deprotonation constants are given in Table 3.3.

.

Metal adsorption is defined by an electrostatic surface complexation model (SCM). Kinetics of metal complexation with functional groups (say carboxyl) as represented in Eq. (3.5) are modelled based on Morel & Hering (1993) as described in Eq. (3.6).

$$Me^{2+} + \equiv X{-}COO^{-} \leftrightarrows \equiv X - COOMe^{+} \tag{3.5}$$

$$\rho_{ads} = k_f A_{Me} S_{\equiv X-COO^-} - k_b S_{\equiv X-COOMe^+} \tag{3.6}$$

where $\equiv X$ represents surface of adsorbent to which functional groups are attached, A_{Me} is the activity of metal ion, $S_{\equiv X-COO^-}$ and $S_{\equiv X-COOMe^+}$ are concentrations of free carboxyl binding site and adsorbed metal on carboxyl binding site respectively. Formation rate constant k_f and desorption rate constant k_d are related by apparent equilibrium constant K_{app} using Eq. (3.7). According to Stumm & Morgan (1996), influence on activity of ions due to interactions between electrostatic field on adsorbent surface and adsorbing metals can be quantified by Eq. (3.8) where K_{int} is the intrinsic equilibrium constant referring to zero surface charge, ΔZ is change in charge of the surface species, F is the Faraday Constant (9.649×10^{-4} coulombs mol^{-1}), ψ is surface potential (volts), R is the universal gas constant (8.314 J mol^{-1} K^{-1}) and T is the absolute temperature (K).

$$K_{app} = k_f / k_b \tag{3.7}$$

$$K_{app} = K_{int} \exp\left(-\frac{\Delta Z F \psi}{RT}\right) \tag{3.8}$$

Surface potential, ψ is calculated using Eq. (3.9) where σ is the surface charge (coulombs m^{-2}), ε is the dielectric constant of water (78.5 at 25 °C), ε_0 is the permittivity of free space (8.854×10^{-12} C V^{-1} m^{-1}) and I is the calculated ionic strength from aqueous phase equilibrium module.

$$\sigma = (8000\, RT\varepsilon\varepsilon_0 I)^{1/2} \sinh\left(\frac{ZF\psi}{2RT}\right) \tag{3.9}$$

Formation rate constant k_f is calculated by multiplying outer sphere complex formation rate constant K_{OS} with intrinsic adsorption rate constant k_{ads} as given in Eq. (3.10). K_{OS} and k_{ads} are obtained by the relation given in Eq. (3.11) and Eq. (3.12) respectively where Z is the charge of adsorbate. Model parameters used in the model are given in Table 3.3.

$$k_f = K_{OS} * k_{ads} \tag{3.10}$$

$$K_{OS} = \exp\left(-\frac{ZF\psi}{RT}\right) \tag{3.11}$$

$$log\, k_{ads} = -4.16 + 0.92\, log\, k_{-w} \tag{3.12}$$

Table 3.3 – Surface complexation model reactions and parameters for metal adsorption

Cell surface characteristics (X, X_I (Yee & Fein, 2001))		
Density of ≡X-COOH (carboxyl sites) = 2×10^{-3} mol/g bacteria		
Density of ≡X-PO_4H (phosphoryl sites) = 0.8×10^{-3} mol/g bacteria		
Density of ≡X-OH (hydroxyl sites) = 1.7×10^{-3} mol/g bacteria		
Surface complexation reactions		
≡X-COOH ⇆ ≡X-COO^- + H^+	log K^{int} = -5.0	(Yee & Fein, 2001)
≡X- PO_4H ⇆ ≡X- PO_4^- + H^+	log K^{int} = -7.2	(Yee & Fein, 2001)
≡X- OH ⇆ ≡X-O^- + H^+	log K^{int} = -9.7	(Yee & Fein, 2001)
≡X-COO^- + Fe^{2+} ⇆ ≡X-$COOFe^+$	log K^{int} = 5.86	(Wightman & Fein, 2005)
≡X-COO^- + Ni^{2+} ⇆ ≡X-$COONi^+$	log K^{int} = 1.95	(Burnett et al., 2007)
≡X-COO^- + Co^{2+} ⇆ ≡X-$COOCo^+$	log K^{int} = 3.41	(Fein et al., 2001)
≡X-COO^- + Ca^{2+} ⇆ ≡X-$COOCa^+$	log K^{int} = 2.3	(Johnson et al., 2007)
≡X-COO^- + Mg^{2+} ⇆ ≡X-$COOMg^+$	log K^{int} = 2.9	(Smith et al., 2002)
≡X-PO_4^- + Ni^{2+} ⇆ ≡X-PO_4Ni^+	log K^{int} = 3.41	(Burnett et al., 2007)
≡X-PO_4^- + Ca^{2+} ⇆ ≡X-PO_4Ca^+	log K^{int} = 1.6	(Johnson et al., 2007)
Surface characteristics (S_I) (Liu & Fang, 2002)		
Density of ≡X-COOH (carboxyl sites) = 6.21×10^{-3} mol/g bacteria		
Density of ≡X-PO_4H (phosphoryl sites) = 0.53×10^{-3} mol/g bacteria		
Density of ≡X-OH (hydroxyl sites) = 6.93×10^{-3} mol/g bacteria		
Surface complexation reactions		
≡X-COOH ⇆ ≡X-COO^- + H^+	log K^{int} = -4.89	(Liu & Fang, 2002)
≡X-PO_4H ⇆ ≡X-PO_4^- + H^+	log K^{int} = -7.30	(Liu & Fang, 2002)
≡X-OH ⇆ ≡X-O^- + H^+	log K^{int} = -10.56	(Liu & Fang, 2002)
≡X-COO^- + Fe^{2+} ⇆ ≡X-$COOFe^+$	log K^{int} = 5.86	(Wightman & Fein, 2005)
≡X-COO^- + Ni^{2+} ⇆ ≡X-$COONi^+$	log K^{int} = 1.95	(Burnett et al., 2007)
≡X-COO^- + Co^{2+} ⇆ ≡X-$COOCo^+$	log K^{int} = 3.41	(Fein et al., 2001)
≡X-COO^- + Ca^{2+} ⇆ ≡X-$COOCa^+$	log K^{int} = 2.3	(Johnson et al., 2007)
≡X-COO^- + Mg^{2+} ⇆ ≡X-$COOMg^+$	log K^{int} = 2.9	(Smith et al., 2002)
≡X-PO_4^- + Ni^{2+} ⇆ ≡X-PO_4Ni^+	log K^{int} = 3.41	(Burnett et al., 2007)
≡X-PO_4^- + Ca^{2+} ⇆ ≡X-PO_4Ca^+	log K^{int} = 1.6	(Johnson et al., 2007)
Surface characteristics (FeS) (Wolthers et al., 2005)		
Density of ≡X-SH (sulfhydryl sites) = 1.2×10^{-3} mol/g bacteria		
Surface complexation reactions		
≡X-SH ⇆ ≡X-S^- + H^+	log K^{int} = -6.5	(Wolthers et al., 2005)
≡X-S^- + Ni^{2+} ⇆ ≡X-SNi^+	log K^{int} = 1.95	(Smith et al., 2002)
≡X-S^- + Co^{2+} ⇆ ≡X-SCo^+	log K^{int} = 3.41	(Smith et al., 2002)

Concentrations of protonated binding sites (say, $S_{\equiv X-COOH}$), deprotonated free binding sites (say, $S_{\equiv X-COO^-}$) and adsorbed metal on binding sites (say, $S_{\equiv X-COOMe^+}$) are calculated from mass balance of the components represented in Eq. (3.13), Eq. (3.14) and Eq. (3.15), respectively, where $D_{\equiv X-COOH}$ is the density of binding sites on adsorbent surface; Y_{ads} is the adsorption yield of metal on the binding surface; $\rho_{formation}$, $\rho_{protonation}$ and ρ_{ads} are formation, protonation and adsorption rates of the binding sites, respectively; $\rho_{formation}$ for biomass, inerts and precipitate FeS are given in Eq. (3.16), Eq. (3.17) and Eq. (3.18), respectively, where ρ_{growth} and ρ_{decay} are the growth and decay rates of biomass; $\rho_{production}$ is the rate of production of inerts during the biochemical reactions in AD; $\rho_{precipitation}$ and $\rho_{dissolution}$ are the precipitation and dissolution rates of the precipitate. Initial volume fractions of free and occupied binding sites are assumed one and zero, respectively.

$$\frac{dS_{\equiv X-COOH}}{dt} = D_{\equiv X-COOH} * \rho_{formation} + \rho_{protonation} \tag{3.13}$$

$$\frac{d\,S_{\equiv X-COO^-}}{dt} = \; - \; \rho_{protonation} - \rho_{ads} \tag{3.14}$$

$$\frac{d\,S_{\equiv X-COOMe^+}}{dt} = Y_{ads}\,\rho_{ads} \tag{3.15}$$

For biomass, $\rho_{formation} = \rho_{growth} \; - \; \rho_{decay}$ (3.16)

For inerts, $\rho_{formation} = \rho_{production}$ (3.17)

For precipitate, $\rho_{formation} = \rho_{precipitation} - \rho_{dissolution}$ (3.18)

3.2.2. Model implementation and simulation

The model is implemented in an original MATLAB code. System of equations are solved using MATLAB ODE solver coupled with multi-dimensional Newton Raphson method. Simulations are performed to test and verify the model under different scenarios. All simulations were performed at neutral pH and 0.1 M ionic strength unless otherwise mentioned. First scenario determines effects of EDTA dosing on metal speciation by varying metal and EDTA dosing concentrations and changing EDTA dosing forms. Second scenario analyses the effect of amino acids in TM speciation and study the model behavior under different concentrations of amino acid compounds (varying substrate). Third scenario investigates the effect of ionic strength on adsorption and metal speciation. Concentration of K^+ and Cl^- ions are varied as a means to change ionic strength of the medium between 0.01 – 0.4 M and influence of salinity due to the added ions is neglected, as beyond the scope of this work. Operational and model input initial conditions used in the model are given in Appendix 3.1.

3.2.3. Model application

3.2.3.1. Experimental set-up

An up-flow anaerobic sludge blanket digestion (UASB) reactor of 3.25 L operated at temperature of 35 ±2 °C was used for performing experiments. The reactor was fed with sodium propionate, trace metal solution excluding Ni, Co and macronutrients. 1.5 L of anaerobic granular sludge collected from a UASB reactor operated at full scale under mesophilic conditions treating brewery wastewater (Heineken Brewery, Seville, Spain) was used as inoculum for the reactor. Influent to the UASB reactor was introduced as two streams to prevent precipitation before feeding the reactor. The first inlet was composed of propionate and trace metals solution with composition as given in Fermoso et al. (2008). Macronutrient solution with composition as reported in the same study was used as the second inlet. Reactor was started at an organic loading rate (OLR) of 1 $gCODL^{-1}d^{-1}$ and hydraulic retention time (HRT) of 12 h. After 4 days of operation, OLR and HRT were changed in steps to 10 $gCODL^{-1}d^{-1}$ and 8 h, respectively.

3.2.3.2. Specific methanogenic activity tests

Maximum specific methanogenic activity (SMA) of the sludge was measured using SMA test assay. Maximum SMA was quantified as the maximum slope of a cumulative methane production rate curve. Activity test assays were performed at 35 °C in 100 mL glass bottles with a working volume of 70 mL. Each bottle was supplemented with 2.2 gCOD/L propionate as substrate and around 2.4 g (wet weight) UASB sludge. Composition of basal medium in the bottles were same as in the UASB reactor with pH around 7.0 ±0.2. Biogas production was quantified manometrically by measuring increase in pressure with volume being kept constant. SMA of the sludge was measured in three conditions (1) control - without Ni and Co in the medium (2) basal medium containing 5 µM Ni (3) basal medium containing 5 µM Co.

3.2.3.3. Analytical methods

UASB reactor performance were monitored by quantifying soluble organic matter, analysed as volatile fatty acids (VFAs) and soluble Chemical Oxygen Demand (sCOD). VFAs were quantified using a gas chromatograph *Shimadzu* GC-2025 in duplicate. American Public Health Association standard methods (APHA, 2007) were used for measuring volatile solids (VS), total solids (TS), sCOD and pH. Dissolved metal concentration was analysed by filtering liquid sample through a 0.20 µm filter and was measured by Inductive Coupled Plasma Mass Spectrometry (ICPMS-Agilent-7800). Composition of biogas (methane, carbon dioxide) from SMA test assays was assessed using a gas chromatograph *Shimadzu* GC-2014.

3.3. RESULTS AND DISCUSSIONS

Results from the developed dynamic model for including trace metal speciation and effects on anaerobic digestion suggests that major processes controlling metal speciation and lability of metals are precipitation followed by complexation and adsorption. Verification of model results from the physicochemical module with Visual MINTEQ outputs (see Appendix 3.1) suggests correct definition of metal speciation processes in the model. Observations from model simulations performed under different scenarios to study adaptability of the model are discussed below.

3.3.1. Effects of EDTA dosing

Decrease in metal precipitation is observed due to formation of strong metal-EDTA complexes during the simulations to study EDTA dosing effects. Effects of EDTA dosing on methane production is shown in Fig 3.2. 0.1 µM of Fe (II) is sub optimal dosing concentration since methane production considerably decreases when Fe dosing is reduced from 1 µM to 0.1 µM. However, when 500 µM EDTA is added with 0.1 µM of Fe (II), cumulative methane production is recovered. Hence EDTA dosing reduces TM dosing concentrations. Vintiloiu et al. (2013) obtained similar results with EDTA addition to an anaerobic system with Ni under sub optimal conditions, i.e. a methane yield increase and a reduced demand of essential TMs to the reactor.

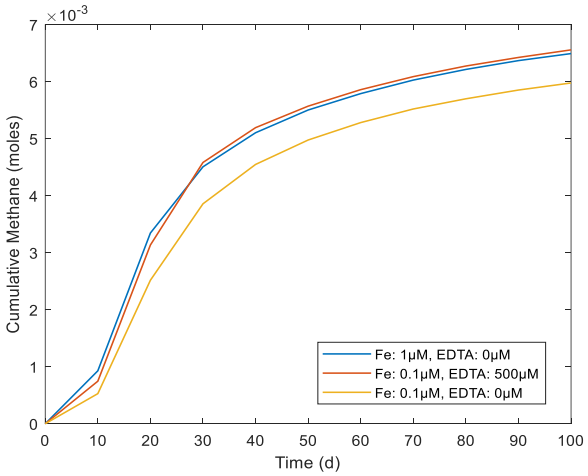

Figure 3.2 – Effects of EDTA dosing on methane production

Influence of EDTA dosing strategy is shown in Fig 3.3. No considerable increase in methane production is observed when EDTA concentration is increased from 0 to 100 µM. However, methane yield increases when EDTA is dosed at 300 µM. Biogas production further increases when EDTA dosing is increased to 400 µM. These effects of EDTA dosing concentration are linked to change in metal speciation and labile metal fraction (i.e. species with fast rate of

ligand displacement reactions and high reactivity in the time frame considered in this study) existing under different dosing concentrations. There is no considerable change in metal labile fraction when EDTA is dosed at 0 - 100 µM whereas dosing EDTA at 300 µM increases metal lability resulting in higher methane production. Nevertheless, increase in methane yield is not observed when EDTA is added to a system with optimal TMs concentrations (data not shown). Furthermore, dosing form of EDTA plays a significant role and is shown in Fig. 3.3(b). It can be observed that dosing EDTA as metal-EDTA complex is more effective than dosing metals and EDTA separately. Similar observation was reported in an experimental study by Thanh et al. (2017) where dosing effects of a similar chelating agent, i.e. EDDS, in an anaerobic system was studied. An improvement in methane yield was observed when supplementing of EDDS was carried out as a complex with Fe instead of dosing EDDS simultaneously with Fe. Such influence of dosing form of chelates on metal bioavailability was also reported by Vintiloiu et al. (2013) and Zhang et al. (2021) for Ni-chelate complexes.

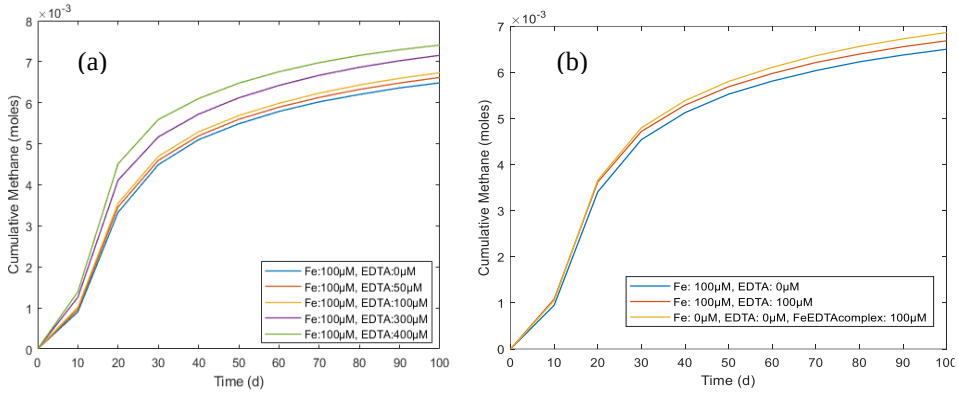

Figure. 3.3 – Effects of EDTA dosing strategy - (a) dosing concentration (b) dosing form

3.3.2. Metal complexation with amino acids

Simulations to study the influence of amino acids during metal limitation with protein rich substrates indicated that trace metals form strong complexes with amino acids thereby keeping the metal concentration below solubility product. Fig. 3.4 shows that metal speciation and cumulative methane production simulated by models with and without amino acid complexation are different. Complexation of amino acids plays a significant role in controlling metal speciation causing decrease or increase in methane production. Model simulations for the system under study showed increase in methane production when metal-amino acid complexation processes are included (Fig. 3.4). Amino acid complexation prevents precipitation and increases labile metal fraction thereby increasing methane production Gonzalez-Gil et al. (2003) reported the importance of amino acids by adding trace doses of yeast extract to anaerobic bioreactors, observing increase in Ni and Co bioavailability due to formation of strong metal-amino acid complexes causing dissolution of metal sulphides.

Amino acid complexation effects are influenced by substrates as shown in Fig. 3.5. Brewery sludge has higher content of amino acid compounds (Cys, Glu, Gly) than sewage and hence forms more metal-amino acid complexes. Accordingly, labile metal fraction formed for system with brewery sludge is higher than that for sewage. Labile fraction in system with brewery sludge reaches inhibitory concentration levels of TMs for the first 40 days. After 40 days, labile metal fraction in the system reduces and reaches stimulatory concentration range thereby increasing methane production (Fig. 3.6). More TM complexation processes with amino acids can be added in future studies, investigating substrates with other predominant amino acid compounds.

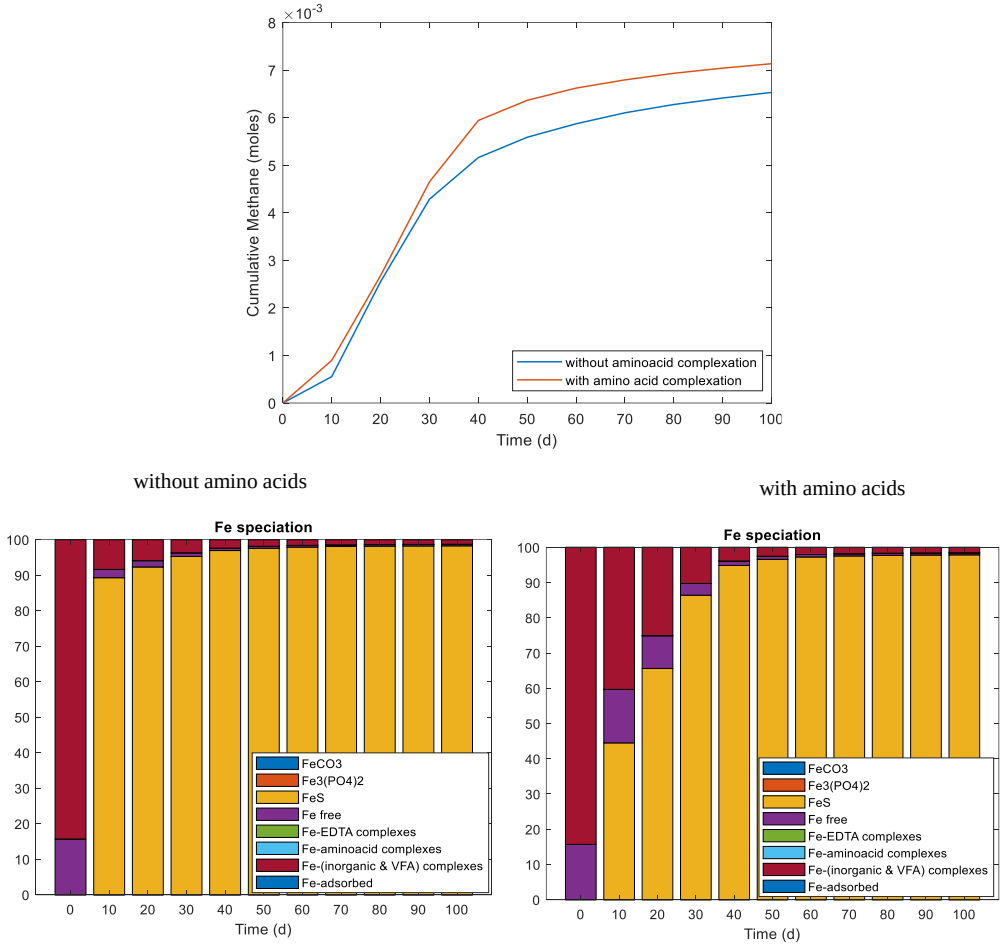

Figure 3.4 – Effect of amino acid complexation on TM speciation with protein rich substrates

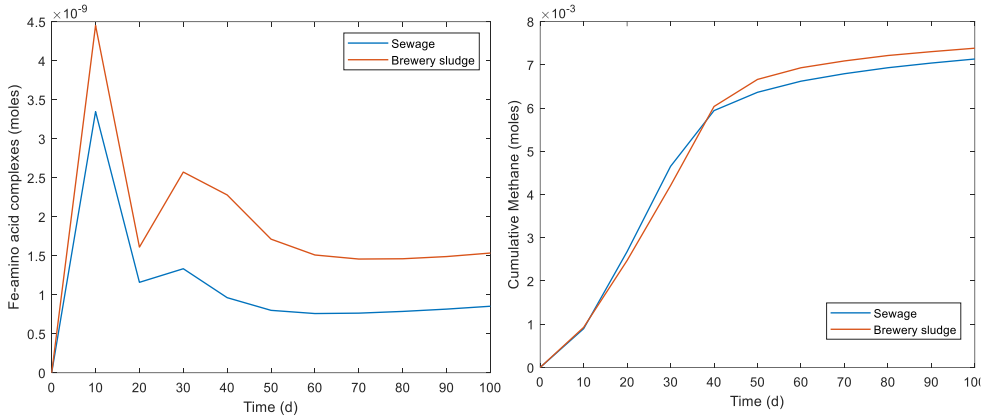

Figure 3.5 – Influence of substrates on amino acid complexation and methane production

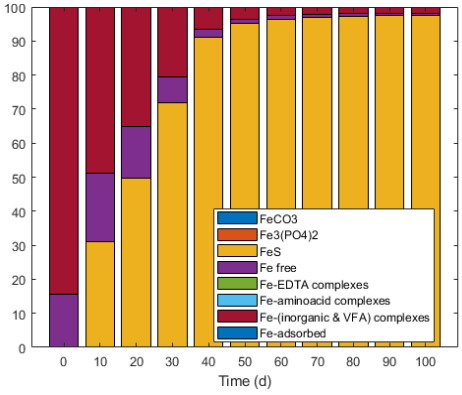

Figure 3.6 – Iron speciation for system with brewery sludge

3.3.3. Effects of ionic strength

Numerical results confirm that ionic strength affects speciation of metals in a system by influencing their chemical activity as also being discussed in the introduction. In an anaerobic system with pH greater than point of zero charge (pH_{pzc}), adsorption of metals increases with increase in ionic strength (Fig. 3.7(a)). At pH above pH_{pzc} (4.7 for the system under consideration), adsorbent surface is negatively charged and surface potential increases (becomes less negative) with ionic strength. Hence the electrostatic interaction with positively charged metal ions increases favouring adsorption. Xu et al. (2009) also reported increase in surface potential with ionic strength at pH above pH_{pzc} and changes in adsorption trend due to electrostatic interactions. Moreover, metal precipitation decreases with ionic strength increase due to decrease in activity of ions (Fig. 3.7(b)). Such effects of ionic strength on precipitation were also reported by George et al. (2023) and Tait et al. (2012). Due to increase in metal adsorption and decrease in metal precipitation, labile metal fraction increases with ionic strength. This causes increase in cumulative methane production with increase in ionic strength (Fig. 3.7(b)). However, since metal speciation is predominantly

affected by precipitation processes, net influence of ionic strength on methane production is controlled by influence of ionic strength on precipitation.

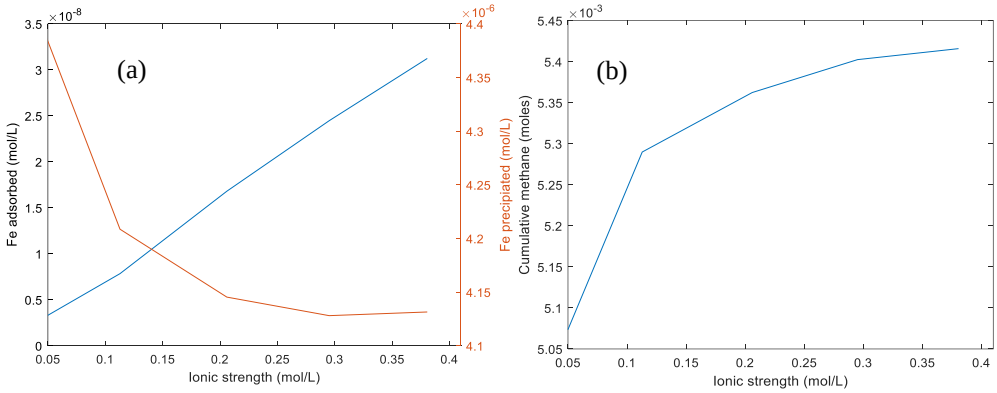

Figure. 3.7 – Influence of ionic strength on (a) metal speciation and (b) digestor performance at pH 6.7 (end of simulation run)

3.3.4. Model application

Experimental results from the UASB reactor showed complete removal of substrate without any VFA accumulation in the effluent until day 49 (Fig. 3.8(a)). About 95% COD removal was observed till day 49. Due to deprivation of Co in the sludge, soluble COD rose to around 861 mgCOD/L within 90 days (71% removal). However, accumulation of acetate was not observed although propionate in the effluent kept increasing (Fig. 3.9(a)). Hence, Co deprivation in the sludge could have mostly affected the propionate oxidisers. Fig. 3.8(b) shows that SMA of the sludge taken from the reactor using propionate as the substrate in mediums without Ni and Co (Control), with Ni and with Co were the same until day 49(~ 0.5gCOD/gVS/d). This suggests that sludge was not deprived of Ni/Co until day 49. A difference in SMA 'with' and 'without Co' was seen from day 49 to day 62 suggesting Co deprivation during those days. SMA difference 'with' and 'without Co' occurred only in the first three weeks of Co deprivation (day 49-62) and no difference in SMA was observed after day 62. Moreover, a continuous decrease in SMA can be observed from day 34 to day 90 suggesting a decline in activity of methanogens over time. Drop in SMA on days 13 and 28 is due to operational limitations in maintaining optimum temperature during those days. Cumulative methane production curve obtained from activity tests performed on day 49 is given in Fig. 3.8(c). It shows evident Co deprivation in the sludge on day 49. Similar curves were obtained from activity tests performed from day 49 to 62 (plots not shown). However, this deprivation of Co in the reactor was not recognizable from measurements of soluble or effluent Co concentrations (Fig. 3.9(b)) as metal deprivation is associated with bioavailable metal concentration and not soluble metal fraction. Significance of the bioavailable metal fraction and the fact that TM effects on AD are not dependent on total or soluble metal concentrations are extensively reported in literature (Fermoso et al., 2009; Thanh et al. 2016).

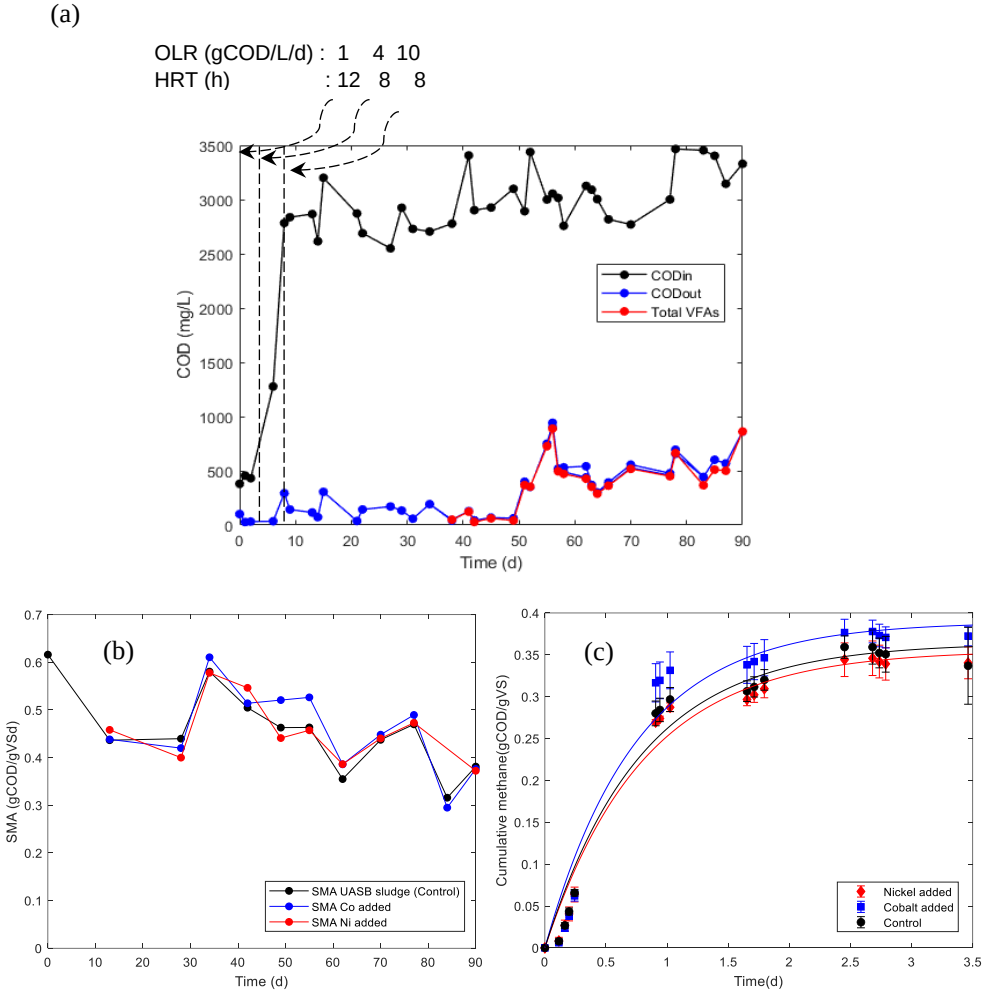

Figure 3.8 – Reactor performance over time: (a) influent COD, effluent COD & effluent VFAs, (b) SMA of the reactor sludge using propionate as substrate, (c) BMP curve on day 49

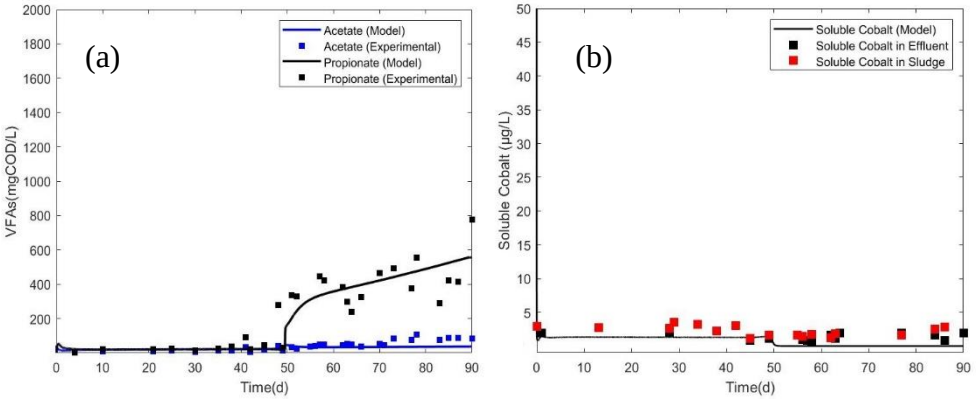

Figure 3.9 – Experimental results and model predictions for concentrations of (a) acetate and propionate, (b) soluble Co in the reactor

The model parameters calibrated to fit model results with experimental observations were the maximum specific uptake rate of acetate degraders $k_{m,ac}$ (14 d^{-1}), the half saturation coefficient of acetate degraders $K_{s,ac}$ (0.49 kgCOD m^{-3}), the CoS precipitation /dissolution rate kr_{CoS} (10^{15} d^{-1}) and the decay rate of propionate degraders $k_{dec,pro}$ (0.01 d^{-1}). Default values were used for the remaining parameters. Fig. 3.9(a) and Fig. 3.9(b) show that the model can reasonably reproduce the experimentally observed values of VFAs (propionate, acetate) and soluble Co concentrations, respectively. Model outputs demonstrated a decline in reactor performance due to decrease in bioavailable Co concentration in the reactor (data not shown).

3.4. CONCLUSIONS

This study developed a complete model based on ADM1 with minimal model input information to study effects of TMs on AD. Speciation of metals in the proposed model is controlled by processes like precipitation, complexation, adsorption, microbial uptake and operational conditions like pH, temperature and ionic strength. The proposed model could reasonably predict trace metal effects like metal deprivation in an anaerobic digestor. Due to experimental/analytical limitations in quantifying the bioavailable metal fractions, this model could be helpful to understand TM effects on AD and design optimum dosing strategies for real case applications.

Model results are also tested and verified under different scenarios. Major observations from the model simulations are outlined below.

- Addition of EDTA reduces trace metal dosing concentration. Concentration of supplemented EDTA influences digestor performance and the effects are driven by labile metal fraction formed under different dosing conditions. Supplementing

EDTA as metal-EDTA complex is found to be more effective than dosing metals and EDTA separately.

- Amino acids form strong complexes with TMs, reduce precipitation and keep metals in solution. Amino acids thus play a significant role in controlling metal labile fraction and methane production for substrates rich in protein content. Moreover, substrate characteristics influence metal speciation since the amount of amino acid compounds is different in different substrates.

- Adsorption of trace metals onto biomass, dead biomass, EPS, SMPs and precipitate FeS is defined considering the effects of pH and ionic strength. Under optimal pH conditions for the performance of an anaerobic digestor, adsorption increases whereas precipitation decreases with increase in ionic strength. Hence metal labile fraction increases resulting in increasing the cumulative methane production.

3.5. REFERENCES

APHA, A. (2007). *WEF (2005) Standard methods for the examination of water and wastewater. American Public Health Association, American Water Works Association, and Water Environment Federation.* https://www.standardmethods.org/

Aquino, S. F., & Stuckey, D. C. (2007). Bioavailability and Toxicity of Metal Nutrients during Anaerobic Digestion. *Journal of Environmental Engineeering*, *133*(1), 28–35. https://doi.org/10.1061/ASCE0733-93722007133:128

Bartacek, J., Fermoso, F. G., Vergeldt, F., Gerkema, E., Maca, J., van As, H., & Lens, P. N. L. (2012). The impact of metal transport processes on bioavailability of free and complex metal ions in methanogenic granular sludge. *Water Science and Technology : A Journal of the International Association on Water Pollution Research*, *65*(10), 1875–1881. https://doi.org/10.2166/WST.2012.030

Burnett, P. G. G., Handley, K., Peak, D., & Daughney, C. J. (2007). Divalent metal adsorption by the thermophile Anoxybacillus flavithermus in single and multi-metal systems. *Chemical Geology*, *244*(3–4), 493–506. https://doi.org/10.1016/J.CHEMGEO.2007.07.006

Cai, Y., Hu, K., Zheng, Z., Zhang, Y., Guo, S., Zhao, X., Cui, Z., & Wang, X. (2019). Effects of adding EDTA and Fe 2+ on the performance of reactor and microbial community structure in two simulated phases of anaerobic digestion. *Bioresource Technology*, *275*, 183–191. https://doi.org/10.1016/J.BIORTECH.2018.12.050

Callander, I. J., & Barford, J. P. (1983). Precipitation, chelation, and the availability of metals as nutrients in anaerobic digestion. I. Methodology. *Biotechnology and Bioengineering*, *25*(8), 1947–1957. https://doi.org/10.1002/BIT.260250805

Davis, J. A., & Kent, D. B. (2018). SURFACE COMPLEXATION MODELING IN AQUEOUS GEOCHEMISTRY. In *Mineral-Water Interface Geochemistry* (pp. 177–260).

Fein, J. B., Martin, A. M., & Wightman, P. G. (2001). *Metal adsorption onto bacterial surfaces: Development of a predictive approach*.

Fermoso, F. G., Bartacek, J., Chung, L. C., & Lens, P. (2008). Supplementation of cobalt to UASB reactors by pulse dosing: CoCl2 versus CoEDTA2− pulses. *Biochemical Engineering Journal*, *42*(2), 111–119. https://doi.org/10.1016/J.BEJ.2008.06.005

Fermoso, F. G., Bartacek, J., Jansen, S., & Lens, P. N. L. (2009). Metal supplementation to UASB bioreactors: from cell-metal interactions to full-scale application. *Science of the Total Environment*, *407*(12), 3652–3667. https://doi.org/10.1016/J.SCITOTENV.2008.10.043

Frunzo, L., Fermoso, F. G., Luongo, V., Mattei, M. R., & Esposito, G. (2019). ADM1-based mechanistic model for the role of trace elements in anaerobic digestion processes.

Journal of Environmental Management, *241*, 587–602. https://doi.org/10.1016/j.jenvman.2018.11.058

George, S., Mattei, M. R., Frunzo, L., Esposito, G., van Hullebusch, E. D., & Fermoso, F. G. (2023). Dynamic modelling the effects of ionic strength and ion complexation on trace metal speciation during anaerobic digestion. *Journal of Environmental Management*, *343*, 118144. https://doi.org/10.1016/j.jenvman.2023.118144

Gonzalez-Gil, G., Jansen, S., Zandvoort, M. H., & van Leeuwen, H. P. (2003). *Effect of Yeast Extract on Speciation and Bioavailability of Nickel and Cobalt in Anaerobic Bioreactors*. https://doi.org/10.1002/bit.10551

Hu, Q. H., Li, X. F., Du, G. C., & Chen, J. (2008). Effect of nitrilotriacetic acid on bioavailability of nickel during methane fermentation. *Chemical Engineering Journal*, *143*(1–3), 111–116. https://doi.org/10.1016/J.CEJ.2007.12.021

Johnson, K. J., Szymanowski, J. E. S., Borrok, D., Huynh, T. Q., & Fein, J. B. (2007). Proton and metal adsorption onto bacterial consortia: Stability constants for metal-bacterial surface complexes. *Chemical Geology*, *239*(1–2), 13–26. https://doi.org/10.1016/J.CHEMGEO.2006.12.002

Liu, H., & Fang, H. H. P. (2002). Characterization of electrostatic binding sites of extracellular polymers by linear programming analysis of titration data. *Biotechnology and Bioengineering*, *80*(7), 806–811. https://doi.org/10.1002/bit.10432

Maharaj, B. C., Mattei, M. R., Frunzo, L., Hullebusch, E. D. van, & Esposito, G. (2019). ADM1 based mathematical model of trace element complexation in anaerobic digestion processes. *Bioresource Technology*, *276*, 253–259. https://doi.org/10.1016/j.biortech.2018.12.064

Maharaj, B. C., Mattei, M. R., Frunzo, L., van Hullebusch, E. D., & Esposito, G. (2018). ADM1 based mathematical model of trace element precipitation/dissolution in anaerobic digestion processes. *Bioresource Technology*, *267*, 666–676. https://doi.org/10.1016/j.biortech.2018.06.099

Maharaj, B. C., Mattei, M. R., Frunzo, L., van Hullebusch, E. D., & Esposito, G. (2021). A general framework to model the fate of trace elements in anaerobic digestion environments. *Scientific Reports*, *11*(1). https://doi.org/10.1038/s41598-021-85403-2

Morel, F., & Hering, J. (1993). *Principles and applications of aquatic chemistry*. https://books.google.com/books?hl=en&lr=&id=lgXpDwAAQBAJ&oi=fnd&pg=PR11&dq=principles+and+applications+of+aquatic+chemistry&ots=Xa4S6T33qn&sig=KF-f_ek6JvGJ9odMMpPyGu40buY

Schwarz, A. O., Bruce, A. E., & Rittmann, E. (2007). A biogeochemical framework for metal detoxification in sulfidic systems. *Biodegradation*, *18*, 675–692. https://doi.org/10.1007/s10532-007-9101-2

Shakeri Yekta, S., Svensson, B. H., Björn, A., & Skyllberg, U. (2014). Thermodynamic modeling of iron and trace metal solubility and speciation under sulfidic and ferruginous

conditions in full scale continuous stirred tank biogas reactors. *Applied Geochemistry*, *47*, 61–73. https://doi.org/10.1016/J.APGEOCHEM.2014.05.001

Smith, D. S., Bell, R. A., & Kramer, J. R. (2002). Metal speciation in natural waters with emphasis on reduced sulfur groups as strong metal binding sites. *Comparative Biochemistry and Physiology - C Toxicology and Pharmacology*, *133*(1–2), 65–74. https://doi.org/10.1016/S1532-0456(02)00108-4

Stumm, W., & Morgan, J. J. (1996). *Aquatic chemistry : chemical equilibria and rates in natural waters* (3rd ed.). Wiley.

Tait, S., Solon, K., Volcke, E. I. P., & Batstone, D. J. (2012). A Unified Approach to Modelling Wastewater Chemistry: Model Corrections. *Procs. 3rd IWA/WEF Wastewater Treatment Modelling Seminar (WWTmod2012), Mont-St-Anne, Quebec, Feb 26–28 (2012)*. https://scholar.google.com/scholar_lookup?title=A%20unified%20approach%20to%20modelling%20wastewater%20chemistry%3A%20model%20corrections&publication_year=2012&author=S.%20Tait&author=K.%20Solon&author=E.I.P.%20Volcke&author=D.J.%20Batstone

Thanh, P. M., Ketheesan, B., Stuckey, D. C., & Zhou, Y. (2017). Dosing of Ethylenediamine-N,N′-disuccinic acid (EDDS) to improve the bioavailability of Fe2+ in the presence of sulfide in a submerged anaerobic membrane bioreactor. *Chemical Engineering Journal*, *330*, 175–182. https://doi.org/10.1016/J.CEJ.2017.07.158

Thanh, P. M., Ketheesan, B., Yan, Z., & Stuckey, D. (2016). Trace metal speciation and bioavailability in anaerobic digestion: A review. In *Biotechnology Advances* (Vol. 34, Issue 2, pp. 122–136). Elsevier Inc. https://doi.org/10.1016/j.biotechadv.2015.12.006

Thanh, P. M., Ketheesan, B., Yan, Z., & Stuckey, D. (2017). Effect of Ethylenediamine-N,N'-disuccinic acid (EDDS) on the speciation and bioavailability of Fe2+ in the presence of sulfide in anaerobic digestion. *Bioresource Technology*, *229*, 169–179. https://doi.org/10.1016/J.BIORTECH.2016.12.113

Tsapekos, P., Alvarado-Morales, M., Tong, J., & Angelidaki, I. (2018). Nickel spiking to improve the methane yield of sewage sludge. *Bioresource Technology*, *270*, 732–737. https://doi.org/10.1016/J.BIORTECH.2018.09.136

van Hullebusch, E. D., Guibaud, G., Simon, S., Lenz, M., Yekta, S. S., Fermoso, F. G., Jain, R., Duester, L., Roussel, J., Guillon, E., Skyllberg, U., Almeida, C. M. R., Pechaud, Y., Garuti, M., Frunzo, L., Esposito, G., Carliell-Marquet, C., Ortner, M., & Collins, G. (2016). Methodological approaches for fractionation and speciation to estimate trace element bioavailability in engineered anaerobic digestion ecosystems: An overview. *Critical Reviews in Environmental Science and Technology*, *46*(16), 1324–1366. https://doi.org/10.1080/10643389.2016.1235943

Vintiloiu, A., Boxriker, M., Lemmer, A., Oechsner, H., Jungbluth, T., Mathies, E., & Ramhold, D. (2013). Effect of ethylenediaminetetraacetic acid (EDTA) on the bioavailability of trace elements during anaerobic digestion. *Chemical Engineering Journal*, *223*, 436–441. https://doi.org/10.1016/J.CEJ.2013.02.104

Wightman, P. G., & Fein, J. B. (2005). Iron adsorption by Bacillus subtilis bacterial cell walls. *Chemical Geology*, *216*(3–4), 177–189. https://doi.org/10.1016/j.chemgeo.2004.11.008

Willett, A. I., & Rittmann, B. E. (2003). Slow complexation kinetics for ferric iron and EDTA complexes make EDTA non-biodegradable. *Biodegradation*, *14*, 105–121.

Wolthers, M., Charlet, L., van der Linde, P. R., Rickard, D., & van der Weijden, C. H. (2005). Surface chemistry of disordered mackinawite (FeS). *Geochimica et Cosmochimica Acta*, *69*(14), 3469–3481. https://doi.org/10.1016/J.GCA.2005.01.027

XU, R., WANG, Y., TIWARI, D., & WANG, H. (2009). Effect of ionic strength on adsorption of As(III) and As(V) on variable charge soils. *Journal of Environmental Sciences*, *21*(7), 927–932. https://doi.org/10.1016/S1001-0742(08)62363-3

Yee, N., & Fein, J. (2001). *Cd adsorption onto bacterial surfaces: A universal adsorption edge?*

Zhang, M., Fan, Z., Hu, Z., & Luo, X. (2021). Enhanced anaerobic digestion with the addition of chelator-nickel complexes to improve nickel bioavailability. *The Science of the Total Environment, 759*. https://doi.org/10.1016/J.SCITOTENV.2020.143458

Zhang, W., Zhang, L., & Li, A. (2015). Enhanced anaerobic digestion of food waste by trace metal elements supplementation and reduced metals dosage by green chelating agent [S, S]-EDDS via improving metals bioavailability. *Water Research*, *84*, 266–277. https://doi.org/10.1016/J.WATRES.2015.07.010

Zhong, T., Liu, Y., & Kang, X. (2019). Synthetic Effect of EDTA and Ni2+ on Methane Production and Microbial Communities in Anaerobic Digestion Process of Kitchen Wastes. *Processes 2019, Vol. 7, Page 590*, *7*(9), 590. https://doi.org/10.3390/PR7090590

APPENDIX 3.1

Table 3A.1 - EDTA processes defined in the model

Species	log K	delta Hr (kJ/mol)	Rate	References
Complexation				
$CaEDTA^{2-}$	12.44	-22	$k_1 S_{EDTA} S_{Ca} - k_{-1} S_{CaEDTA}$	(Gustafsson, 2018)
$CaHEDTA^{-}$	3.1	0	$k_1 S_{CaEDTA} S_H - k_{-1} S_{CaHEDTA}$	(Smith et al., 2004)
$CoEDTA^{2-}$	18.16	-15	$k_1 S_{EDTA} S_{Co} - k_{-1} S_{CoEDTA}$	(Gustafsson, 2018)
CoH_2EDTA	1.7	0	$k_1 S_{CoHEDTA} S_H - k_{-1} S_{CoH2EDTA}$	(Smith et al., 2004)
$CoHEDTA^{-}$	3	-7.9	$k_1 S_{CoEDTA} S_H - k_{-1} S_{CoHEDTA}$	(Smith et al., 2004)
$FeEDTA^{2-}$	16.01	-16	$k_1 S_{EDTA} S_{Fe} - k_{-1} S_{FeEDTA}$	(Gustafsson, 2018)
$FeHEDTA^{-}$	6.82	-4	$k_1 S_{HEDTA} S_{Fe} - k_{-1} S_{FeHEDTA}$	(Smith et al., 2004)
$FeOHEDTA^{3-}$	11.9	0	$k_1 S_{EDTA} S_{FeOH} - k_{-1} S_{FeOHEDTA}$	(Smith et al., 2004)
$MgEDTA^{2-}$	10.58	17	$k_1 S_{EDTA} S_{Mg} - k_{-1} S_{MgEDTA}$	(Gustafsson, 2018)
$MgHEDTA^{-}$	4	0	$k_1 S_{MgEDTA} S_H - k_{-1} S_{MgHEDTA}$	(Smith et al., 2004)
$NiEDTA^{2-}$	20.11	-30	$k_1 S_{EDTA} S_{Ni} - k_{-1} S_{NiEDTA}$	(Gustafsson, 2018)
NiH_2EDTA	0.9	0	$k_1 S_{NiHEDTA} S_H - k_{-1} S_{NiH2EDTA}$	(Smith et al., 2004)
$NiHEDTA^{-}$	3.1	-7.5	$k_1 S_{NiEDTA} S_H - k_{-1} S_{NiHEDTA}$	(Smith et al., 2004)
$NiOHEDTA^{3-}$	11.9	-46.5	$k_1 S_{EDTA} S_{NiOH} - k_{-1} S_{NiOHEDTA}$	(Smith et al., 2004)
Protonation/deprotonation				
$HEDTA^{3-}$	10.948	-21	$k_{HEDTA}(S_{EDTA} S_H - K_{HEDTA} S_{HEDTA})$	(Smith et al., 2004)
H_2EDTA^{2-}	6.273	-15	$k_{H2EDTA}(S_{HEDTA} S_H - K_{HEDTA} S_{H2EDTA})$	(Smith et al., 2004)
H_3EDTA^{-}	2.69	7.1	$k_{H3EDTA}(S_{H2EDTA} S_H - K_{HEDTA} S_{H3EDTA})$	(Smith et al., 2004)
H_4EDTA	2	1	$k_{H4EDTA}(S_{H3EDTA} S_H - K_{HEDTA} S_{H4EDTA})$	(Smith et al., 2004)
H_5EDTA^{+}	1.5	2	$k_{H5EDTA}(S_{H4EDTA} S_H - K_{HEDTA} S_{H5EDTA})$	(Smith et al., 2004)
H_6EDTA^{2+}	0	8	$k_{H6EDTA}(S_{H5EDTA} S_H - K_{HEDTA} S_{H6EDTA})$	(Smith et al., 2004)

Table 3A.2 - Rate constants for EDTA complexation processes (Morel & Hering, 1993)

Species ↓	k_w (h^{-1})	K_{OS} (M^{-1}) (I=0.1 M)	$k_1 = k_w * K_{OS}$ (M^{-1} h^{-1})
$CaEDTA^{2-}$	$2.6*10^{12}$	$5.8*10^{2}$	$1.51*10^{13}$
$CaHEDTA^{-}$	$2.6*10^{12}$	2.09	$5.43*10^{10}$
$CoEDTA^{2-}$	$7.2*10^{9}$	$5.8*10^{2}$	$4.18*10^{10}$
CoH_2EDTA	$7.2*10^{9}$	0.118	$8.50*10^{6}$
$CoHEDTA^{-}$	$7.2*10^{9}$	2.09	$1.50*10^{8}$
$FeEDTA^{2-}$	$1.44*10^{10}$	$5.8*10^{2}$	$8.35*10^{10}$
$FeHEDTA^{-}$	$1.44*10^{10}$	2.09	$3.01*10^{8}$
$FeOHEDTA^{3-}$	$1.44*10^{10}$	$5.8*10^{2}$	$8.35*10^{10}$
$MgEDTA^{2-}$	$1.08*10^{9}$	$5.8*10^{2}$	$6.26*10^{9}$
$MgHEDTA^{-}$	$1.08*10^{9}$	2.09	$2.26*10^{7}$
$NiEDTA^{2-}$	$1.08*10^{8}$	$5.8*10^{2}$	$6.26*10^{8}$
NiH_2EDTA	$1.08*10^{8}$	0.118	$1.27*10^{5}$
$NiHEDTA^{-}$	$1.08*10^{8}$	2.09	$2.26*10^{6}$
$NiOHEDTA^{3-}$	$1.08*10^{8}$	$5.8*10^{2}$	$6.26*10^{8}$

Table 3A.3 - Amino acid compounds in different substrates (Liu et al., 2022)

Amino acid	Sewage (%)	Brewery sludge (%)
Glutamic acid (Glu)	8.1	12.2
Glycine (Gly)	4.9	7.1
Cysteine (Cys)	2.1	2.7

Table 3A.4 - Amino acid complexation processes defined in the model (Morel & Hering, 1993, Berthon, 1995)

Component → / Species ↓	log K	delta Hr (kJ/mol)	Cys^{-1}	Glu^{-2}	Gly^{-1}	Ca^{2+}	Mg^{2+}	Fe^{2+}	Ni^{2+}	Co^{2+}	H^{+1}
$Ca\text{-}Cys^{+}$	2.5	0	1			1					
$Ca\text{-}Gly^{+}$	1.4	-4			1	1					
Ca-Glu	2.1	0		1		1					
$Mg\text{-}Cys^{+}$	2.749	0	1				1				
$Mg\text{-}Gly^{+}$	2.7	25			1		1				
Mg-Glu	2.8	0		1			1				
$Fe\text{-}Cys^{+}$	6.2	0	1					1			
$Fe\text{-}(Cys)_2$	11.77	0	2					1			
Fe-Glu	4.6	0		1				1			
$Fe\text{-}(Gly)_2$	8.31	0			2			1			
$Fe\text{-}Gly^{+}$	4.3	-15			1			1			
$Fe\text{-}(Gly)_3^{-}$	9.48	0			3			1			
$Co\text{-}Cys^{+}$	8.8	0	1							1	
$Co\text{-}(Cys)_2$	16.2	0	2							1	
Co-Glu	5.4	0		1						1	
$Co\text{-}(Glu)_2^{2-}$	8.7	0		2						1	
$Co\text{-}(Gly)_2$	9.0	-26			2					1	
$Co\text{-}Gly^{+}$	5.1	-12			1					1	
$Co\text{-}(Gly)_3^{-}$	11.6	-41			3					1	
$Ni\text{-}Cys^{+}$	10.7	0	1						1		
$Ni\text{-}(Cys)_2$	20.9	0	2						1		
Ni-Glu	6.5	0		1					1		
$Ni\text{-}(Glu)_2^{2-}$	10.6	-30		2					1		
$Ni\text{-}(Gly)_2$	11.1	-38			2				1		
$Ni\text{-}Gly^{+}$	6.2	-18			1				1		
$Ni\text{-}(Gly)_3^{-}$	14.2	-62.3			3				1		
H-Cys	10.77	0	1								1
$H_2\text{-}Cys^{+}$	19.13	0	1								2
$H_3\text{-}Cys^{2+}$	20.84	0	1								3
$H\text{-}Glu^{-}$	9.95	-40		1							1
$H_2\text{-}Glu$	14.47	-43		1							2
$H_3\text{-}Glu^{+}$	16.70	-46		1							3
H-Gly	9.78	-44.35			1						1
$H_2\text{-}Gl^{+}$	12.13	-48.35			1						2

Table 3A.5 - Operational and initial model input conditions

Parameter	Variable	Value	Unit
Digester volume	V_{liq}	0.75	m^3
Headspace volume	V_{gas}	0.25	m^3
Influent flow rate	q_{in}	0	$m^3\ d^{-1}$
Temperature	T	308.15	K
Monosaccharides	S_{su}	0	kgCOD m^{-3}
Amino acids	S_{aa}	0	kgCOD m^{-3}
Long chain fatty acids	S_{fa}	0	kgCOD m^{-3}
Total Valerate	S_{va}	0	kgCOD m^{-3}
Total Butyrate	S_{bu}	0	kgCOD m^{-3}
Total Propionate	S_{pro}	0	kgCOD m^{-3}
Total Acetate	S_{ac}	0	kgCOD m^{-3}
Hydrogen	S_{h2}	0	kgCOD m^{-3}
Methane	S_{ch4}	0	kgCOD m^{-3}
Inorganic carbon	S_{IC}	0.0025	kmole m^{-3}
Inorganic nitrogen	S_{IN}	0.001	kmole m^{-3}
Soluble inerts	S_I	0.0000001	kgCOD m^{-3}
Composites	X_c	1	kgCOD m^{-3}
Carbohydrates	X_{ch}	0	kgCOD m^{-3}
Proteins	X_{pr}	0	kgCOD m^{-3}
Lipids	X_{li}	0	kgCOD m^{-3}
Sugar degraders	X_{su}	0.012	kgCOD m^{-3}
Amino acid degraders	X_{aa}	0.012	kgCOD m^{-3}
LCFA degraders	X_{fa}	0.012	kgCOD m^{-3}
Valerate and butyrate degraders	X_{c4}	0.012	kgCOD m^{-3}
Propionate degraders	X_{pro}	0.012	kgCOD m^{-3}
Acetate degraders	X_{ac}	0.012	kgCOD m^{-3}
Hydrogen degraders	X_{h2}	0.012	kgCOD m^{-3}
Particulate inerts	X_I	0.000001	kgCOD m^{-3}
Total dissolved Calcium	S_{Ca}	0.002	kmole m^{-3}
Total dissolved Magnesium	S_{Mg}	0.0025	kmole m^{-3}
Total dissolved Nickel	S_{Ni}	variable (0.000001 – 0.00001)	kmole m^{-3}
Total dissolved Cobalt	S_{Co}	variable (0.0000001 – 0.000001)	kmole m^{-3}
Total dissolved Iron	S_{Fe}	variable (0.0000001- 0.0001)	kmole m^{-3}
Inorganic phosphorous	S_{po4}	0.006	kmole m^{-3}
Inorganic sulphur	S_{hs}	0.0002	kmole m^{-3}
Potassium	S_K	variable (0 - 0.4)	kmole m^{-3}
Chlorine	S_{Cl}	variable (0 - 0.4)	kmole m^{-3}
Precipitates	X_{prec}	0.00000001	kmole m^{-3}
Gases	S_{gases}	0	kgCOD m^{-3}
EDTA	S_{EDTA}	variable (0 - 0.0004)	kmole m^{-3}
Biomass carboxyl binding site	≡X_COOH	0.002*0.012*7/1.4	kmole m^{-3}
Biomass phosphoryl binding site	≡X_PO_4H	0.0008*0.012*7/1.4	kmole m^{-3}
Biomass hydroxyl binding site	≡X_OH	0.00017*0.012*7/1.4	kmole m^{-3}
Particulate inert carboxyl binding site	≡XI_COOH	0.002*0.000001/1.4	kmole m^{-3}
Particulate inert phosphoryl binding sit	≡XI_PO_4H	0.0008*0.000001/1.4	kmole m^{-3}
Particulate inert hydroxyl binding site	≡XI_OH	0.00017*0.000001/1.4	kmole m^{-3}
Soluble inert carboxyl binding site	≡SI_COOH	0.00621*0.0000001/1.4	kmole m^{-3}
Soluble inert phosphoryl binding site	≡SI_PO_4H	0.00053*0.0000001/1.4	kmole m^{-3}
Soluble inert hydroxyl binding site	≡SI_OH	0.00693*0.0000001/1.4	kmole m^{-3}
FeS sulfyhydrl binding site	≡XP_SH	$93*10^{-6}$*0.00000001	kmole m^{-3}

Table 3A.6 - Validation of model results (precipitation and complexation) with Visual MINTEQ outputs

INPUT											I		pH		Precipitates formed out of 13 selected precipitates		EDTA complexes formed out of all selected EDTA complexes	
NH_4^+	CO_3^{2-}	PO_4^{3-}	Ca^{2+}	Mg^{2+}	Co^{2+}	Ni^{2+}	Fe^{2+}	K^+	Cl^-	$EDTA^{4-}$	Model	MINTEQ	Model	MINTEQ	Model	MINTEQ	Model	MINTEQ
0.1	0.02	0.0006	0.0002	0.00025	$5*10^{-7}$	$5*10^{-4}$	$5*10^{-4}$	0.1	0.2	0.0001	0.203	0.20269	5.694	5.712	$NiCO_3$: 10^{-4} $Fe_3(PO_4)_2$: 10^{-4}	$NiCO_3$: 10^{-4} $Fe_3(PO_4)_2$: 10^{-4}	CoEDTA_tot: 10^{-9} FeEDTA_tot: 10^{-10} NiEDTA_tot : 10^{-5}	CoEDTA_tot: 10^{-9} FeEDTA_tot : 10^{-10} NiEDTA_tot: 10^{-5}
0	0	0.05	$2.5*10^{-6}$	$2.5*10^{-5}$	$5*10^{-7}$	$5*10^{-4}$	0.05	0	0	0.00001	0.01629	0.01163	3.494	3.495	$Fe_3(PO_4)_2$: 10^{-2}	$Fe_3(PO_4)_2$: 10^{-2}	CoEDTA_tot: 10^{-11} FeEDTA_tot: 10^{-9} NiEDTA_tot: 10^{-6}	CoEDTA_tot: 10^{-11} FeEDTA_tot: 10^{-9} NiEDTA_tot: 10^{-6}
0	0	0.05	$2.5*10^{-6}$	$2.5*10^{-5}$	$5*10^{-7}$	$5*10^{-4}$	0.05	0.1	0.02	0.00001	0.2238	0.2240	1.623	1.619	Nil	Nil	CoEDTA_tot: 10^{-11} FeEDTA_tot: 10^{-7} NiEDTA_tot: 10^{-6}	CoEDTA_tot : 10^{-10} FeEDTA_tot: 10^{-8} NiEDTA_tot: 10^{-6}

Table 3A.6 – *(Continued)*

INPUT											I		pH		Precipitates formed out of 13 selected precipitates		EDTA complexes formed out of all selected EDTA complexes	
NH_4^+	CO_3^{2-}	PO_4^{3-}	Ca^{2+}	Mg^{2+}	Co^{2+}	Ni^{2+}	Fe^{2+}	K^+	Cl^-	$EDTA^{4-}$	Model	MINTEQ	Model	MINTEQ	Model	MINTEQ	Model	MINTEQ
0	0	0.0006	0.0002	0.00025	$5*10^{-7}$	$5*10^{-4}$	$5*10^{-4}$	0.1	0.02	0.0001	0.09556	0.09560	12.437	12.438	$Ca_3(PO_4)_2$: 10^{-4}	$Ca_3(PO_4)_2$: 10^{-5}	CaEDTA_tot: 10^{-7} CoEDTA_tot: 10^{-8} FeEDTA_tot: 10^{-6} MgEDTA_tot: 10^{-7} NiEDTA_tot: 10^{-5}	CaEDTA_tot: 10^{-8} CoEDTA_tot: 10^{-9} FeEDTA_tot: $10^{\wedge-5}$ MgEDTA_tot: 10^{-8} NiEDTA_tot: 10^{-5}
0	0	0.0006	0.0002	0.00025	$5*10^{-7}$	$5*10^{-4}$	$5*10^{-4}$	0.1	0.2	0.0001	0.19775	0.19780	1.158	1.161	Nil	Nil	CoEDTA_tot: 10^{-9} FeEDTA_tot: 10^{-9} NiEDTA_tot: 10^{-4}	CoEDTA_tot: 10^{-9} FeEDTA_tot: 10^{-9} NiEDTA_tot: 10^{-5}
0	0	0.0006	0.0002	0.00025	$5*10^{-7}$	$5*10^{-4}$	$5*10^{-4}$	0.01	0.02	0.0001	0.02237	0.02237	2.505	2.539	Nil	Nil	CoEDTA_tot: 10^{-9} FeEDTA_tot: 10^{-9} NiEDTA_tot: 10^{-5}	CoEDTA_tot: 10^{-9} FeEDTA_tot: 10^{-9} NiEDTA_tot: 10^{-5}

CHAPTER 4

Model Based Analysis of Trace Metal Dosing Strategies to Improve Methane Yield in Anaerobic Digestion Systems

ABSTRACT: Favourable effects of trace metals (TMs) on regulating anaerobic digestion (AD) performance are extensively utilised to improve methane yield in anaerobic digesters. There are various decision factors before supplementing TMs to AD systems. This study discusses a model-based approach to find out the best strategies to dose TMs into anaerobic digesters. The model considers major processes influencing metal speciation in AD including precipitation, complexation (with inorganics, metabolites, chelates) and adsorption (on biomass, soluble inerts, precipitates). TM speciation model in AD has been applied to compare continuous, preloading, pulse dosing and in-situ loading. A comparison between high concentration at low dosing frequency and low dosage at high dosing frequency is performed with model simulations. Simulations were also carried out to comprehend appropriate dosing form, dosing time and quantity of metals to be dosed. Model results show that the best way to dose TMs is repeated pulse dosing at optimum low concentration levels with high frequency. Preferable dosing form depends on reactor configuration and retention times. Metal chloride dosing is favourable over metal-EDTA complexes for continuous reactor due to wash out of metals through effluent when dosed as highly soluble metal chelates like EDTA complexes. For a batch or semi-continuous reactor, metal-EDTA complexes are the preferred way to dose. Influence of reactor configuration on dosing form has also been verified after model calibration with experimental data.

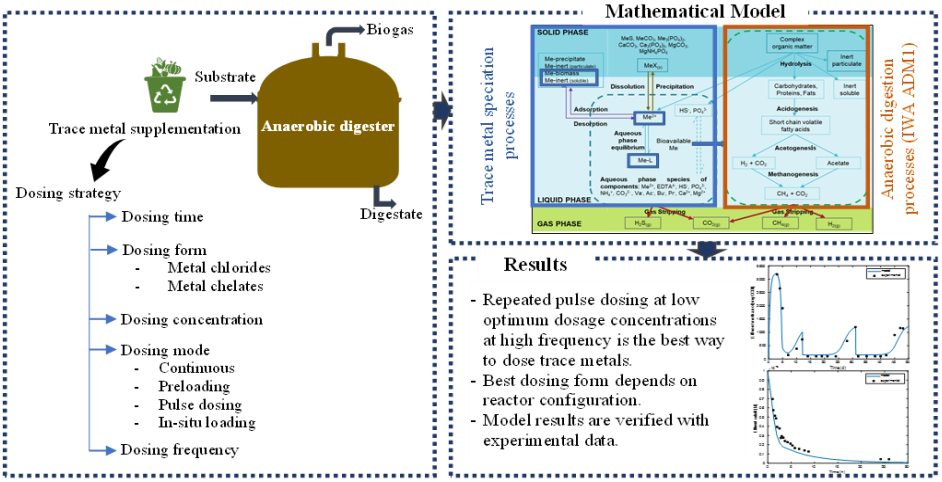

4.1. INTRODUCTION

Poor performance of anaerobic digestors due to trace metal deficiency for the microorganisms present in different anaerobic digestion pathways is widely accepted. Numerous studies have reported improvement in digestor performance and biogas yield for reactors under deprivation by supplementing TMs (Y. Cai, Hua, et al., 2017; Feng et al., 2010; Molaey et al., 2018; Wei et al., 2014; Wintsche et al., 2016). Influence of dosing strategy on TM effects are also widely reported (Aquino & Stuckey, 2007; W. Cai et al., 2018; Fermoso et al., 2010; Yu et al., 2015).

Dosing form of TMs is one major factor influencing TM response of an anaerobic reactor. TMs are commonly dosed in form of metal ions (as chlorides), metal chelate complexes (ethyleneaminetetraacetic acid (EDTA), ethylenediamine-N,N′-disuccinic acid (EDDS), citrate, nitrilotriacetic acid (NTA)) or through feedstock containing trace metals. Supplementing chelates like EDTA to an AD system improved metal bioavailability by forming strong soluble TM-EDTA complexes (Chapter 3). Moreover, further improvement in digestor performance was observed when TMs were dosed as TM-EDTA complexes instead of supplementing TMs and EDTA simultaneously (Chapter 3).

Another decision factor regarding dosing strategy that can influence metal requirement is the procedure/mode of dosing – continuous, pulse or preloading. Continuous and pre-loading of metals can result in loss of metals through the effluent (Zandvoort et al., 2002, 2004). Pulse dosing procedure requires less amount of metals and wastage is minimum compared to other forms of dosing (Fermoso et al., 2008). This makes the dosing frequency a decision-making factor. Optimal frequency of dosing TMs at low concentrations can simultaneously increase reactor performance and decrease sludge metal losses. Timing of dosing is another major factor to be considered while dosing. Fermoso et al. (2008) observed that Co dosing both in form of pulse and continuous addition during high acetate concentrations stimulated acidification due to Co dependence of enzymes involved in acetogenesis.

Quantity/concentration of metals reported in literature to stimulate reactor performance vary significantly (Thanh et al., 2016). This is because TM effects classified as stimulation, inhibition and toxicity depend on the bioavailable metal fraction. Absence of TMs or presence of TMs below optimum levels can cause metal deprivation whereas metals supplied in excess can cause toxicity. Hence, maintaining optimum TM concentration in the system is significant, thereby adding another factor to decide during metal supplementation, i.e. dosing concentration.

TM effects on microorganisms depend on metal speciation, which is influenced by the equilibrium and kinetics of processes influencing metals. Metal bioavailability and dosing strategy are therefore dependent on factors like operational conditions, labile metal fraction and type of microorganisms involved. Reactor operational conditions include operational pH (acidogenic/methanogenic), redox potential, ionic strength, operational temperature

(mesophilic/thermophilic), organic loading rate (OLR), metal retention capacity of the reactor which is dependent on factors like hydraulic retention time (HRT), solid retention time (SRT) and existing metal concentration in the reactor influenced by feedstock characteristics and digestion operating mode (mono/co-digestion).

Due to wide variation in environmental conditions for the microbes existing in different systems, metal requirement and dosing response shown by different systems vary. For instance, effect of EDTA on improving metal lability depends on reactor configuration and metal retention capacity. Supplementation of Co-EDTA^{2-} to an upflow anaerobic sludge blanket (UASB) reactor reduced metal retention capacity from 90% (when it was dosed as $CoCl_2$) to 8% as the metal EDTA complexes were highly soluble and were easily washed out (Fermoso et al., 2008). However, Vintiloiu et al. (2013) observed an increase in metal bioavailability when Ni-EDTA complex was supplemented in a batch system.

A model-based approach will help to easily optimise the best dosing strategy applicable for each individual system. In Chapter 2 and Chapter 3, models are developed for TM speciation during AD using Anaerobic Digestion Model 1 (ADM1) and the capability of the model in predicting major processes (precipitation, complexation, adsorption) affecting metal speciation was verified. This paper aims to apply the trace metal speciation model in AD for optimising the dosing strategies applicable to individual systems. No model-based studies have been carried out so far to completely define a best trace metal dosing protocol in anaerobic digestors. Objectives of this study are to calibrate/verify the model with experimental data and to optimise the TMs dosing strategy in terms of mode of dosing (continuous, pulse, preloading, in-situ loading), dosing frequency (high dosage, low frequency versus low dosage, high frequency, concentration of dosing), dosing form (metal chlorides versus meta-EDTA complex) and time of dosing.

4.2. METHODOLOGY

4.2.1. Mathematical model

Model consisting of algebraic equilibrium reactions and ordinary differential equations (ODEs) for kinetic processes is implemented in MATLAB platform. Algebraic equations are solved by multi-dimensional Newton Raphson method coupled with simulated annealing algorithm to reduce initial guess dependency. ODE 15s solver in MATLAB run in sequential iteration with Newton Raphson method is used to solve ODEs (Chapter 2).

4.2.2. Aqueous phase model

Liquid-liquid processes considered in the model include acid base reactions, all possible inorganic complexes formed from cations and anions defined in the model, organic complexation with metabolites like amino acids (cystine, glutamine, glycine), volatile fatty acids (VFAs - butyrate, valerate, propionate, acetate) and chelate additives like EDTA. All aqueous phase reactions except EDTA complexation are defined as equilibrium reactions as they occur rapidly. Ion activity is used instead of molar concentration to consider ionic

strength effects (Chapter 2). Non-linear algebraic equations used to describe equilibrium reactions are based on material conservation principle (Eq. (4.1) and Eq. (4.2)) where A_i, S_i and A_j, S_j are the activity and concentration of specie i and component j. k_i is equilibrium coefficient with temperature corrections, $\nu_{i,j}$ is the stoichiometric coefficient of the j^{th} component in specie i. $S_{j,tot}$ is the total dissolved concentration, N_s is the number of considered species and N_c is the number of components. γ is the corresponding activity coefficient that depends on ionic strength calculated from Davies equation.

$$\boldsymbol{A_i = k_i \prod_{j=1}^{N_c} A_j^{\nu_{i,j}}}\,, \tag{4.1}$$

$$\boldsymbol{S_{j,tot} = S_j + \sum_{i=1}^{N_s} \nu_{i,j} S_i = \frac{A_j}{\gamma} + \sum_{i=1}^{N_s} \nu_{i,j} \frac{A_i}{\gamma}}\,. \tag{4.2}$$

4.2.2.1. EDTA complexation model

Protonation/deprotonation reactions of EDTA and complexation of cations including TMs with EDTA are defined in the model as kinetic rate reactions (Eq. (4.3))

$$\rho_{comp} = k_1 A_{EDTA} A_{Me} - k_{-1} A_{MeEDTA}\,, \tag{4.3}$$

where ρ_{comp} is the EDTA complexation rate, A_{EDTA}, A_{Me} *and* A_{MeEDTA} are the activities of EDTA, metal ions and metal-EDTA complex. k_1 and k_{-1} are formation and dissociation rate constants respectively (Chapter 3).

4.2.3. Precipitation model

Precipitation reactions are modelled as reversible reactions based on saturation index (SI) calculated based on Eq. (4.4) (Chapter 2). If solution is supersaturated (SI>1), precipitation reaction mathematically expressed as Eq. (4.5) is activated and re-dissolution (Eq. (4.6)) occurs when SI<1.

$$\text{SI} = \frac{(A_{M^{\nu+}})^x (A_{N^{\nu-}})^y}{K_{sp}}\,, \tag{4.4}$$

$$\rho_{prec} = k_r' \left(((A_{M^{\nu+}})^x (A_{N^{\nu-}})^y)^{1/\nu} - {K_{sp}}^{1/\nu}\right)^n\,, \tag{4.5}$$

$$\rho_{diss} = -k_r' \left(((A_{M^{\nu+}})^x (A_{N^{\nu-}})^y)^{1/\nu} - {K_{sp}}^{1/\nu}\right)^n \frac{1}{1 + (K/S_{M_xN_y})}\,. \tag{4.6}$$

$A_{M^{\nu+}}$and $A_{N^{\nu-}}$ are the activities of cations and anions. x and y are the number of cations and anions. K_{sp} is the solubility product, k_r' is the rate constant, ν is the sum of cations and anions,

$S_{M_xN_y}$ is the concentration of precipitate and K is the dissolution hyperbolic inhibition constant.

4.2.4. Adsorption model

Adsorption of TMs on surfaces of biomass, particulate inerts (dead biomass), soluble inerts (soluble microbial products and extracellular polymeric substances) and precipitate FeS is modelled by electrostatic surface complexation model (Eq. (4.7)) where metal undergoes surface complexation with deprotonated carboxyl, hydroxyl, phosphoryl and sulfhydryl functional groups present on the adsorbent surface (Chapter 3).

$$\rho_{ads} = k_f A_{Me} S_{\equiv X-COO^-} - k_b S_{\equiv X-COOMe^+} \quad (4.7)$$

k_f and k_b are the formation and desorption rate constants, A_{Me} is the activity of metal ion, $S_{\equiv X-COO^-}$ and $S_{\equiv X-COOMe^+}$ are concentrations of free binding site (carboxyl in this case) and adsorbed metal on binding site.

4.2.5. Coupling physiochemical trace metal effects to biological reactions

Biochemical module in ADM1 is modified by adding metal uptake during biological reactions and release of TMs during disintegration of organic matter as explained in Chapter 2. Stimulation and inhibition effect of TMs is coupled to microbial processes using a modified dose response function defined by Eq. (4.8) as limiting factor

$$I_{Me} = I_0 + \frac{I_{max} - I_0}{(1+\frac{EC_{50}}{Me_{labile}})^a (1+\frac{Me_{labile}}{IC_{50}})^b}, \quad (4.8)$$

where I_0 is the baseline of limiting factor at concentration levels approaching zero, I_{max} is the maximum response, EC_{50} is the concentration of TM where 50% maximum effect is observed, IC_{50} is the TM concentration when 50% inhibition/toxicity is achieved, a and b are parameters affecting slope of left- and right-hand sides of the curve respectively. The dose response function has been modified in this chapter to explicitly capture differential response of microbes to different trace metals. Labile metal fraction (Me_{labile}) used in the dose response function consists of dissolved metal, metal complexed with EDTA and adsorbed metal on biomass and soluble inerts solved from the physicochemical module. More details on the biochemical module and stoichiometry matrix for biochemical and physicochemical module can be found in Chapter 2 and Chapter 3.

4.2.6. Dosing strategy model scenarios

Model is tested under different scenarios of dosing strategies to check model capability for experimental and industrial applications. Main dosing strategies are mode of dosing, dosing frequency, concentration of dosing, dosing form and time of dosing. In the first scenario, simulations are run for a continuous reactor at a concentration of 5 µM with different modes of dosing – pulse addition, continuous dosing, preloading and in-situ loading. For the same

overall dosing concentration, pulse dosing frequency is tested at different intervals in the second scenario. Different concentrations of TM (Co) are dosed in the third scenario to check stimulatory and inhibitory effects of trace metal on AD performance in a batch reactor system. Pulse dosing is done at variable times in a continuous reactor system under metal deprivation to check the influence of time of dosing in the fourth scenario. Cobalt addition is done as $CoCl_2$ and Co-EDTA complex for continuous and semi-continuous reactors in the fifth scenario to check the best form of dosing suitable for different reactor configurations. Operational conditions, initial and influent values of state variables for different scenarios are given in Appendix 4.1.

4.2.7. Model application

The model is applied to simulate experimental observations reported in Fermoso et al. (2008) for checking best form of dosing in a continuous reactor. Two 3.25 L continuous reactors fed with methanol operating at OLR of 8.5 gCOD L^{-1} $D^{-1}$and HRT of 8 hours were dosed with 5 µM Co in form of $CoCl_2$ and Co-EDTA complex, respectively.

The UASB reactors are modelled as CSTRs using ODEs formulated based on mass conservation principle defining dynamics of model components: soluble and particulate species (similar to ADM1), dissolved metal Me_i (Eq. (4.9), precipitate $Me_{p,i}$ (Eq. (4.10)), metal-EDTA complex $Me_{c,i}$ (Eq. (4.11)), adsorbed metal $Me_{a,i}$ (Eq. (4.12)), protonated binding site $BS_{pro,i}$ (Eq. (4.13)) and de-protonated/free binding site $BS_{free,i}$ (Eq. (4.14))

$$\frac{dV_{liq}\,Me_i}{dt} = q_{in}\,Me_{in,i} - q_{out}\,Me_i + V_{liq}\sum_{j=1}^{m_1}\alpha_{i,j}\rho_{uptake,j}\,(t, Me) - V_{liq}\sum_{j=1}^{m_2}\beta_{i,j}\rho_{prec,j}\,(t, Me, Me_p) + V_{liq}\sum_{j=1}^{m_2}\beta_{i,j}\rho_{diss,j}\,(t, Me, Me_p)\,) - V_{liq}\sum_{j=1}^{m_3}\gamma_{i,j}\rho_{comp,j}\,(t, Me, Me_c) - V_{liq}\sum_{j=1}^{m_4}\delta_{i,j}\rho_{ads,j}\,(t, Me, Me_a),\ i = 1,..,n_1, \quad (4.9)$$

$$\frac{d\,V_{liq}\,Me_{p,i}}{dt} = q_{in}Me_{in,p,i} - q_{out}\,f_{p,removal}\,Me_{p,i} + V_{liq}\beta_{i,j}\rho_{prec,j}(t, Me, Me_p) - V_{liq}\beta_{i,j}\rho_{diss,j}(t, Me, Me_p),\ i = 1,..,m_2\,, \quad (4.10)$$

$$\frac{d\,V_{liq}\,Me_{c,i}}{dt} = q_{in}Me_{in,c,i} - q_{out}Me_{c,i} + V_{liq}\gamma_{i,j}\rho_{comp,j}(t, Me, Me_c), i = 1,..,m_3, \quad (4.11)$$

$$\frac{d\,V_{liq}\,Me_{a,i}}{dt} = q_{in}Me_{in,a,i} - q_{out}Me_{a,i} + V_{liq}\delta_{i,j}\rho_{ads,j}(t, Me, BS_{free}, Me_a),\ i = 1,..,m_4, \quad (4.12)$$

$$\frac{d\,BS_{pro,i}}{dt} = q_{in}BS_{in,pro,i} - q_{out}Me_{in,pro,i} + D_{BS,i}\rho_{form} + \rho_{prot}(t, BS_{pro}, BS_{free}), i = 1,..,n_2, \quad (4.13)$$

$$\frac{d\,BS_{free,i}}{dt} = q_{in}BS_{in,free,i} - q_{out}BS_{in,free,i} - \rho_{prot}(t, BS_{pro}, BS_{free}) - \delta_{i,j}\rho_{ads,j}(t, Me, BS_{free}, Me_a),\ i = 1,..,n_2, \quad (4.14)$$

where V_{liq} is the reactor volume, q_{in} and q_{out} are the influent and effluent flow rates, ρ_{uptake}, ρ_{prec}, ρ_{diss}, ρ_{comp}, ρ_{ads}, ρ_{form} and ρ_{prot} are the kinetic rate expressions for metal uptake, precipitation, dissolution, complexation, adsorption, binding site formation and protonation processes respectively for component i. $Me_{in,i}$, $Me_{in,p,i}$, $Me_{in,c,i}$, $Me_{in,a,i}$, $BS_{in,pro,i}$ and $BS_{in,free,i}$ denote influent concentrations of metal dissolved, precipitated, complexed, adsorbed, protonated binding sites and free binding sites respectively. Number of soluble metal species and binding sites is represented as n_1 and n_2. m_1, m_2, m_3 and m_4 denote number of uptake processes, precipitation/dissolution processes, EDTA complexation and adsorption processes under consideration. $\alpha_{i,j}$, $\beta_{i,j}$, $\gamma_{i,j}$, $\delta_{i,j}$ represent stoichiometric coefficient of species i on j^{th} uptake, precipitation/dissolution process, complexation and adsorption processes. $f_{p,removal}$ is the factor of precipitate in the sludge that is removed through the effluent. $D_{BS,i}$ is the density of binding site i on surfaces of biomass, inert and precipitate. Rate of binding site formation (ρ_{form}) on each of these surfaces is given in Eq. (4.15), Eq. (4.16), Eq. (4.17) where ρ_{growth}, ρ_{decay} and $\rho_{production}$ represent biomass growth rate, decay rate and production rate of inert, respectively.

For biomass, $\rho_{form} = \rho_{growth} - \rho_{decay}$, (4.15)

For inert, $\rho_{form} = \rho_{production}$, (4.16)

For precipitate, $\rho_{form} = \rho_{prec} - \rho_{diss}$. (4.17)

4.2.8. Sensitivity analysis

By considering the complexity of model and number of parameters, a local sensitivity analysis (LSA) based on one-factor-at-a-time method is chosen to identify the most influential parameters on model outputs. The first-order partial derivative of the output variable with respect to the parameter under consideration is computed in order to analyse the impact of a changing parameter (Zi, 2011). Sensitivity Index $SI_{i,j}$ for each parameter j with respect to i^{th} output state variable is calculated using Eq. (4.18)

$$SI_{i,j} = \frac{\partial y_i}{\partial u_j}\,\frac{u_j}{y_i}, \quad (4.18)$$

where $\frac{\partial y_i}{\partial u_j}$ is the highest of absolute maximum or absolute minimum value of the computed partial derivative of i^{th} output variable with respect to the j^{th} parameter at the instant time t, for t ranging from zero to final duration. 5% change in parameter value is considered for computing partial derivatives. u_j represents initial parameter value and y_i represents value of

output state variable *i* obtained using initial parameter values. Initial parameter values are set to roughly fit experimental data with values adopted from the acceptable ranges reported in literature (Table 4.4). Values reported in Batstone et al. (2002) are used for ADM1 stoichiometric parameters and metal speciation process parameters as reported in Chapter 2 and Chapter 3.

Only those parameters with unknown values or with high variability in reported values from literature are selected for performing sensitivity analysis. Some parameters whose values are theoretically calculated like those in complexation and adsorption models are also excluded from sensitivity analysis. Sensitivity of the parameters given in Table 4.4 are calculated with respect to output state variables, substrate (methanol) and cumulative methane production. Numerical analysis is carried out in MATLAB using an ode solver coupled with *sens_sys* tool (Molla & Padilla, 2002).

4.2.9. Model calibration

Parameters with highest sensitivity for both chosen model output state variables, methanol and cumulative methane production are calibrated using a trial and error method to fit experimental data. Each selected parameter is individually calibrated in the order of their sensitivity index until a reasonable fitness with experimental data is obtained (Sin et al., 2008). Accuracy of model calibration is determined from performance indicators (Janssen & Heuberger, 1995), namely index of agreement (IoA), root mean square error (RMSE) and normalised root mean square error (NRMSE) as expressed in Eq. (4.19), Eq. (4.20) and Eq. (4.21), respectively.

$$\mathrm{IoA} = 1 - \frac{\sum_{i=1}^{N}(P_i - O_i)^2}{\sum_{i=1}^{N}(|P_i - \bar{O}| + |O_i - \bar{O}|)^2}, \tag{4.19}$$

$$\mathrm{RMSE} = \sqrt{\frac{\sum_{i=1}^{N}(P_i - O_i)^2}{N}}, \tag{4.20}$$

$$\mathrm{NRMSE} = \frac{RMSE}{O_{i,max} - O_{i,min}}. \tag{4.21}$$

P_i and O_i are the i^{th} model predicted and observed values. $\bar{O}$, $O_{i,max}$ and $O_{i,min}$ are the mean, maximum and minimum of observed value respectively and N is the number of observations.

4.3. RESULTS AND DISCUSSION

4.3.1. Dosing strategy simulations

Simulations to study various dosing strategies indicate that model results coincide with the outcomes obtained from experimental studies. Best protocol of dosing in terms of dosing mode, dosing frequency, dosing form, quantity and time of trace metals to be dosed is discussed in sections below.

4.3.1.1. Mode of dosing

Simulation results from a continuous AD model reactor system supplemented with trace metal Co by various modes of dosing showed different responses (Fig. 4.1). Maximum methane production is observed for 5 µM continuous dosing mode. However, metal lost through the effluent in continuous dosing is comparatively high (in the range of 10^{-5} moles). This observation agrees with Gonzalez-Gil et al. (1999) and Zandvoort et al., (2002). Gonzalez-Gil et al. (1999) compared continuous addition with single pulse additions and found improved Co bioavailability and methane production with continuous dosing. Restricted Co dosing due to relatively higher loss of Co through the effluent during continuous dosing was recommended by Zandvoort et al. (2002).

A comparison with other modes of dosing namely preload, in-situ loading for 24 hours on day 20 and pulse load at day 5 and day 20 at concentrations of 5 µM suggests pulse and preloading to be better options. Though methane production is almost the same with these conditions, metal lost through the effluent is high for in-situ loading for 24 hours. This contradicts the observation reported in Zandvoort et al. (2004). This is because of lower Co concentration adopted in Zandvoort et al. (2004) for in-situ loading as compared to preloading condition. Only 16 % of mass of cobalt present in preloaded sludge was used for in-situ loading.

Later, simulations were performed to compare pulse and preloading for further improving methane production. Concentration of preloading is increased from 5 µM to 5 mM and pulse loading at 5 µM is done at more frequent intervals (5 days intervals). Preloading at 5 mM increased cumulative methane production to 0.0025 M while 5 µM pulse loading at 5 days intervals gives higher methane production (0.0052 M). Moreover, cobalt lost through the effluent for 5 µM pulse loading at 5 days intervals (range of 10^{-7} moles) is less than that for preloading at 5 mM (range of 10^{-5} moles). Hence, best dosing strategy for the system under consideration is 5 µM pulse loading at 5 days intervals as it gives maximum methane production (almost same as continuous loading) and low metal loss through the effluent. Likewise, Fermoso et al. (2008) demonstrated that repeated pulse dosing of low concentrations of $CoCl_2$ (5 µM) as a compromise between continuous, pre-loading and pulse dosing at high Co concentrations to overcome metal limitation without significant metal loss through the effluent. Moreover, pulse dosing at regular intervals is a more cost-effective strategy than continuous addition thereby helping in minimising operational costs.

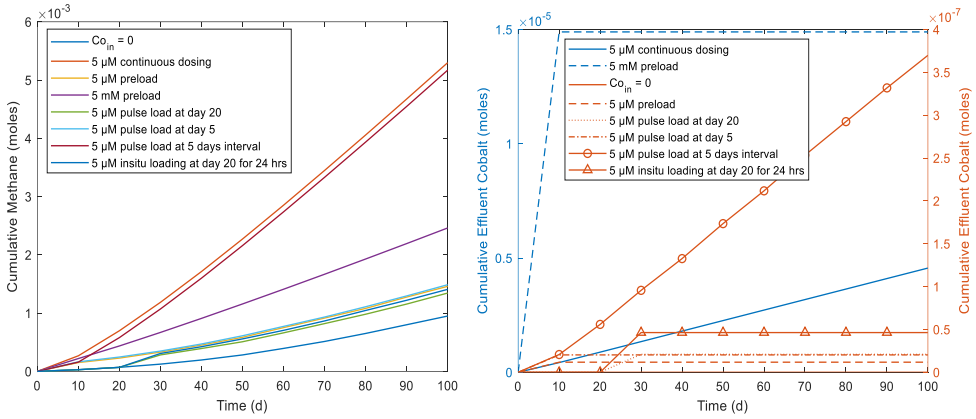

Figure 4. 1 - Effect of different modes of dosing on (a) methane production (b) effluent cobalt

4.3.1.2. Frequency of dosing

Since repeated pulse dosing is found to be the best mode of dosing from the previous section, simulations were performed to find best dosing frequency. For the same overall metal dosing, three different conditions were chosen for comparison - 5 µM at 5 days intervals, 10 µM at 10 days intervals and 24 µM at 20 days intervals. Maximum cumulative methane production is obtained for 5 µM at 5 days intervals (Fig. 4.2). Hence low dosing concentration at higher frequency is better than high dosage, low frequency dosing strategy. Cao et al. (2019) compared these strategies for mitigating sulphide and methane production in sewers and reported that high dosage, low frequency suppressed methanogenic activity and methane production as compared to low dosage, high frequency ferric dosing strategy. Moreover, a comparison between 5 µM at 5 days intervals and 5 µM at 10 days intervals shows that methane production increases with increase in dosing frequency for the same dosing concentration. Wang et al. (2020) reported Fe^{2+} dosing frequency of 5 days to be more effective than 10 days and 20 days during mesophilic and thermophilic dry anaerobic digestion processes. They observed weakening of metal effect when dosing frequency was increased from 5 days to 20 days. Similarly, a comparison between 5 µM at 10 days intervals and 10 µM at 10 days intervals shows increase in methane production with increase in concentration (within optimum dosing levels) for the same frequency of dosing.

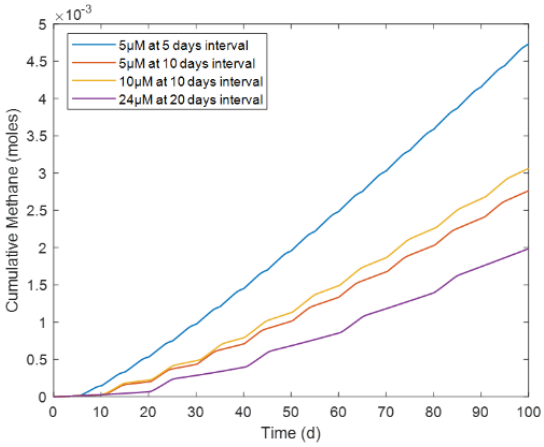

Figure. 4.2 - Effect of frequency of dosing on methane production

4.3.1.3. Concentration of dosing

Fig. 4.3(a) shows the effect of dosing concentration of trace metal (iron) on cumulative methane production in a batch reactor system. Methane production increased when iron concentration is increased stepwise from 0 μM to 100 μM. This shows stimulatory effects of iron on anaerobic digestion. However, when iron dosing concentration is further increased to 1 mM, methane production drastically decreased due to inhibitory effects of iron on methane production. The results show that an increase in metal supplementation will not necessarily improve methane production. Dosing metals in excess of their optimum levels cause metal toxicity (Y. Cai, Zhao, et al., 2017; Facchin et al., 2013).

4.3.1.4. Time of dosing

Fig. 4.3(b) shows that effect of TM dosing on AD is influenced by time of dosing. For a continuous reactor system under Co deprivation, single pulse dosing at different time gives different reactor performances. Methane production observed for dosing at day 5 is greater than at day 20 which is greater than at day 60. Therefore, the earliest dosing time following a metal deficit is the preferred time to dose. Delay in dosing a deprived metal can minimize the effects of TM dosing on AD. Fermoso et al. (2008) stated that metal addition to a metal deprived methanogenic granular sludge reactor has to be done prior to VFA accumulation in the effluent. Reactor performance could not be recovered when deprived metal was added to the reactor after VFA accumulation in the reactor.

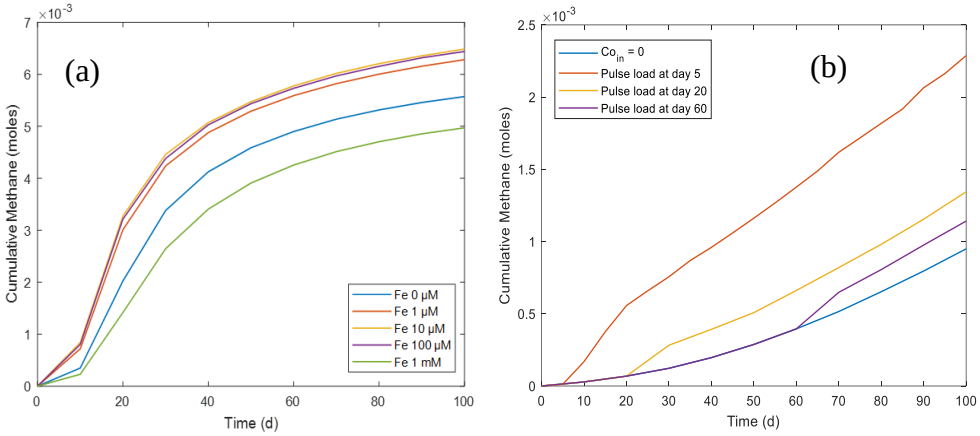

Figure. 4.3 - Effect of (a) dosing concentration and (b) time of dosing on methane production

4.3.1.5. Form of dosing

Trace metals are usually dosed to reactors as chlorides (get easily dissociated) or strong chelates like EDTA complexes. For a continuous UASB reactor system, Co supplemented as $CoCl_2$ has better and long-term effects on daily methane production than Co-EDTA complex (Fig. 4.4(a)). This is due to high solubility of metal-EDTA complex and complete washout of supplemented Co through the effluent as can be found in Fig. 4.4(a)). When Co is supplemented on day 5 as $CoCl_2$, it remains accumulated (mainly in form of precipitates) in the sludge and labile Co will be available for an extended period through dissolution of the precipitates accumulated in the sludge. Similar observations are reported by Fermoso et al. (2008). Application of the model to simulate experimental outcomes from Fermoso et al. (2008) where two continuous reactors were supplemented with Co in form of $CoCl_2$ and Co-EDTA complex is discussed in Section 4.3.3. For a batch reactor system, dosing TMs as metal EDTA complexes is more effective than supplementing them as chlorides or supplementing metals and EDTA separately (Thanh et al., 2017; Zhang et al., 2015; Chapter 3). Fig. 4.4(b) shows comparison between the two forms of dosing for a semi-continuous reactor system with HRT of 30 days where Co is supplemented along with the feed at 10 days intervals. Similar to a batch reactor, for a semi-continuous reactor system, Co-EDTA complex dosing is ideal than $CoCl_2$. This is due to higher dissolved Co concentration and metal lability when Co is supplemented as Co-EDTA as discussed by Chapter 3 for a batch reactor system. Hence, best dosing form for TMs can depend on reactor configuration and retention times.

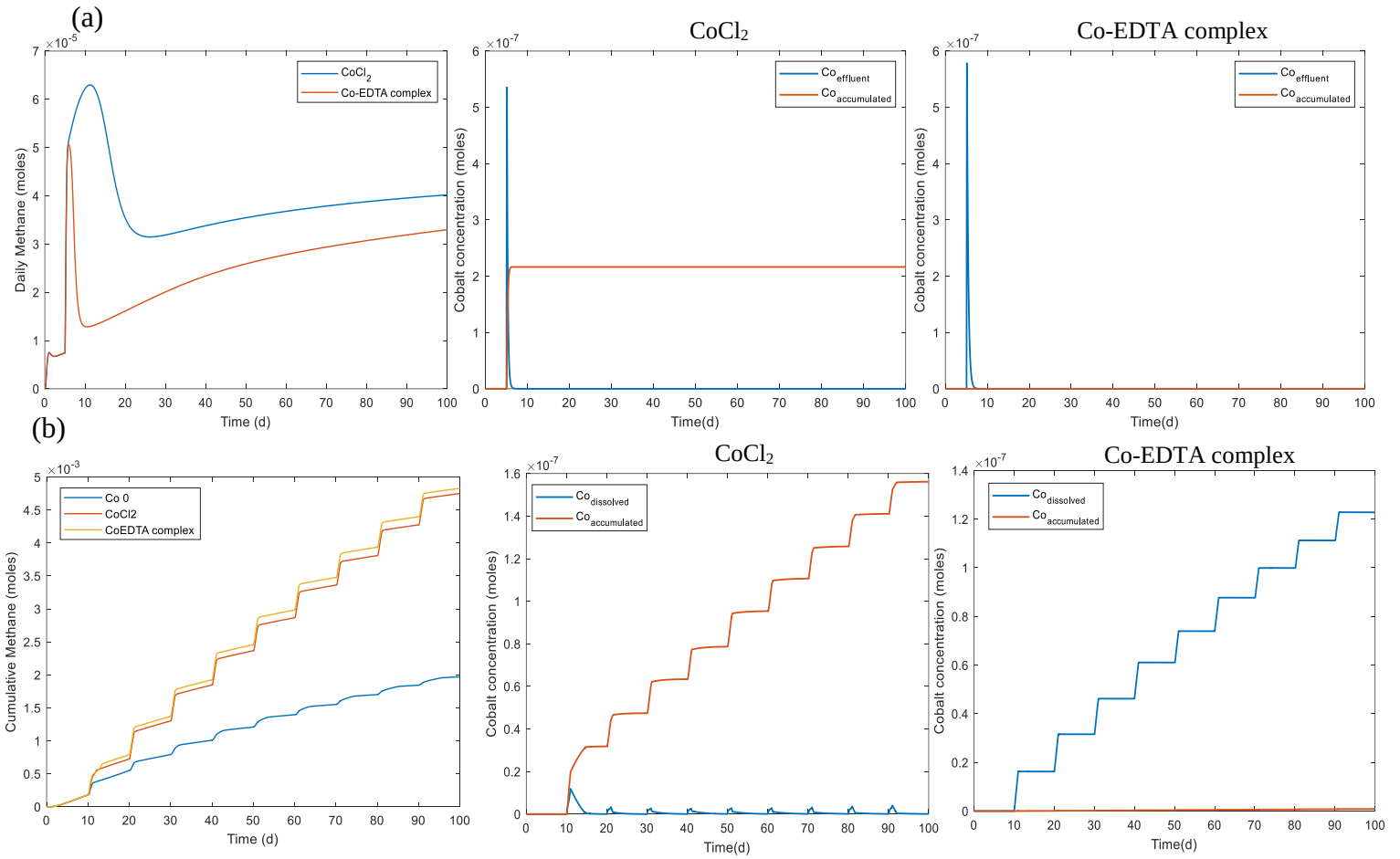

Figure 4.4 - Effect of dosing form on methane production and Co concentration in (a) continuous reactor and (b) semi-continuous reactor

4.3.2. Sensitivity analysis and model calibration

Sensitivity indices of parameters considered in the study with respect to outputs, methane and substrate (methanol) are given in Table 4.4. Few parameters have substantial influence on the model outputs. Results show that most sensitive parameters for both the outputs are maximum specific uptake rate of sugar degraders $k_{m,su}$, factor of CoS removal from reactor $f_{CoS,removal}$, half saturation coefficient of sugar degraders $K_{s,su}$, factor of $CoCO_3$ removal from reactor $f_{CoCO3,removal}$, CoS precipitation/dissolution rate kr_{CoS}, yield coefficient of sugar degraders Y_{su} and decay rate of sugar degraders $k_{dec,su}$. Therefore, only these parameters were calibrated with the experimental data reported in Fermoso et al. (2008). Default values were retained for other stoichiometric parameters. Calibrated values of sensitive parameters for both model applications ($CoCl_2$ and Co-EDTA complex pulse dosing) are given in Table 4.5. Estimation of parameters related to biological pathways ($k_{m,su}$, $K_{s,su}$, Y_{su}, $k_{dec,su}$) are critical during ADM1 applications as reported in previous literatures (Batstone et al., 2002; Razaviarani & Buchanan, 2015). Moreover, since cobalt deprivation is the limiting factor controlling both scenario conditions, reactor performance is limited by the parameters controlling cobalt speciation which includes $f_{CoS,removal}$ $f_{CoCO3,removal}$ and kr_{CoS}. The parameter $f_{CoS,removal}$ depends on the reactor configuration. For a batch and continuous reactor, $f_{CoS,removal}$ is zero. However, since the UASB reactor in this system is modelled as a CSTR, $f_{CoS,removal}$ was introduced to consider retention time of the precipitate. The calibrated model gave an adequate representation of the experimentally measured outputs (Fig. 4.5 and Fig. 4.6).

Performance indicators or goodness of fit indices calculated with respect to outputs, effluent methanol and Co concentrations are given in Table 4.6. As can be observed from the table, IoA coefficients are close to 1, NRMSE values are close to 0 and values of RMSE are small with respect to the actual output values. The values of IoA, NRMSE and RMSE confirmed adequate calibration procedure.

Table 4.4. Initial values and sensitivity indices of parameters considered for sensitivity analysis

Description	Parameter	Initial value	SI with respect to methane	SI with respect to substrate
Maximum specific uptake rate of sugar degraders	$k_{m,su}$	50	941.1235	12.04579
Factor of CoS removal from reactor	$f_{CoS,removal}$	0.2	307.901	4.363645
Half saturation coefficient of sugar degraders	$K_{s,su}$	0.5	252.3188	3.466411
Factor of $CoCO_3$ removal from reactor	$f_{CoCO3,removal}$	0	192.6832	3.027888
CoS precipitation/dissolution rate	kr_{CoS}	10^{10}	189.1311	1.231456
Yield coefficient of sugar degraders	Y_{su}	0.06	149.9254	2.82943
Decay rate of sugar degraders	$k_{dec,su}$	0.02	97.0554	1.276066

Table 4.4 *(Continued)*

Description	Parameter	Initial value	SI with respect to methane	SI with respect to substrate
Yield coefficient of acetate degraders	Y_{ac}	0.05	53.72972	0.05719
Maximum specific uptake rate of acetate degraders	$k_{m,ac}$	14	28.18952	0.07705
Yield coefficient of hydrogen degraders	Y_{h2}	0.06	22.35413	0.031692
Half saturation coefficient of acetate degraders	$K_{s,ac}$	0.15	20.9656	0.024418
FeS precipitation/dissolution rate	kr_{FeS}	10^{12}	18.695	0.112076
Decay rate of sugar degraders	$k_{dec,ac}$	0.02	12.68626	0.246651
Max specific uptake rate of H_2 degraders	$k_{m,h2}$	35	11.77339	0.062758
$FeCO_3$ precipitation/dissolution rate	kr_{FeCO3}	10^{3}	9.503294	0.060051
$CoCO_3$ precipitation/dissolution rate	kr_{CoCO3}	10^{3}	8.333298	0.130756
NiS precipitation/dissolution rate	kr_{NiS}	10^{10}	8.285852	0.05839
Decay rate of hydrogen degraders	$k_{dec,h2}$	0.02	8.22042	0.074521
$Fe_3(PO_4)_2$ precipitation/dissolution rate	$kr_{Fe3(PO4)2}$	10^{5}	6.500763	0.039296
Factor of FeS removal from reactor	$f_{FeS,removal}$	0	5.825193	0.042595
Disintegration constant	k_{dis}	0.5	4.067934	0.160193
Co release from composites	$f_{Co,xc}$	10^{-12}	0.49132	0.007012
Fe release from composites	$f_{Fe,xc}$	10^{-6}	0.47059	0.006002
Ni release from composites	$f_{Ni,xc}$	10^{-7}	0.400512	0.005097
Half saturation coefficient of H_2 degraders	$K_{s,h2}$	7×10^{-6}	0.01093	5×10^{-6}
$MgNH_4PO_4$ precipitation/dissolution rate	$kr_{MgNH4PO4}$	10^{8}	3.7×10^{-31}	4.28×10^{-39}
Factor of NiS removal from reactor	$f_{NiS,removal}$	0	0	0
Co content in microbes	$f_{Co,uptake}$	10^{-10}	0	0
Fe content in microbes	$f_{Fe,uptake}$	10^{-6}	0	0
Ni content in microbes	$f_{Ni,uptake}$	10^{-7}	0	0
Phosphate release from composites	$f_{PO4,xc}$	6×10^{-5}	0	0
Sulphide release from composites	$f_{HS,xc}$	6×10^{-5}	0	0
$CaCO_3$ precipitation/dissolution rate	kr_{CaCO3}	10^{7}	0	0
$MgCO_3$ precipitation/dissolution rate	kr_{MgCO3}	10^{5}	0	0
$NiCO_3$ precipitation/dissolution rate	kr_{NiCO3}	10^{3}	0	0
$Ca_3(PO_4)_2$ precipitation/dissolution rate	$kr_{Ca3(PO4)2}$	10^{8}	0	0
$Ni_3(PO_4)_2$ precipitation/dissolution rate	$kr_{Ni3(PO4)2}$	10^{5}	0	0
$Co_3(PO_4)_2$ precipitation/dissolution rate	$kr_{Co3(PO4)2}$	10^{5}	0	0
Factor of $Co_3(PO_4)_2$ removal from reactor	$f_{Co3(PO4)2,removal}$	0	0	0
Factor of precipitate removal from reactor	$f_{p,removal}$	0	0	0

Table 4.5. Values after calibration for the sensitive parameters

Parameter	$CoCl_2$ dosing	Co-EDTA complex dosing
$k_{m,su}$ (d^{-1})	30	30
$f_{CoS,removal}$	0.25	0.25
Y_{su}	0.02	0.096
$K_{s,su}$ (kgCOD m^{-3})	0.9	0.9
kr_{CoS} (d^{-1})	10^{15}	10^{15}
$k_{dec,su}$ (d^{-1})	0.02	0.15
$f_{CoCO3,removal}$	0.25	0.25

Table 4.6. Performance indicators

Dosing condition	Objective variables for calibration	Performance indicators		
		IoA	NRMSE	RMSE
$CoCl_2$	Effluent Co	0.9417	0.1253	8.1647×10^{-8} (M)
	Effluent methanol	0.9546	0.1167	359.6671(mgCOD/L)
Co-EDTA complex	Effluent Co	0.9576	0.1054	5.6072×10^{-7}(M)
	Effluent methanol	0.9117	0.1990	569.1405(mgCOD/L)

4.3.3. Pulse dosing of $CoCl_2$ versus Co-EDTA complex

Model results from the first scenario of model application show recovery of a reactor undergoing Co deprivation by repetitive pulse dosing of 5 µM $CoCl_2$. Fig. 4.5 shows that the model reproduced experimental data accurately. Pulse dosing of $CoCl_2$ on days 12 and 31 performed after accumulation of methanol in the effluent recovered methanol removal efficiency (Fig. 4.5(a)). Maximum Co concentration in the effluent simulated for 30 hours after first 5 µM $CoCl_2$ pulse dosing showed only around 1 µM concentration in the effluent (Fig. 4.5(b)).

Fig. 4.6 shows comparison of model simulation results with experimental outcomes during second case of model application, i.e. Co-EDTA complex pulse dosing. The experimental data (Fermoso et al., 2008) reported a start-up period for this reactor as 20 days. Hence, model results before day 20 can be ignored as the reactor has not reached steady state. Following an increase in effluent methanol concentration, pulse dosing of Co-EDTA complex at 5 µM on day 28 improved methanol removal efficiency. However, the effect of dosing was short term (7 days) and methanol concentration started increasing further. A second pulse dose of Co-EDTA complex given on day 46 improved methanol removal though removal efficiency was not recovered completely. Model result on effluent cobalt concentrations during 30 h after first 5 µM Co-EDTA pulse dosing shows a maximum effluent Co concentration of around 4.5 µM (Fig. 4.6(b)). This demonstrates that majority of the dosed Co was washed out through the effluent when it was dosed as EDTA complex.

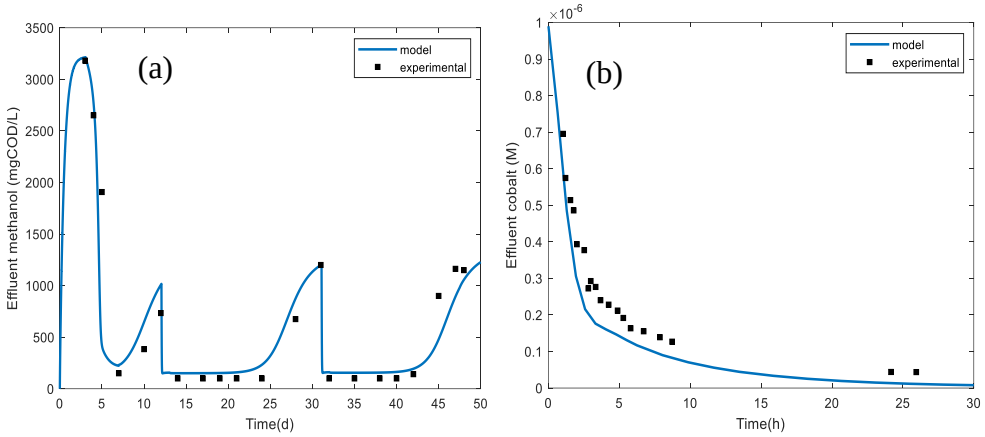

Figure 4.5 - Model predictions and experimental results of (a) effluent methane and (b) effluent cobalt after first pulse dose during $CoCl_2$ pulse dosing.

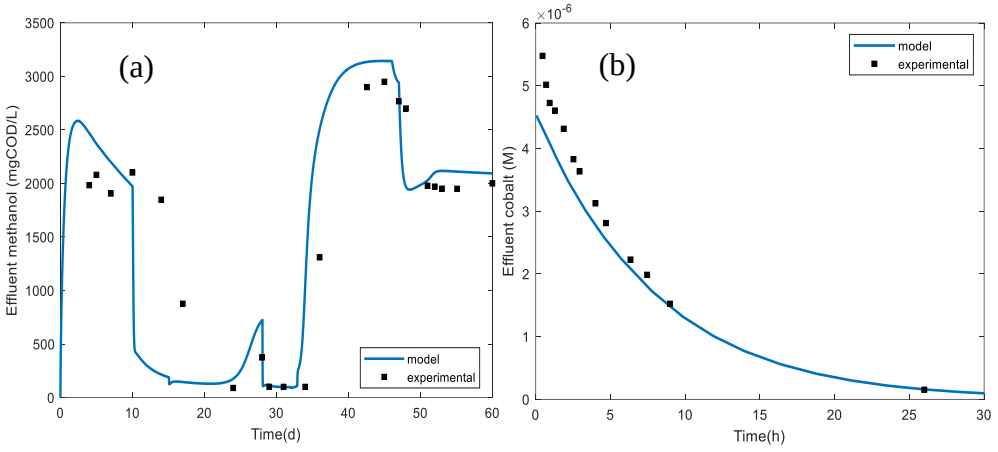

Figure 4.6 - Model predictions and experimental results of (a) effluent methane and (b) effluent cobalt after first pulse dose during Co-EDTA complex pulse dosing.

A model-based comparison between two different dosing forms, $CoCl_2$ and Co-EDTA complex in form of repetitive pulses in a continuous UASB reactor confirmed that $CoCl_2$ pulse dose is preferable over Co-EDTA. Effect of dosing $CoCl_2$ lasted longer than dosing Co-EDTA complex. Moreover, effluent Co concentrations observed after first pulse dose showed that metal-EDTA complexes get easily washed out than $CoCl_2$ as explained in Section 4.3.1.5.

4.4. CONCLUSIONS

This study proposed ideal ways to supplement trace metals to anaerobic digesters for improving methane yield. A comparison between different dosing modes, namely continuous, single pulse, preloading, in-situ loading and repeated pulse dosing revealed that repeated pulse dosing is the best way to dose TM. Low TM concentration at high dosing frequency is preferable over high dosage at low frequency. Trace metals should be supplemented at the earliest time possible after metal deficit at optimum concentration levels. An excess of metal supplementation can result in toxicity. Preferred dosing form depends on reactor configuration. Easily dissociable metal forms like metal chlorides are ideal in continuous reactors whereas strong metal chelates like EDTA complexes are advisable for reactors with high retention times like batch or semi-continuous reactors.

4.5. REFERENCES

Aquino, S. F., & Stuckey, D. C. (2007). Bioavailability and Toxicity of Metal Nutrients during Anaerobic Digestion. *Journal of Environmental Engineering*, *133*(1), 28–35. https://doi.org/10.1061/ASCE0733-93722007133:128

Batstone, D. J., Keller, J., Angelidaki, I., Kalyuzhnyi, S. V., Pavlostathis, S. G., Rozzi, A., Sanders, W. T., Siegrist, H., & Vavilin, V. A. (2002). The IWA Anaerobic Digestion Model No 1 (ADM1). *Water Science and Technology*, *45*(10), 65–73. https://doi.org/10.2166/WST.2002.0292

Cai, W., Jin, M., Zhao, Z., Lei, Z., Zhang, Z., Adachi, Y., & Lee, D. J. (2018). Influence of ferrous iron dosing strategy on aerobic granulation of activated sludge and bioavailability of phosphorus accumulated in granules. *Bioresource Technology Reports*, *2*, 7–14. https://doi.org/10.1016/J.BITEB.2018.03.004

Cai, Y., Hua, B., Gao, L., Hu, Y., Yuan, X., Cui, Z., Zhu, W., & Wang, X. (2017). Effects of adding trace elements on rice straw anaerobic mono-digestion: Focus on changes in microbial communities using high-throughput sequencing. *Bioresource Technology*, *239*, 454–463. https://doi.org/10.1016/j.biortech.2017.04.071

Cai, Y., Zhao, X., Zhao, Y., Wang, H., Yuan, X., Zhu, W., Cui, Z., & Wang, X. (2017). Optimization of Fe2+ supplement in anaerobic digestion accounting for the Fe-bioavailability. https://doi.org/10.1016/j.biortech.2017.07.151

Cao, J., Zhang, L., Hong, J., Sun, J., & Jiang, F. (2019). Different ferric dosing strategies could result in different control mechanisms of sulfide and methane production in sediments of gravity sewers. *Water Research*, *164*. https://doi.org/10.1016/j.watres.2019.114914

Evranos, B., & Demirel, B. (2015). The impact of Ni, Co and Mo supplementation on methane yield from anaerobic mono-digestion of maize silage. *Environmental Technology*, *36*(12), 1556–1562. https://doi.org/10.1080/09593330.2014.997297

Facchin, V., Cavinato, C., Fatone, F., Pavan, P., Cecchi, F., & Bolzonella, D. (2013). Effect of trace element supplementation on the mesophilic anaerobic digestion of food waste in batch trials: The influence of inoculum origin. *Biochemical Engineering Journal*, *70*, 71–77. https://doi.org/10.1016/J.BEJ.2012.10.004

Feng, X. M., Karlsson, A., Svensson, B. H., & Bertilsson, S. (2010). Impact of trace element addition on biogas production from food industrial waste - Linking process to microbial communities. *FEMS Microbiology Ecology*, *74*(1), 226–240. https://doi.org/10.1111/j.1574-6941.2010.00932.x

Fermoso, F. G., Bartacek, J., Chung, L. C., & Lens, P. (2008). Supplementation of cobalt to UASB reactors by pulse dosing: CoCl2 versus CoEDTA2− pulses. *Biochemical Engineering Journal*, *42*(2), 111–119. https://doi.org/10.1016/J.BEJ.2008.06.005

Fermoso, F. G., Bartacek, J., Manzano, R., van Leeuwen, H. P., & Lens, P. N. L. (2010). Dosing of anaerobic granular sludge bioreactors with cobalt: Impact of cobalt

retention on methanogenic activity. *Bioresource Technology*, *101*(24), 9429–9437. https://doi.org/10.1016/j.biortech.2010.07.053

George, S., Mattei, M. R., Frunzo, L., Esposito, G., van Hullebusch, E. D., & Fermoso, F. G. (2023). Dynamic modelling the effects of ionic strength and ion complexation on trace metal speciation during anaerobic digestion. *Journal of Environmental Management*, *343*, 118144. https://doi.org/10.1016/j.jenvman.2023.118144

Gonzalez-Gil, G., Kleerebezem, R., & Lettinga, G. (1999). Effects of nickel and cobalt on kinetics of methanol conversion by methanogenic sludge as assessed by on-line CH4 monitoring. *Applied and Environmental Microbiology*, *65*(4), 1789–1793. https://doi.org/10.1128/AEM.65.4.1789-1793.1999/ASSET/63618013-8F45-4D61-934F-70FD0BA4739B/ASSETS/GRAPHIC/AM0491171003.JPEG

Janssen, P. H. M., & Heuberger, P. S. C. (1995). Calibration of process-oriented models. *Ecological Modelling*, *83*(1–2), 55–66. https://doi.org/10.1016/0304-3800(95)00084-9

Molaey, R., Bayrakdar, A., Sürmeli, R. Ö., & Çalli, B. (2018). Influence of trace element supplementation on anaerobic digestion of chicken manure: Linking process stability to methanogenic population dynamics. *Journal of Cleaner Production*, *181*, 794–800. https://doi.org/10.1016/j.jclepro.2018.01.264

Molla, V. M. G., & Padilla, R. G. (2002). *Description of the MATLAB functions SENS_SYS and SENS_IND.* Universidad Politécnica de Valencia, Spain. https://scholar.google.com/scholar_lookup?title=Description%20of%20the%20MATLAB%20functions%20SENS_SYS%20and%20SENS_IND&author=V.%20Molla&publication_year=2002

Razaviarani, V., & Buchanan, I. D. (2015). Calibration of the Anaerobic Digestion Model No. 1 (ADM1) for steady-state anaerobic co-digestion of municipal wastewater sludge with restaurant grease trap waste. *Chemical Engineering Journal*, *266*, 91–99. https://doi.org/10.1016/j.cej.2014.12.080

Roussel, J., Carliell-Marquet, C., Braga, A. F. M., Garuti, M., Serrano, A., Fermoso, F. G., van Hullebusch, E., Collins, G., Mucha, A. P., & Esposito, G. (2019). *Engineering of trace-element supplementation from the book Trace Elements in Anaerobic Biotechnologies*. http://creativecommons.org/licenses/by/4.0/

Sin, G., De Pauw, D. J. W., Weijers, S., & Vanrolleghem, P. A. (2008). An efficient approach to automate the manual trial and error calibration of activated sludge models. *Biotechnology and Bioengineering*, *100*(3), 516–528. https://doi.org/10.1002/BIT.21769

Thanh, P. M., Ketheesan, B., Yan, Z., & Stuckey, D. (2016). Trace metal speciation and bioavailability in anaerobic digestion: A review. In *Biotechnology Advances* (Vol. 34, Issue 2, pp. 122–136). Elsevier Inc. https://doi.org/10.1016/j.biotechadv.2015.12.006

Thanh, P. M., Ketheesan, B., Yan, Z., & Stuckey, D. (2017). Effect of Ethylenediamine-N,N'-disuccinic acid (EDDS) on the speciation and bioavailability of Fe2+ in the

presence of sulfide in anaerobic digestion. *Bioresource Technology*, *229*, 169–179. https://doi.org/10.1016/j.biortech.2016.12.113

Vintiloiu, A., Boxriker, M., Lemmer, A., Oechsner, H., Jungbluth, T., Mathies, E., & Ramhold, D. (2013). Effect of ethylenediaminetetraacetic acid (EDTA) on the bioavailability of trace elements during anaerobic digestion. *Chemical Engineering Journal*, *223*, 436–441. https://doi.org/10.1016/J.CEJ.2013.02.104

Wang, S., Yuan, R., Liu, C., & Zhou, B. (2020). Effect of Fe2+ adding period on the biogas production and microbial community distribution during the dry anaerobic digestion process. *Process Safety and Environmental Protection*, *136*, 234–241. https://doi.org/10.1016/j.psep.2019.12.031

Wei, Q., Zhang, W., Guo, J., Wu, S., Tan, T., Wang, F., & Dong, R. (2014). Performance and kinetic evaluation of a semi-continuously fed anaerobic digester treating food waste: Effect of trace elements on the digester recovery and stability. *Chemosphere*, *117*(1), 477–485. https://doi.org/10.1016/j.chemosphere.2014.08.060

Wintsche, B., Glaser, K., Sträuber, H., Centler, F., Liebetrau, J., Harms, H., & Kleinsteuber, S. (2016). Trace Elements Induce Predominance among Methanogenic Activity in Anaerobic Digestion. *Frontiers in Microbiology*, *7*(DEC), 2034. https://doi.org/10.3389/fmicb.2016.02034

Yu, B., Shan, A., Zhang, D., Lou, Z., Yuan, H., Huang, X., Zhu, N., & Hu, X. (2015). Dosing time of ferric chloride to disinhibit the excessive volatile fatty acids in sludge thermophilic anaerobic digestion system. *Bioresource Technology*, *189*, 154–161. https://doi.org/10.1016/j.biortech.2015.03.144

Zandvoort, M. H., Geerts, R., Lettinga, G., & Lens, P. N. L. (2002). Effect of long-term cobalt deprivation on methanol degradation in a methanogenic granular sludge bioreactor. *Biotechnology Progress*, *18*(6), 1233–1239. https://doi.org/10.1021/BP020078E

Zandvoort, M. H., Gieteling, J., Lettinga, G., & Lens, P. N. L. (2004). Stimulation of methanol degradation in UASB reactors: In situ versus pre-loading cobalt on anaerobic granular sludge. *Biotechnology and Bioengineering*, *87*(7), 897–904. https://doi.org/10.1002/BIT.20200

Zhang, W., Zhang, L., & Li, A. (2015). Enhanced anaerobic digestion of food waste by trace metal elements supplementation and reduced metals dosage by green chelating agent [S, S]-EDDS via improving metals bioavailability. *Water Research*, *84*, 266–277. https://doi.org/10.1016/J.WATRES.2015.07.010

Zi, Z. (2011). Sensitivity analysis approaches applied to systems biology models. *IET Systems Biology*, *5*(6), 336–346. https://doi.org/10.1049/IET-SYB.2011.0015/CITE/REFWORKS

APPENDIX 4.1

Table 4A.1 - Operational, initial and influent conditions considered for numerical simulations

Parameter	Variable	Value				Unit
		Scenario 1, 2 & 4: dosing mode, dosing frequency and dosing time	Scenario 5: Form of dosing		Scenario 3: dosing concentration	
			Continuous reactor	Semi-continuous reactor		
Digester volume	V_{liq}	$3*10^{-3}$	$3*10^{-3}$	$1.5*10^{-3}$	0.75	m^3
Headspace volume	V_{gas}	$0.05*10^{-3}$	$0.05*10^{-3}$	$0.025*10^{-3}$	0.25	m^3
Influent flow rate	q_{in}	$9.3*10^{-3}$	$9.3*10^{-3}$	0, $5*10^{-6}$	0	$m^3\ d^{-1}$
Temperature	T	308.15	308.15	308.15	308.15	K
Inorganic carbon	S_{IC}	0.0025	0.0025	0.0299	0.0025	kmole m^{-3}
Inorganic nitrogen	S_{IN}	0.001	0.001	$5.2*10^{-3}$	0.001	kmole m^{-3}
Composites	X_c	0	0	0	1	kgCOD m^{-3}
Sugar degraders	X_{su}	0.8	0.8	38.84	0.012	kgCOD m^{-3}
Amino acid degraders	X_{aa}	0.8	0.8	1.602	0.012	kgCOD m^{-3}
LCFA degraders	X_{fa}	0.8	0.8	1.18	0.012	kgCOD m^{-3}
Valerate and butyrate degraders	X_{c4}	0.8	0.8	3.35	0.012	kgCOD m^{-3}
Propionate degraders	X_{pro}	0.8	0.8	4.145	0.012	kgCOD m^{-3}

Table 4A.1 *(Continued)*

Parameter	Variable	Value				Unit
		Scenario 1, 2 & 4: dosing mode, dosing frequency and dosing time	Scenario 5: Form of dosing		Scenario 3: dosing concentration	
			Continuous reactor	Semi-continuous reactor		
Acetate degraders	X_{ac}	0.8	0.8	11.38	0.012	kgCOD m^{-3}
Hydrogen degraders	X_{h2}	0.8	0.8	7.38	0.012	kgCOD m^{-3}
Particulate inerts	X_I	0.000001	0.000001	0.000001	0	kgCOD m^{-3}
Total dissolved Calcium	S_{Ca}	0.002	0.002	$6.8*10^{-6}$	0.002	kmole m^{-3}
Total dissolved Magnesium	S_{Mg}	0.0025	0.0025	0.0004	0.0025	kmole m^{-3}
Total dissolved Nickel	S_{Ni}	$0.5*10^{-6}$	$0.5*10^{-6}$	$0.5*10^{-6}$	0.000005	kmole m^{-3}
Total dissolved Cobalt	S_{Co}	0	0	0	0.000005	kmole m^{-3}
Total dissolved Iron	S_{Fe}	$1*10^{-4}$	$1*10^{-4}$	$5*10^{-6}$	Variable (0 - 10^{-3})	kmole m^{-3}
Inorganic phosphorous	S_{po4}	0.006	0.006	0.0018	0.006	kmole m^{-3}
Inorganic sulphur	S_{hs}	0.0001	0.0001	0.0004	0.0025	kmole m^{-3}

Table 4A.1 *(Continued)*

Parameter	Variable	Value				Unit
		Scenario 1, 2 & 4: dosing mode, dosing frequency and dosing time	Scenario 5: Form of dosing		Scenario 3: dosing concentration	
			Continuous reactor	Semi-continuous reactor		
FeS	X_{prec}	0.00000001	0.00000001	0.00000001	0	kmole m^{-3}
EDTA	S_{EDTA}	0	0	0	0	kmole m^{-3}
Biomass carboxyl binding site	≡X_COOH	0.002*0.012*7/1.4	0.002*0.012*7/1.4	0.002*0.012*7/1.4	0.002*0.012 *7/1.4	kmole m^{-3}
Biomass phosphoryl binding site	≡X_PO_4H	0.0008*0.012*7/1.4	0.0008*0.012*7/1.4	0.0008*0.012*7/1.4	0.0008*0.012*7/ 1.4	kmole m^{-3}
Biomass hydroxyl binding site	≡X_OH	0.00017*0.012* 7/1.4	0.00017*0.012*7/1.4	0.00017*0.012*7/1.4	0.00017* 0.012*7/1.4	kmole m^{-3}
Particulate inert carboxyl binding site	≡XI_COOH	0.002*0.000001/1.4	0.002*0.000001/1.4	0.002*0.000001/1.4	0.002* 0.000001/1.4	kmole m^{-3}
Particulate inert phosphoryl binding site	≡XI_PO_4H	0.0008* 0.000001/1.4	0.0008*0.000001/1.4	0.0008*0.000001/1.4	0.0008* 0.000001/1.4	kmole m^{-3}
Particulate inert hydroxyl carboxyl binding site	≡XI_OH	0.00017* 0.000001/1.4	0.00017*0.000001/1.4	0.00017*0.000001/1.4	0.00017* 0.000001/1.4	kmole m^{-3}

Table 4A.1 *(Continued)*

Parameter	Variable	Value			Unit
		Scenario 1, 2 & 4: dosing mode, dosing frequency and dosing time	Scenario 5: Form of dosing		Scenario 3: dosing concentration	
			Continuous reactor	Semi-continuous reactor		
Soluble inert carboxyl binding site	≡SI_COOH	0.00621* 0.0000001/1.4	0.00621* 0.0000001/1.4	0.00621*0.0000001/1.4	0.00621* 0.0000001/1.4	kmole m^{-3}
Soluble inert phosphoryl binding site	≡SI_PO_4H	0.00053* 0.0000001/1.4	0.00053* 0.0000001/1.4	0.00053*0.0000001/1.4	0.00053* 0.0000001/1.4	kmole m^{-3}
Soluble inert hydroxyl binding site	≡SI_OH	0.00693* 0.0000001/1.4	0.00693* 0.0000001/1.4	0.00693*0.0000001/1.4	0.00693* 0.0000001/1.4	kmole m^{-3}
FeS sulfyhydrl binding site	≡XP_SH	$93*10^{-6}$* 0.00000001	$93*10^{-6}$*0.00000001	$93*10^{-6}$*0.00000001	$93*10^{-6}$* 0.00000001	kmole m^{-3}
Influent sugar	S_{su}_in	1	1	600	0	kgCOD m^{-3}
Influent inorganic carbon	S_{IC}_in	0.1	0.1	0.0299	0	kmole m^{-3}
Influent inorganic nitrogen	S_{IN}_in	0.1383	0.1383	0.6	0	kmole m^{-3}
Influent Ca	S_{Ca}_in	0.0225	0.0225	$6.8*10^{-6}$	0	kmole m^{-3}
Influent Mg	S_{Mg}_in	0.04155	0.04155	0.0004	0	kmole m^{-3}
Influent Ni	S_{Ni}_in	$0.5*10^{-6}$	$0.5*10^{-6}$	$0.5*10^{-6}$	0	kmole m^{-3}
Influent Co	S_{Co}_in	Variable (0, $5*10^{-6}$)	Variable (0, $5*10^{-6}$)	Variable (0, $5*10^{-6}$)	0	kmole m^{-3}
Influent Fe	S_{Fe}_in	0.007125	$5*10^{-6}$	$5*10^{-6}$	0	kmole m^{-3}

Table 4A.1 *(Continued)*

Parameter	Variable	Value				Unit
		Scenario 1, 2 & 4: dosing mode, dosing frequency and dosing time	Scenario 5: Form of dosing		Scenario 3: dosing concentration	
			Continuous reactor	Semi-continuous reactor		
Influent phosphate	S_{PO4}_in	0.00002	0.007125	0.0018	0	kmole m^{-3}
Influent sulphide	S_{HS}_in	0	0.00002	0.0004	0	kmole m^{-3}
Influent cation	S_{cation}_in	0.175894	0	0.033	0	kmole m^{-3}
Influent anion	S_{anion}_in	0	0.175894	0		kmole m^{-3}
Influent chloride	S_{Cl}_in	Variable (0, $10*10^{-6}$)	Variable (0, $10*10^{-6}$)	$5.23*10^{-3}$	0	kmole m^{-3}
Influent K	S_K_in	0.007125	0.007125	0.0018	0	kmole m^{-3}
Influent CoEDTA	S_{CoEDTA}_in	0	Variable ($5*10^{-6}$, 0)	Variable ($5*10^{-6}$, 0)	0	kmole m^{-3}

Value of all other state variables not mentioned in the table is considered to be zero

CHAPTER 5

Application of the Trace Metal Speciation Model Framework to a Full-Scale Anaerobic Digester

ABSTRACT: Co-digestion helps in improving digester performance and influence of trace metals during co-digestion is very significant. Trace metals (TMs) are commonly supplied to biogas plants facing metal deprivation through feedstocks. Bioavailability of TMs greatly varies with feedstock characterisation. Trace metal influence during co-digestion is mostly determined by two main characteristics of feedstock – sulphur content and trace metal concentration. This study presents a model-based analysis on effect of concentration of sulphur and trace metals in feedstock on methane production during co-digestion. Despite the wide application of iron dosage method to remove H_2S from biogas, amount of iron salts to be added is not quantified. Hence, optimum iron dosing concentration is also analysed in the study during co-digestion as well as sewage sludge digestion. Trace metal speciation model based on ADM1 is adopted to study the effects. Data collected from anaerobic digestor in a full-scale wastewater treatment plant is used for model application. Model results shows influence of trace metal and sulphur concentration present in the substrate on co-digestion process and significance of optimum iron dosing to improve methane yield.

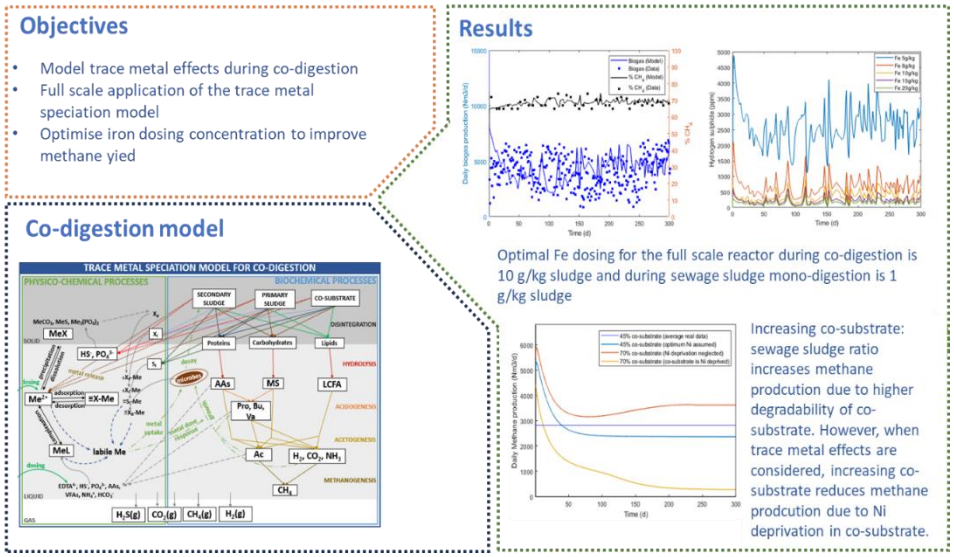

5.1. INTRODUCTION

Sewage sludge from wastewater treatments (WWTPs) are commonly treated by anaerobic digestion (AD) process as it is a sustainable, economical and effective technology for reducing excess sludge and generating energy rich biogas. Often co-substrates like food wastes, animal manure and crop residue are added along with sewage sludge to overcome drawbacks of mono-digestion. Biogas produced after anaerobic digestion is burnt in heat and power generation plants for meeting the energy demands of the WWTPs and excess is often supplied to the power grid for community use. Biogas is composed of methane, carbon dioxide and traces of other gases like, hydrogen sulphide (H_2S). Composition of biogas is determined by the type of feedstock treated and pathways of production. Methane content of biogas normally ranges between 45% – 75%. Biomethane which is the pure methane obtained after biogas upgrading has a lower heating value (LHV) of around 36 megajoules per cubic metre (MJ/m^3).

Sulphate-reducing bacteria in the digestors such as Desulfovibrio or Desulfotamaculum reduces sulphate present in the substrate to produce H_2S (Lens and LW Hulshoff, 2020). Depending on sulphur content of the feed, concentration of H_2S in biogas varies from 100 to 10,000 ppmv (Vu et al., 2022). H_2S generated from anaerobic digestion of sewage sludge releases around 500 – 2500 ppmv (Nguyen et al., 2021). Sulphur content in sewage sludge is around 115 mg S/kg raw sludge while cattle manure has high levels of sulphur of around 600 mg S/kg raw sludge (Chen et al., 2019; Choudhury et al., 2019). Due to competition of substrates between sulphate reducing bacteria and methanogens, high levels of sulphur can inhibit methanogenesis during anaerobic digestion (Song et al., 2018). Moreover, H_2S gas is toxic to methanogens at concentration levels of 50 to 220 mg S/L at pH 7 – 8 (Dykstra and Pavlostathis, 2021).

Highly corrosive SO_2 or SO_3 released after combustion of H_2S in biogas causes corrosion of plant equipments used for heat and power generation from biogas. Deublein and Steinhauser (2011) suggest to maintain concentration of H_2S less than 100–500 mg/N m^3 to prevent corrosion of steel in the plant equipments. Trace levels of H_2S can also damage ion exchange membrane in fuel cells used for converting biogas to electricity (Vu et al., 2022). Moreover, H_2S gas can cause catalyst poisoning during reformation of steam (Ghimire et al., 2021). Considering concerns of health and occupational safety, H_2S exposure limit of around 10 ppm is set across different countries as a standard as H_2S concentrations at 50–100 ppm cause eye irritation and exposure at 300–500 ppm can lead to severe poisoning that may result in unconsciousness and death (Firer et al., 2008). Specifications are also set by countries for safe biogas applications like around 3–4 ppmv H_2S for automotive fuel/natural gas replacement. Engine and fuel cell manufacturers specify limit of 100 ppmv H_2S and 5 ppmv H_2S respectively for power generation (Vu et al., 2022).

Various ex situ and in situ technologies are employed for removal of biogas contaminants like H_2S. In-situ methods include regulating operational parameters or addition of chemicals

to the digestor. Addition of iron salts enable sulphide precipitation while oxidative chemical addition promote conversion of H_2S to elemental sulphur that can be removed from digestate. Adding iron salts to precipitate sulphur as insoluble iron sulphide (FeS) thereby preventing H_2S stripping is widely adapted due to its simple operation and relative low cost of iron salts.

Iron in form of chlorides, oxides or phosphates is added along with the influent. Iron (II) salts such as ferrous chloride ($FeCl_2$), ferrous sulphate ($FeSO_4$) or iron (III) salts such as ferric hydroxide ($Fe(OH)_3$), ferric chloride ($FeCl_3$) are moslty used. Eq. (5.1), Eq. (5.2) and Eq. (5.3) represent formation of FeS after addition of $FeCl_2$, $FeCl_3$ and $Fe(OH)_3$ respectively.

$$Fe^{2+} + H_2S \rightarrow FeS_{(s)} + 2H^+ \quad (5.1)$$

$$2FeCl_3 + H_2S \rightarrow S_{(s)} + 2FeCl_2 + 2HCl \quad (5.2)$$

$$2Fe(OH)_3 + 3H_2S \rightarrow Fe_2S_3 + 6H_2O \quad (5.3)$$

Despite the wide application of iron dosage method to remove H_2S from biogas, amount of iron salts to be added is not quantified. Hence, their application is based on empirical experience which is mostly site specific. In most cases, high dosage of iron is practised maintaining high iron to sulphide molar ratio, which is often much higher than the stoichiometric requirements. Iron is an important trace metal influencing anaerobic digestion pathways. Iron is the most abundant TM required in AD followed by Ni, Co and Mo (Glass and Orphan, 2012; Scherer and Sahm, 1981). However, presence of excess bioavailable Fe in AD system can inhibit the microbes causing reduction in methane yield. George et al. (2023) demonstrated that when iron to sulphide ratio is more than 1, iron exists in the system predominantly as labile fraction thereby reaching inhibitory and toxic concentration levels of iron on the microorganisms. This study analyses optimum concentration of Fe to be supplemented to anaerobic digestors with emphasis to achieve less H_2S contamination in biogas and avoid any possible inhibition effects in AD process caused by addition of Fe.

Moreover, TMs are commonly supplied to biogas plants through feedstocks. Bioavailability of TMs greatly varies with feedstock characterisation, mainly classified as phosphate rich, sulphur rich, lignocellulose rich and lipid rich feedstock (Roussel et al., 2019). Wheat stillage for example has low TMs with high sulphur concentration and is not an ideal substrate for AD whereas swine wastewater contains high concentrations of Cu and Zn (Thanh et al., 2016). Characterisation of maize silage indicated deficiency of Ni and Co (Evranos & Demirel, 2015). Trace metal influence during co-digestion is mostly determined by two main characteristics of feedstock – sulphur content and trace metal concentration. This study presents a model-based analysis on effect of concentration of sulphur and trace metals in feedstock on methane production during co-digestion. Trace metal speciation model based on ADM1 is adopted to study the effects. Data collected from anaerobic digestor in a full-scale wastewater treatment plant is used for model application.

5.2. METHODOLOGY

5.2.1. Full scale plant and anaerobic digester details

The anaerobic digester modelled in this study is from a municipal wastewater treatment plant (EMASESA Metropolitana) located in Seville, Spain. The plant has a treatment capacity of 90,000 m^3/day designed for a population of 350,000 equivalent inhabitants. This plant serves the population of Alcalá de Guadaíra and the eastern part of Seville, as well as the industrial area between the two nuclei. The raw water entering the WWTP has characteristics of 33,300 kg BOD/d (370 mg/L), 920 mg COD/L, 400 mg TSS/L, 280 mg VSS/L, ammoniacal nitrogen of 42 mg N/L and total phosphorous of 8.5 mg/L.

Primary sludge and centrifugally thickened activated sludge from the biological secondary treatment unit are anaerobically co-digested. Co-substrate added along with sewage sludge is mixed food waste and it includes wastes from industries producing dairy products, biofuels, beer, juices, meat, and fish. Anaerobic digestion (AD) is carried out in a single stage with a retention period of 23 days and external heating. The plant contains three anaerobic digesters of diameter 20 m with a unit volume of 5,810 m^3. Agitation is carried out by means of submerged vertical agitators and recirculation pumps. The heating system of the plant maintains the digestion temperature at 35º C. The plant has a lime dosing facility to correct pH deviations in the digester and ferric chloride dosing for fixation of H_2S. They are dosed directly into the thickened mixed sludge tank.

5.2.2. Data analysis

Data used for model application is obtained by continuous monitoring of the digester during January – October 2022. Flow rate, temperature, pH, acidity/alkalinity, total solids (TS), volatile solids (VS) are monitored in the digesters. TS, VS, COD and flow rate are monitored in the influent to the digesters whereas TS, VS, flow rate, biogas volume and biogas composition (CH_4, CO_2, H_2S) are monitored in the digester effluent. Quantity of $FeCl_3$ consumed to fix H_2S in biogas is also monitored. Flowrate, TS, VS, COD and sulphates are analysed for primary sludge, secondary sludge and co-substrates. Parameters are determined by standard methods used for analysis in water and wastewater treatment plants. Sulphate concentration of sewage sludge and co-substrates are 155 mg/L and 6614 mg/L respectively. Average characteristics of the substrates, influent and effluent are given in Table 5.1.

Table 5.1 - Parameters monitored in anaerobic digester

Parameters	**Measurements** (Average)
Primary sludge	
Flow (m^3/d)	138.76+7.63
% TS	5.1+0.25
% VS	56.89+0.91
Total COD (mg/L)	34621+1306
Soluble COD (mg/L)	1,780 +42
Secondary sludge before thickening	
Flow (m^3/d)	1483+28
% TS	3.96+0.09
% VS	74.38+5.7
Total COD (mg/L)	14888+2106
Soluble COD (mg/L)	3559.88+206
Secondary sludge after thickening	
Flow (m^3/d)	416 + 6
% TS	3.01 +0.04
% VS	74.38+5.7
Co-substrate	
Flow (m^3/d)	59.4 +4
% TS	7.1 +0.10
% VS	82.9 + 6.2
Total COD (mg/L)	335681+6841
Soluble COD (mg/L)	5290.0 + 346
Influent	
Flow (m^3/d)	582+13
% TS	4.29+0.15
% VS	72.8+0.46
Total COD (mg/L)	69471+2503
Soluble COD (mg/L)	8133.10 + 1409
Digester 1	
Flow (m^3/d)	259.44 + 3.22
% TS	2.75 + 0.017
% VS	58.36 + 0.546
Acidity/Alkalinity	0.06 + 0.004
Acidity (mg/L)	230 + 15.48
Alkalinity (mg/L)	4000 + 36.82
Ph	7.2 + 0.03
Temperature (ºC)	37.35 + 0.08

Table 5.1 *(Continued)*

Parameters	**Measurements** (Average)
Digester 3	
Flow (m^3/d)	398.06 + 2.8
% TS	2.91 + 0.03
% VS	56.55 +0.48
Acidity/Alkalinity	0.04+0.002
Acidity (mg/L)	175 + 8.4
Alkalinity (mg/L)	4400 +29.8
pH	7.10 +0.02
Temperature (ºC)	35.57 +0.05
Effluent	
% TS	2.79 + 0.02
% VS	58 + 0.439
Total COD (mg/L)	24841.40 + 3408
Acidity/Alkalinity	0.07 + 0.003
Acidity (mg/L)	293.35 + 6.49
Alkalinity (mg/L)	4161.75 + 93.16
pH	6.94 + 0.007
Retention time (d)	21.79 +1.36
Yield (%)	44.25 + 2.17
Biogas (Nm^3/d)	4069 + 196
m^3 biogas generated/kg COD fed	0.26 +0.02
% CH_4	68 + 0.001
% CO_2	29 + 0.001
H_2S(ppm)	243 +3.33
Ferric chloride consumed (kg/d)	514 + 7.87
Temperature (ºC)	32 + 1.54

5.2.3. Model application and scenarios

The dynamic trace metal (TM) speciation model for anaerobic digestion presented in Chapter 4 as represented in Fig. 5.1 is used for model application with the data from full scale anaerobic digester. ADM1 is modified to include TM effects on AD. Precipitation processes defined in the model include precipitation/dissolution of $CaCO_3$, $Ca_3(PO_4)_2$, $MgCO_3$, $MgNH_4PO_4$ and precipitation/dissolution of TMs (Fe, Co, Ni) with sulphates, carbonates, and phosphates. Ion pairing and acid-base equations are considered for monitoring the effects of pH and ionic strength. Complexation processes include complexation with inorganic ligands and AD metabolites like volatile fatty acids (VFAs) and amino acids (AAs). TM adsorption on biomass, microbial products and inerts like precipitates are also defined in the model. Initial variable values of biomass concentrations were obtained by running the simulations until steady state using the average input parameter values. Since the model does not consider

sulphate reduction pathways by sulphate reducing bacteria, sulphide in the system is calculated based on the fraction of sulphate in the influent reduced to sulphides in AD systems in the study from Flores-Alsina et al. (2016). Kinetic and stoichiometric parameters in the biochemical module are according to Batstone et al. (2002) for mesophilic AD system. Physiochemical values used in Chapter 4 are adapted in the model. Model is implemented in an in-house code developed on MATLAB platform where the model equations are solved by multidimensional Newton Raphson method and built-in ode solver of MATLAB.

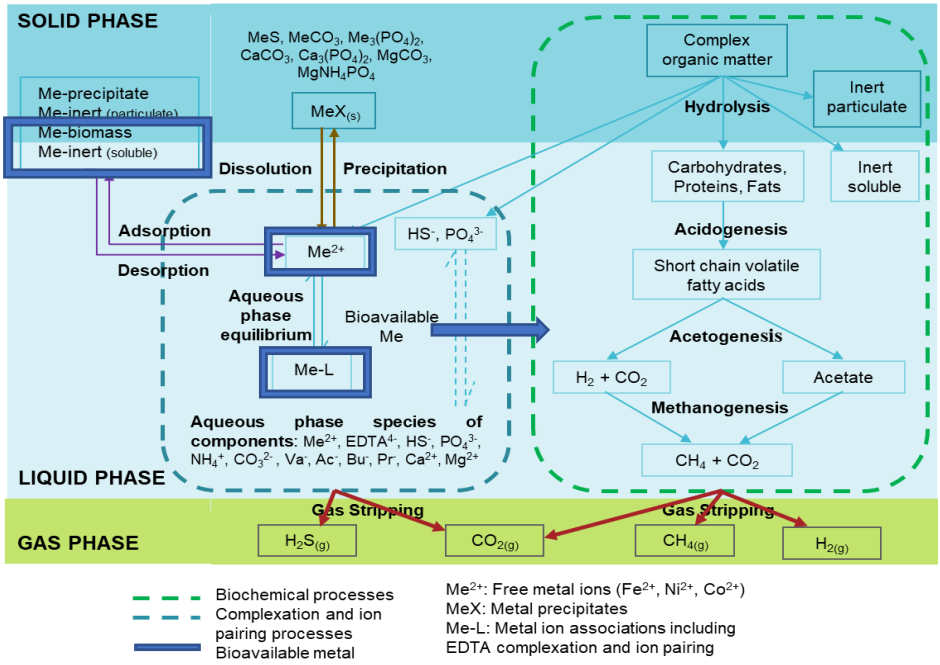

Figure 5.1 - Schematic representation of the model

Two approaches are followed to model co-digestion. In the first approach, influent to the model (complex organic matter in Fig. 5.1 is defined as mixed substrate (primary sludge, secondary sludge and co-substrate) where influent characterisation (carbohydrate, protein and lipid) and hydrolysis rates were calibrated to fit the data. In the second approach, separate influent is defined for each of the feedstock (Fig. 5.2) and fractions of carbohydrate, protein and lipid for each substrate are taken from literature (default ADM1 parameters for primary sludge, Montecchio et al. (2019) for secondary sludge and co-substrate/food waste). Release of trace metals and sulphur are considered during the disintegration process. Particulate matter from biomass decay has the degradation pathway as secondary sludge like proposed by Ozyildiz et al. (2023). Co-substrate/food waste is assumed to be deprived of Ni and sewage sludge as Ni rich based on the study from Habagil et al. (2020).

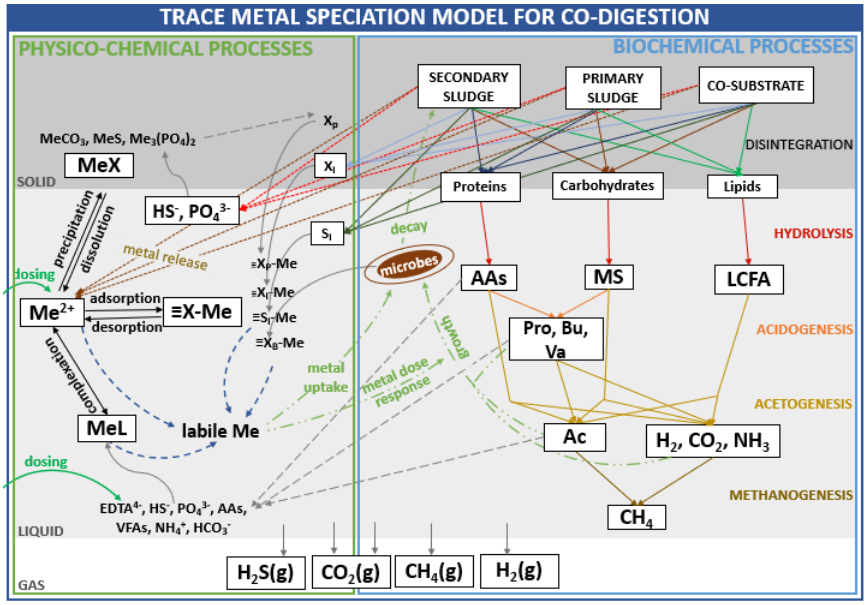

Me^{2+}: Free metal ions (Fe, Ni, Co)
MeX: Metal precipitates
MeL: Metal ion associations
AAs: Amino acids
MS: Monosaccarides
LCFA: Long chain fatty acids
Pro: Propionic acid
Bu: Butyric acid
Va: Valeric acid
Ac: Acetic acid

VFAs: Volatile fatty acids
EDTA: Ethyleneaminetetraacetic acid
≡X-Me: Absorbed metal
MeS: Metal sulphides
$MeCO_3$: Metal carbonates
$Me_3(PO_4)_2$: Metal phosphates
$\equiv X_P$-Me: Metal absorbed on precipitates
$\equiv X_I$-Me: Metal absorbed on particulate inerts
$\equiv S_I$-Me: Metal absorbed on soluble inerts

Figure 5.2 - Schematic representation of TM speciation model for co-digestion

Three model scenarios are simulated to study influence of dosing iron concentration and trace metals on methane production and H_2S concentration in biogas. First set of simulations replicate full scale anaerobic digester plant data where iron is dosed at 10 g/kg sludge. Simulations are performed at iron dosing conditions of 5 - 20 g/kg sludge to optimise iron dosing concentration. Second set of simulations are aimed to estimate the optimum iron quantity to be dosed for a lower sulphate input concentration of 150 mg/kg sludge (average sulphate concentration in sewage sludge). Third scenario analyses the effect of Ni concentration in the feedstock with the assumption that other trace metals are at optimum concentration levels.

5.3. RESULTS AND DISCUSSION

5.3.1. Model application to full scale anaerobic digester

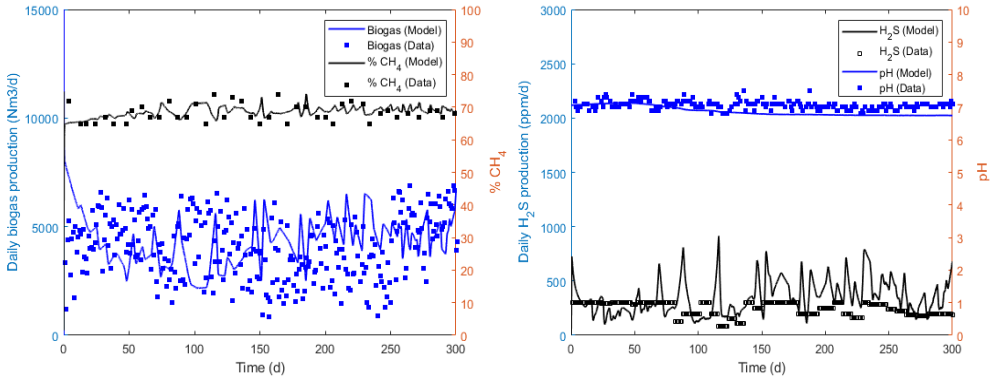

Figure 5.3 - Comparison of plant data with model results.

Model results where co-digestion is defined based on mixed substrate influent along with real data from the full-scale anaerobic digester can be found in Fig. 5.3. As can be observed, the model could reasonably predict digester performance and influence of trace metal Fe. Values of parameters obtained after calibration are 0.10 for $f_{si,xc}$ (soluble inerts from composites), 0.40 for $f_{ch,xc}$ (carbohydrates from composites), 0.20 for $f_{pr,xc}$ (proteins from composites), 0.25 for $f_{li,xc}$ (lipids from composites), 0.05 for $f_{xi,xc}$ (particulate inerts from composites), 10 d^{-1} for disintegration rate and 50 d^{-1} for hydrolysis rates of carbohydrate, protein and lipids. However, it is noteworthy that proper calibration and validation of the model is required to accurately predict metal dynamics and its influence on full-scale digester performance which would require further substrate characterisation. Average biogas production from the anaerobic digester is around 3000 Nm^3/d with around 68 % methane content. pH of the digestor is maintained around 7.00. H_2S content in the biogas is controlled to around 300 ppm with addition of 514 kg $FeCl_3$/d which corresponds to 10g Fe/kg sludge (Fig. 5.3).

Flores-Alsina et al. (2016) illustrated presence of HS^- and H_2S in absence of Fe and abundance of $FeHS^-$ and consequently FeS when iron is added. The study reported drop in H_2S partial pressure and precipitation of almost all sulphide when Fe: S molar ratio is greater than 1. Similar behaviour in sulphide with addition of Fe^{3+} is reported in Liu et al. (2015) and Zhang et al. (2013). In the absence of sulphide, Fe precipitated as phosphates resulting in reduced struvite precipitation (Flores-Alsina et al., 2016). Nevertheless, rate of iron phosphate precipitation is not high as iron sulphide. Hence excess Fe exists as labile fraction that could even reach inhibitory concentration levels of iron on microbes when Fe: S molar ratio is far higher than 1 (Chapter 2).

5.3.2. Effect of iron dosing concentration

Simulations performed to study effect of dosing iron concentration showed increase in H_2S content in biogas with decrease in dosing concentration. As iron dosing concentration decreases, sulphide concentration in the system increases due to decrease in FeS precipitation (plots not shown) resulting in increase of H_2S in biogas. However, same trend in methane production can be observed regardless of decreasing Fe dosing concentrations (Fig. 5.4). No effects were observed in methane production as the dosing concentrations are within the optimum levels considering metal effects on microbes. Iron requirement by the microbes is met with the dosing concentrations simulated during the study. Similar observations were also reported by Frunzo et al. (2019) where effect of iron supply is investigated on anaerobic digestion of food waste. The study reported increase in FeS precipitation with increasing Fe dosage with consequent decrease of H_2S in biogas during anaerobic digestion of food waste. Flores-Alsina et al. (2016) observed decrease in methane production at high S:COD ratios due to inhibition of sulphide on hydrogenotrophic and acetoclastic methanogens. This effect is not observed in the model results as inhibition on methanogens due to excess sulphide concentrations in the system is not included in the model as the primary focus of the work is to study trace metal inhibition effects.

Not all simulated Fe concentrations are optimum considering H_2S production. At Fe concentrations of 5 g/kg, H_2S production rose to around 3000 ppm. With increase in Fe to 8 g/kg, H_2S production decreases drastically to around 700 ppm. Dosing concentration of 10g/kg is optimum as it keeps H_2S production within the requirements. No further significant decrease in H_2S production can be observed with additional Fe supplementation of 15g/kg and 20 g/kg. Supplementing iron more than stoichiometric requirements does not reduce H_2S production and contributes to additional chemical costs. In an experimental study, (Wang and Banks (2006) reported optimum $FeCl_3$ dosing of 7.4 g/L for anaerobic digestion of sulphate rich landfill leachate (sulphate concentration of 8700 mg/L). Of the tested dosing concentrations of 5 g/L, 10 g/L and 15 g/L in the study, sulphate concentration of 7.4 g/L corresponding to theoretically obtained 0.7 – 1 mole of $FeCl_3$ to counteract the effects of 1 mole of H_2S was reported to be optimum.

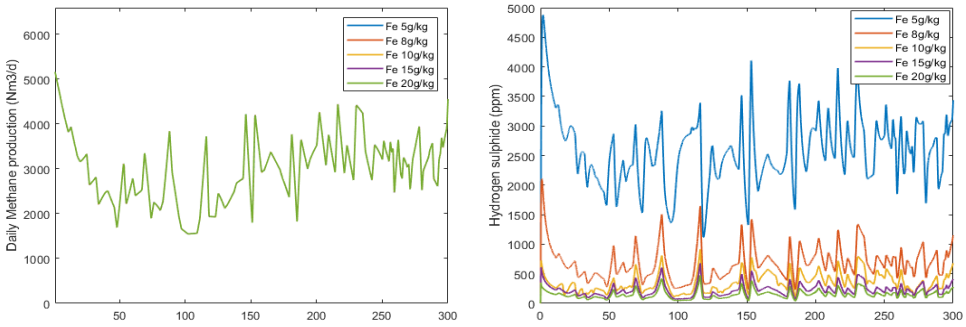

Figure 5.4 - Effect of dosing $FeCl_3$ concentration of methane production and H_2S content

5.3.3. Influence of sulphate concentration

This set of simulations showed that dosage of $FeCl_3$ depends predominantly on sulphate concentration in the substrate. For a sewage sludge anaerobic digester with average influent sulphate concentration of 150 mg SO_4/kg sludge (Chen et al., 2019; Vu et al., 2022), 1 g $FeCl_3$/kg sludge is found to be optimum (Fig. 5.5). However, for the previous set of simulations where co-digestion is carried out, $FeCl_3$ requirement was high as around 10 g/ kg sludge. H_2S content in biogas rose to 1500 ppm without $FeCl_3$ supplementation whereas dosing 1 gFe/kg sludge reduces H_2S concentration to 200 ppm. If the goal is to keep H_2S content in biogas below 100 ppm, $FeCl_3$ concentration of 5 g/kg can be used. Increasing concentration to 10 gFe/kg sludge contributes to unnecessary chemical costs as it does not reduce sulphide levels below the concentration levels achieved by 5 g/kg dosing.

Firer et al. (2008) suggests iron to sulphide ratio of around 1.3:1 for ferrous salts and 0.9:1 for ferric salts to achieve dissolved sulphide concentrations lower than 0.1 mg/L. Díaz et al. (2015) reported around 760 g $FeCl_3/m^3$ raw sludge or equivalently, 0.017 kg $FeCl_3$/kg total solids influent to reduce dissolved sulphide concentration from 50 mg/L to 0.2 mg/L. Erdirencelebi and Kucukhemek (2018) established a linear relationship between $FeCl_3$ dosage and sulphide in full-scale ADs at a largescale municipal wastewater treatment plant. The authors indicated $FeCl_3$ dosing at 2.27 – 6.82 g $FeCl_3$ per 1 g of sulphide, corresponding to 1.17 – 3.5 g Fe^{3+} per g of sulphide. Optimum $FeCl_3$ dosing reported in this study falls in this range.

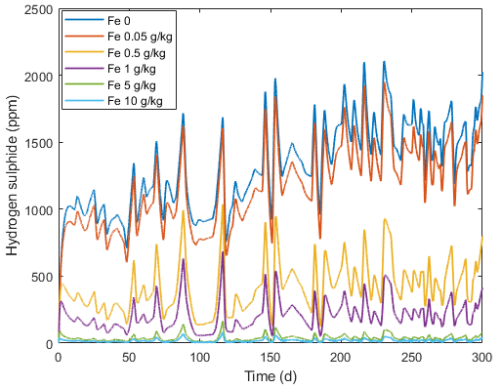

Figure 5.5 - H_2S concentrations in AD during sewage sludge digestion.

5.3.4. Effect of trace metals during co-digestion

Model results where influent is defined separately (primary sludge, secondary sludge, co-substrate) along with real full-scale digester data is shown in Fig. 5.6(a). Defining influent separately helps in defining influence of feedstock characterisation better. When substrate is well characterised, this model approach is recommended to define trace metal effects during co-digestion. Co-substrate/food waste is assumed to be deprived of Ni and sewage sludge as Ni rich based on the study from Habagil et al. (2020). Other trace metals such as Fe or Co

are assumed to be at optimum concentrations. Real data from the digester shows 45% influent COD as co-substrate and 55% sewage sludge. Concentration of Ni at this mixing ratio is assumed to be optimum for biomass. When Ni effects on anaerobic digestion is neglected, increasing co-substrate to 70% of COD increases methane production due to higher degradable fraction of COD in food waste (Fig. 5.6(b)). However, when Ni effects are considered, increasing co-substrate to 70% reduces methane production as food waste in this study is Ni deprived. Increasing co-substrate fraction of COD reduces overall Ni content in the system and the reactor shows Ni deprivation effects on methane production. Influence of other substrates based on their trace metal characteristics can also be tested in future studies.

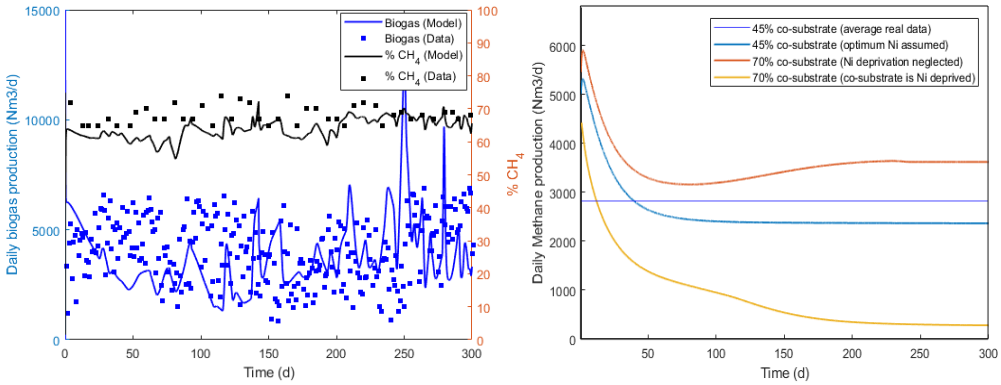

Figure 5.6 - Simulation results from trace metal speciation model for co-digestion (a) comparison with real data (b) influence of co-substrate characteristics.

5.4. CONCLUSIONS

The study highlights trace metal effects during co-digestion and the importance of optimising dosing concentration of iron to anaerobic digestors. High dosage of iron at high iron to sulphide ratio will not only result in reduction of methane yield due to inhibition of Fe but also is not useful for H_2S removal from biogas. Hence ideal dosage of iron is maintaining iron to sulphide ratio around 1. Moreover, extra costs due to adding excess of $FeCl_3$ can be reduced by the optimised dosing concentration levels. Substrate characteristics such as sulphur content and trace metal concentration influence co-digestion. In case of metal deprivation, co-digestion can be performed using co-substrates rich in trace metals to overcome metal limitation. However, optimum mixing ratio should be maintained to ensure sufficient metal bioavailability.

5.5. REFERENCES

Allison, J.D., Brown, D.S., 1995. MINTEQA2/PRODEFA2—A Geochemical Speciation Model and Interactive Preprocessor, in: Chemical Equilibrium and Reaction Models. John Wiley & Sons, Ltd, pp. 241–252. https://doi.org/10.2136/sssaspecpub42.c12

Appels, L., Baeyens, J., Degrève, J., Dewil, R., 2008. Principles and potential of the anaerobic digestion of waste-activated sludge. Prog. Energy Combust. Sci. 34, 755–781. https://doi.org/10.1016/j.pecs.2008.06.002

Appels, L., Lauwers, J., Degrève, J., Helsen, L., Lievens, B., Willems, K., Van Impe, J., Dewil, R., 2011. Anaerobic digestion in global bio-energy production: Potential and research challenges. Renew. Sustain. Energy Rev. 15, 4295–4301. https://doi.org/10.1016/j.rser.2011.07.121

Artola, A., Balaguer, M.D., Rigola, M., 1997. Heavy metal binding to anaerobic sludge. Water Res. 31, 997–1004. https://doi.org/10.1016/S0043-1354(96)00345-4

Batstone, D., Flores-Alsina, X. (Eds.), 2022. Generalised Physicochemical Model (PCM) for Wastewater Processes. IWA Publishing. https://doi.org/10.2166/9781780409832

Batstone, D.J., Keller, J., Angelidaki, I., Kalyuzhnyi, S.V., Pavlostathis, S.G., Rozzi, A., Sanders, W.T., Siegrist, H., Vavilin, V.A., 2002. The IWA Anaerobic Digestion Model No 1 (ADM1). Water Sci. Technol. 45, 65–73. https://doi.org/10.2166/WST.2002.0292

Callander, I.J., Barford, J.P., 1983. Precipitation, chelation, and the availability of metals as nutrients in anaerobic digestion. I. Methodology. Biotechnol. Bioeng. 25, 1947–1957. https://doi.org/10.1002/BIT.260250805

Chen, S., Dong, B., Dai, X., Wang, H., Li, N., Yang, D., 2019. Effects of thermal hydrolysis on the metabolism of amino acids in sewage sludge in anaerobic digestion. Waste Manag. 88, 309–318. https://doi.org/10.1016/J.WASMAN.2019.03.060

Choudhury, A., Shelford, T., Felton, G., Gooch, C., Lansing, S., 2019. Evaluation of Hydrogen Sulfide Scrubbing Systems for Anaerobic Digesters on Two U.S. Dairy Farms. Energies 12, 4605. https://doi.org/10.3390/en12244605

Deublein, D., Steinhauser, A., 2011. Biogas from Waste and Renewable Resources: An Introduction. John Wiley & Sons.

Díaz, I., Ramos, I., Fdz-Polanco, M., 2015. Economic analysis of microaerobic removal of H2S from biogas in full-scale sludge digesters. Bioresour. Technol. 192, 280–286. https://doi.org/10.1016/j.biortech.2015.05.048

Dykstra, C.M., Pavlostathis, S.G., 2021. Hydrogen sulfide affects the performance of a methanogenic bioelectrochemical system used for biogas upgrading. Water Res. 200, 117268. https://doi.org/10.1016/j.watres.2021.117268

Erdirencelebi, D., Kucukhemek, M., 2018. Control of hydrogen sulphide in full-scale anaerobic digesters using iron (III) chloride: performance, origin and effects. Water SA 44. https://doi.org/10.4314/wsa.v44i2.04

Fang, H.H.P., Liu, Y., 1995. X-ray analysis of anaerobic granules. Biotechnol. Tech. 9, 513–518. https://doi.org/10.1007/BF00159568

Fermoso, F.G., Bartacek, J., Jansen, S., Lens, P.N.L., 2009. Metal supplementation to UASB bioreactors: from cell-metal interactions to full-scale application. Sci. Total Environ. 407, 3652–3667. https://doi.org/10.1016/J.SCITOTENV.2008.10.043

Ferry, J.G., 1999. Enzymology of one-carbon metabolism in methanogenic pathways. FEMS Microbiol. Rev. 23, 13–38. https://doi.org/10.1111/j.1574-6976.1999.tb00390.x

Filgueiras, A.V., Lavilla, I., Bendicho, C., 2002. Chemical sequential extraction for metal partitioning in environmental solid samples. J. Environ. Monit. 4, 823–857. https://doi.org/10.1039/b207574c

Firer, D., Friedler, E., Lahav, O., 2008. Control of sulfide in sewer systems by dosage of iron salts: Comparison between theoretical and experimental results, and practical implications. Sci. Total Environ. 392, 145–156. https://doi.org/10.1016/j.scitotenv.2007.11.008

Fletcher, P., Beckett, P.H.T., 1987. The chemistry of heavy metals in digested sewage sludge—II. Heavy metal complexation with soluble organic matter. Water Res. 21, 1163–1172. https://doi.org/10.1016/0043-1354(87)90167-9

Flores-Alsina, X., Solon, K., Kazadi Mbamba, C., Tait, S., Gernaey, K.V., Jeppsson, U., Batstone, D.J., 2016. Modelling phosphorus (P), sulfur (S) and iron (Fe) interactions for dynamic simulations of anaerobic digestion processes. Water Res. 95, 370–382. https://doi.org/10.1016/j.watres.2016.03.012

Frunzo, L., Fermoso, F.G., Luongo, V., Mattei, M.R., Esposito, G., 2019. ADM1-based mechanistic model for the role of trace elements in anaerobic digestion processes. J. Environ. Manage. 241, 587–602. https://doi.org/10.1016/j.jenvman.2018.11.058

Fuentes, A., Lloréns, M., Sáez, J., Isabel Aguilar, M., Ortuño, J.F., Meseguer, V.F., 2008. Comparative study of six different sludges by sequential speciation of heavy metals. Bioresour. Technol. 99, 517–525. https://doi.org/10.1016/j.biortech.2007.01.025

George, S., Mattei, M.R., Frunzo, L., Esposito, G., van Hullebusch, E.D., Fermoso, F.G., 2023. Dynamic modelling the effects of ionic strength and ion complexation on trace metal speciation during anaerobic digestion. J. Environ. Manage. 343, 118144. https://doi.org/10.1016/j.jenvman.2023.118144

Ghimire, A., Gyawali, R., Lens, P.N.L., Lohani, S.P., 2021. Chapter 11 - Technologies for removal of hydrogen sulfide (H2S) from biogas, in: Aryal, N., Mørck Ottosen, L.D., Wegener Kofoed, M.V., Pant, D. (Eds.), Emerging Technologies and Biological Systems for Biogas Upgrading. Academic Press, pp. 295–320. https://doi.org/10.1016/B978-0-12-822808-1.00011-8

Glass, J.B., Orphan, V.J., 2012. Trace metal requirements for microbial enzymes involved in the production and consumption of methane and nitrous oxide. Front. Microbiol. 3. https://doi.org/10.3389/fmicb.2012.00061

Gujer, W., Zehnder, A.J.B., 1983. Conversion Processes in Anaerobic Digestion. Water Sci. Technol. 15, 127–167. https://doi.org/10.2166/wst.1983.0164

Habagil, M., Keucken, A., Horváth, I.S., 2020. Biogas production from food residues—the role of trace metals and co-digestion with primary sludge. Environ. - MDPI 7. https://doi.org/10.3390/environments7060042

Henze, M., 2008. Biological wastewater treatment : principles, modelling and design. IWA Pub.

Hullebusch, E.D.V., Utomo, S., Zandvoort, M.H., Piet, P.N., 2005. Comparison of three sequential extraction procedures to describe metal fractionation in anaerobic granular sludges. Talanta 65, 549–558. https://doi.org/10.1016/J.TALANTA.2004.07.024

Jansen, S., 2004. Speciation and bioavailability of cobalt and nickel in anaerobic wastewater treatment.

Jong, T., Parry, D.L., 2004. Adsorption of Pb(II), Cu(II), Cd(II), Zn(II), Ni(II), Fe(II), and As(V) on bacterially produced metal sulfides. J. Colloid Interface Sci. 275, 61–71. https://doi.org/10.1016/j.jcis.2004.01.046

Kaksonen, A.H., Riekkola-Vanhanen, M.L., Puhakka, J.A., 2003. Optimization of metal sulphide precipitation in fluidized-bed treatment of acidic wastewater. Water Res. 37, 255–266. https://doi.org/10.1016/S0043-1354(02)00267-1

Katz, S.A., 1991. The analytical biochemistry of chromium. Environ. Health Perspect. 92, 13–16. https://doi.org/10.1289/ehp.919213

Kazadi Mbamba, C., Tait, S., Flores-Alsina, X., Batstone, D.J., 2015. A systematic study of multiple minerals precipitation modelling in wastewater treatment. Water Res. 85, 359–370. https://doi.org/10.1016/j.watres.2015.08.041

Khalid, A., Arshad, M., Anjum, M., Mahmood, T., Dawson, L., 2011. The anaerobic digestion of solid organic waste. Waste Manag. 31, 1737–1744. https://doi.org/10.1016/j.wasman.2011.03.021

Lens, P., LW Hulshoff, P., 2020. Environmental Technologies to Treat Sulfur Pollution: Principles and Engineering. IWA Publishing. https://doi.org/10.2166/9781789060966

Maharaj, B.C., Mattei, M.R., Frunzo, L., van Hullebusch, E.D., Esposito, G., 2018. ADM1 based mathematical model of trace element precipitation/dissolution in anaerobic digestion processes. Bioresour. Technol. 267, 666–676. https://doi.org/10.1016/j.biortech.2018.06.099

Marcato, C.-E., Pinelli, E., Cecchi, M., Winterton, P., Guiresse, M., 2009. Bioavailability of Cu and Zn in raw and anaerobically digested pig slurry. Ecotoxicol. Environ. Saf. 72, 1538–1544. https://doi.org/10.1016/j.ecoenv.2008.12.010

Mata-Alvarez, J., Macé, S., Llabrés, P., 2000. Anaerobic digestion of organic solid wastes. An overview of research achievements and perspectives. Bioresour. Technol. 74, 3–16. https://doi.org/10.1016/S0960-8524(00)00023-7

Mathivanan, K., Chandirika, J.U., Vinothkanna, A., Yin, H., Liu, X., Meng, D., 2021. Bacterial adaptive strategies to cope with metal toxicity in the contaminated environment – A review. Ecotoxicol. Environ. Saf. 226, 112863. https://doi.org/10.1016/j.ecoenv.2021.112863

Mo, R., Guo, W., Batstone, D., Makinia, J., Li, Y., 2023. Modifications to the anaerobic digestion model no. 1 (ADM1) for enhanced understanding and application of the anaerobic treatment processes – A comprehensive review. Water Res. 244, 120504. https://doi.org/10.1016/j.watres.2023.120504

Montecchio, D., Astals, S., Di Castro, V., Gallipoli, A., Gianico, A., Pagliaccia, P., Piemonte, V., Rossetti, S., Tonanzi, B., Braguglia, C.M., 2019. Anaerobic co-digestion of food waste and waste activated sludge: ADM1 modelling and microbial analysis to gain insights into the two substrates' synergistic effects. Waste Manag. 97, 27–37. https://doi.org/10.1016/j.wasman.2019.07.036

Morel, F., Hering, J., 1993. Principles and applications of aquatic chemistry.

Nguyen, L.N., Kumar, J., Vu, M.T., Mohammed, J.A.H., Pathak, N., Commault, A.S., Sutherland, D., Zdarta, J., Tyagi, V.K., Nghiem, L.D., 2021. Biomethane production from anaerobic co-digestion at wastewater treatment plants: A critical review on development and innovations in biogas upgrading techniques. Sci. Total Environ. 765, 142753. https://doi.org/10.1016/j.scitotenv.2020.142753

Oleszkiewicz, J.A., Sharma, V.K., 1990. Stimulation and Inhibition of Anaerobic Processes by Heavy MetalsmA Review.

Osuna, M.B., Zandvoort, M.H., Iza, J.M., Lettinga, G., Lens, P.N.L., 2003. Effects of trace element addition on volatile fatty acid conversions in anaerobic granular sludge reactors. Environ. Technol. U. K. 24, 573–587. https://doi.org/10.1080/09593330309385592

Ozyildiz, G., Zengin, G.E., Güven, D., Cokgor, E., Özdemir, Ö., Hauduc, H., Takács, I., Insel, G., 2023. Restructuring anaerobic hydrolysis kinetics in plant-wide models for accurate prediction of biogas production. Water Res. 245, 120620. https://doi.org/10.1016/j.watres.2023.120620

Parker, D.R., Norvell, W.A., Chaney, R.L., 1995. GEOCHEM-PC—A Chemical Speciation Program for IBM and Compatible Personal Computers, in: Chemical Equilibrium and Reaction Models. John Wiley & Sons, Ltd, pp. 253–269. https://doi.org/10.2136/sssaspecpub42.c13

Roussel, J., 2013. Metal behaviour in anaerobic sludge digesters supplemented with trace nutrients.

Sauvé, S., Parker, D.R., 2005. Chemical Speciation of Trace Elements in Soil Solution, in: Chemical Processes in Soils. John Wiley & Sons, Ltd, pp. 655–688. https://doi.org/10.2136/sssabookser8.c14

Schecher, W.D., McAvoy, D.C., 1992. MINEQL+: A software environment for chemical equilibrium modeling. Comput. Environ. Urban Syst. 16, 65–76. https://doi.org/10.1016/0198-9715(92)90053-T

Scherer, P., Sahm, H., 1981. Effect of trace elenments and vitamins on the growth of Methanosarcina barkeri. Acta Biotechnol. 1, 57–65; ISSN: 1618-2863.

Schink, B., 2002. Synergistic interactions in the microbial world. Antonie Van Leeuwenhoek 81, 257–261. https://doi.org/10.1023/A:1020579004534

Siegel, F.R., 2002. Environmental Geochemistry of Potentially Toxic Metals. Springer, Berlin, Heidelberg. https://doi.org/10.1007/978-3-662-04739-2

Solon, K., Flores-Alsina, X., Mbamba, C.K., Volcke, E.I.P., Tait, S., Batstone, D., Gernaey, K.V., Jeppsson, U., 2015. Effects of ionic strength and ion pairing on (plant-wide) modelling of anaerobic digestion. Water Res. 70, 235–245. https://doi.org/10.1016/j.watres.2014.11.035

Song, X., Luo, W., Hai, F.I., Price, W.E., Guo, W., Ngo, H.H., Nghiem, L.D., 2018. Resource recovery from wastewater by anaerobic membrane bioreactors: Opportunities and challenges. Bioresour. Technol. 270, 669–677. https://doi.org/10.1016/j.biortech.2018.09.001

Staicu, L.C., Simon, S., Guibaud, G., Yekta, S.S., Calli, B., Bartacek, J., Fermoso, F.G., Van Hullebusch, E.D., Van Hullebusch, E., Collins, G., Roussel, J., Mucha, A.P., Esposito, G., 2019. Chapter 2 Biogeochemistry of trace elements in anaerobic digesters from the book Trace Elements in Anaerobic Biotechnologies.

Templeton, D.M., Ariese, F., Cornelis, R., Danielsson, L.-G., Muntau, H., Leeuwen, H.P. van, Lobinski, R., 2000. Guidelines for terms related to chemical speciation and fractionation of elements. Definitions, structural aspects, and methodological approaches (IUPAC Recommendations 2000). Pure Appl. Chem. 72, 1453–1470. https://doi.org/10.1351/pac200072081453

Tessier, A., Campbell, P.G.C., Bisson, M., 1979. Sequential extraction procedure for the speciation of particulate trace metals. Anal. Chem. 51, 844–851. https://doi.org/10.1021/ac50043a017

Thanh, P.M., Ketheesan, B., Yan, Z., Stuckey, D., 2016. Trace metal speciation and bioavailability in anaerobic digestion: A review. Biotechnol. Adv. 34, 122–136. https://doi.org/10.1016/j.biotechadv.2015.12.006

van der Veen, A., Fermoso, F.G., Lens, P.N.L., 2007. Bonding Form Analysis of Metals and Sulfur Fractionation in Methanol-Grown Anaerobic Granular Sludge. Eng. Life Sci. 7, 480–489. https://doi.org/10.1002/ELSC.200720208

Van Hullebusch, E.D., Gieteling, J., Zhang, M., Zandvoort, M.H., Daele, W.V., Defrancq, J., Lens, P.N.L., 2006. Cobalt sorption onto anaerobic granular sludge: Isotherm and spatial localization analysis. J. Biotechnol. 121, 227–240. https://doi.org/10.1016/J.JBIOTEC.2005.07.011

van Hullebusch, E.D., Guibaud, G., Simon, S., Lenz, M., Yekta, S.S., Fermoso, F.G., Jain, R., Duester, L., Roussel, J., Guillon, E., Skyllberg, U., Almeida, C.M.R., Pechaud, Y., Garuti, M., Frunzo, L., Esposito, G., Carliell-Marquet, C., Ortner, M., Collins, G., 2016. Methodological approaches for fractionation and speciation to estimate trace element bioavailability in engineered anaerobic digestion ecosystems: An overview. Crit. Rev. Environ. Sci. Technol. 46, 1324–1366. https://doi.org/10.1080/10643389.2016.1235943

Vu, H.P., Nguyen, L.N., Wang, Q., Ngo, H.H., Liu, Q., Zhang, X., Nghiem, L.D., 2022. Hydrogen sulphide management in anaerobic digestion: A critical review on input control, process regulation, and post-treatment. Bioresour. Technol. 346, 126634. https://doi.org/10.1016/j.biortech.2021.126634

Wang, Z., Banks, C.J., 2006. Report: Anaerobic digestion of a sulphate-rich high-strength landfill leachate: the effect of differential dosing with FeCl3. Waste Manag. Res. J. Sustain. Circ. Econ. 24, 289–293. https://doi.org/10.1177/0734242X06065232

Watson, J.H.P., Ellwood, D.C., Deng, Q., Mikhalovsky, S., Haytert, C.E., Evanst, J., 1995. HEAVY METAL ADSORPTION ON BACTERIALLY PRODUCED FeS, Minerals Engineering.

Yekta, S.S., Skyllberg, U., Danielsson, Å., Björn, A., Svensson, B.H., 2017. Chemical speciation of sulfur and metals in biogas reactors – Implications for cobalt and nickel bio-uptake processes. J. Hazard. Mater. 324, 110–116. https://doi.org/10.1016/J.JHAZMAT.2015.12.058

Zheng, X., Wu, K., Sun, P., Zhouyang, S., Wang, Y., Wang, H., Zheng, Y., Li, Q., 2021. Effects of substrate types on the transformation of heavy metal speciation and bioavailability in an anaerobic digestion system. J. Environ. Sci. 101, 361–372. https://doi.org/10.1016/j.jes.2020.08.032

CHAPTER 6

Conclusions and Recommendations for Future Work

6.1. CONCLUSIONS

The thesis presented a model-based approach to assess trace metal speciation effects during anaerobic digestion. ADM1, the most widely used model for anaerobic digestion, is extended to incorporate processes influencing TM effects. The thesis discussed the progressive development of the trace metal speciation model and different potential applications of the model linked to metal effects in AD.

The first chapter highlighted the need to develop a trace metal speciation model in anaerobic digestion. The chapter gave a background on role of various trace metals in different anaerobic digestion pathways. Existing methods to assess TM speciation in AD are reviewed and major processes influencing the speciation of metals are identified. General findings of the chapter are summarised below.

- Major processes to be considered for modelling trace metal speciation during anaerobic digestion are precipitation (with sulphides, carbonates, phosphates), complexation (inorganic and organic), adsorption and microbial uptake.
- Analytical methods to determine metal speciation in AD have limitations and there are no technologies available to date to quantify bioavailable concentration of metals.
- Currently, geochemical equilibrium softwares are used as a model approach to understand metal speciation. However, they can only be used concurrently with analytical measurements and they have limitations in adding process kinetics and biological reactions.
- Need for a dynamic mechanistic model to define trace metal speciation in anaerobic digestion systems is found essential and existing dynamic models need rigorous improvements in terms of model development, calibration and application.

The second chapter addressed one of the limitations in existing model framework for trace metal speciation modelling in anaerobic digestion. The chapter discussed three different model approaches to define aqueous phase chemistry in anaerobic digestors – (i) existing TM speciation model framework (Frunzo et al., 2019; Maharaj et al., 2018, 2019, 2021), (ii) with ionic activity correction and (iii) with ionic activity correction and ion pairing. Since bioavailability of a trace metal and its effects on AD relies on accurate description of metal speciation, this study showed the significance of considering non-ideal aqueous phase chemistry (ionic strength correction and ion pairing) in modelling trace metal dynamics. Major conclusions drawn from the chapter are outlined below:

- Both ion activity corrections and ion pairing influence trace metal effects on anaerobic digestion performance and methane production by changing the total dissolved and labile metal fraction. Hence, it is highly recommended to consider physicochemical framework for non-ideal aqueous phase chemistry in modelling trace metal effects in AD.

- Anaerobic digestion performance increases with increase in ionic strength and ion pairing due to decrease in precipitation and increase in metal labile fractions.
- The proposed model can reasonably simulate the trace metal speciation effects on AD. Few examples like stimulatory and inhibitory effects of trace metals and influence of iron to sulphide ratio on metal speciation and digestion performance are tested and verified. Dosing iron increased methane production and decreased H_2S concentration. However, when iron to sulphide ratio is greater than 1, methane production decreases due to increase in dissolved Fe thereby reaching inhibitory levels of Fe.

In the third chapter, a complete trace metal speciation model for application in anaerobic digesters has been proposed. The model presented in Chapter 2 has been improved to incorporate major trace metal speciation processes like complexation (with inorganic species, chelates, metabolites) and adsorption (on biomass, soluble inerts, precipitates) along with TM precipitation (with sulphides, carbonates, phosphates), biouptake, dose response and TM release during disintegration process. Lab experiments carried out and described in Chapter 3 facilitated model calibration and application to simulate metal deprivation conditions in a UASB reactor at lab scale. Given below are the major conclusions gained from the chapter.

- Model could reasonably predict trace metal effects like metal deprivation in an anaerobic digestor as being observed during comparison with the experimental data.
- In addition to precipitation process, ionic strength also influences TM adsorption and hence ionic strength is an important operational parameter controlling the system.
- Model results have been verified under various scenarios to analyse effect of EDTA and amino acids. Model results verified that amino acids play a significant role in controlling metal labile fraction for substrates rich in protein content. Moreover, as being reported earlier in different experimental studies, addition of EDTA reduces trace metal dosing concentration.

Fourth chapter presented another potential application of the model. Model is tested under different scenarios of dosing strategies to check model capability for experimental and industrial applications. Main dosing strategies such as mode of dosing, dosing frequency, concentration of dosing, dosing form and time of dosing are simulated with the model. Model results are verified with existing observations from experimental studies. Influence of reactor configuration on dosing form has also been verified after model calibration with literature experimental data. Key findings from the chapter are listed below.

- Best ways to dose trace metals to anaerobic digesters for improving methane yield are analysed. Repeated pulse dosing is the best mode to dose TM in comparison with other modes of dosing such as continuous, single pulse, preloading and in-situ loading.

- Low TM concentration at high dosing frequency is preferable over high dosage at low frequency.
- Trace metals should be supplemented at the earliest time possible after metal deficit at optimum concentration levels. An excess of metal supplementation can result in toxicity.
- Preferred dosing form depends on reactor configuration. Easily dissociable metal forms like metal chlorides are ideal in continuous reactors whereas strong metal chelates like EDTA complexes are advisable for reactors with high retention times like batch or semi-continuous reactors.

Application of the trace metal speciation model in the context of a full-scale reactor is presented in the fifth chapter. The most common trace metal supplemented in chemical form to a full-scale reactor is iron with the objective to reduce H_2S content in the biogas. Trace metal speciation model developed in the thesis is adopted to analyse optimum concentration of Fe to be supplemented to anaerobic digestors with emphasis to achieve less H_2S contamination in biogas and avoid any possible inhibition effects in AD process caused by addition of Fe. Moreover, effect of trace metals during co-digestion has been investigated. Data collected from anaerobic digestor in a full-scale wastewater treatment plant is used for model application. Major conclusions from the chapter are highlighted below.

- High dosage of iron will not only result in reduction of methane yield due to inhibition of Fe but also is not useful for H_2S removal from biogas. Hence ideal dosage of iron is maintaining iron to sulphide ratio around 1.
- Increasing co-substrate: sewage sludge ratio increases methane production due to higher degradability of co-substrate. However, when trace metal effects are considered, increasing co-substrate reduces methane production due to Ni deprivation in co-substrate.
- Substrate characteristics such as sulphur content and trace metal concentration influence co-digestion. In case of metal deprivation, co-digestion can be performed using co-substrates rich in trace metals to overcome metal limitation. However, optimum mixing ratio should be maintained to ensure sufficient metal bioavailability.

6.2. RECOMMENDATIONS FOR FUTURE WORK

A mechanistic model to study influence of trace metals during anaerobic digestion based on knowledge on the topic from evident proofs from literature and expert knowledge is presented in this thesis. The model has been verified to reproduce some common trends widely reported in literature. The model has also been calibrated and verified with lab scale experimental data generated during this study as well as data available from literature. Theoretical values are used for estimation of few parameters such as kinetic rate constants for adsorption-desorption processes. A complete set of data to precisely calibrate all the parameters introduced in the model is missing and this would require ad hoc experiments to be carried out. The model needs to be calibrated and validated under different conditions as well as reactor configurations to check its capability and adaptability. This also points out the need of a sensitivity analysis to identify the most influential parameters. Local sensitivity analysis has been carried in this thesis. However, there is a scope for performing global sensitivity analysis for better identification of influential parameters in the model. A systematic analysis on effect of initial conditions can be performed as it was found to be very influential for accurate model results.

Scalability of the model also needs to be extensively studied. Though Chapter 5 highlighted potential application of the model in the full-scale reactor context, the model needs to be validated for full scale applications. Improving the model to study TM influence during co-digestion facilitating selection of suitable substrates under metal deprivation conditions would be another interesting domain of application of the model.

Regarding further model development, complete knowledge about forms of metal species that are bioavailable as well as differential response of various microbial communities to various metal species are lacking, and the analytical research in this direction is still in progress. The model can be further improved if more knowledge is available in this context. For example, metal species that are considered to be labile in the dose response function of the model can be defined better if more information regarding this is available in the future. The terms EC 50 and IC 50 are used as a means to capture differential response of microbes to different trace metals. Another approach would be to use distinct inhibitory effect functions on different biological pathways. Further consideration of compounds such as complexation of TMs with proteins, organic compounds (humic substances) or biogenic products such as SMPs or EPS can be included. Currently, complexation of TMs with EPS and SMPs is considered only in the disintegration step. However, it can be incorporated in other digestion pathways.

Both anaerobic digestion and trace metal bioavailability are complex fields and hence developing a combined mechanistic model for both phenomena to a level of capturing all the known knowledge can get extremely complex. An ideal model will be the simplest model with the capability to accurately predict targeted objectives for potential applications of the model. However, few improvements that can be made to the proposed model if the user

objectives demand can be identified in the incorporation of other TMs in the model such as Selenium or Molybdenum, modelling redox reactions and more detailed definition of TM influence on the biological pathways. Anaerobic digestion pathways defined in ADM1 can be improved by introducing new pathways based on their differential response to trace metals and TM influence on metabolic pathways can be defined further.

LIST OF SCIENTIFIC PUBLICATIONS FROM THE THESIS

Peer reviewed papers

George, S., Mattei, M. R., Frunzo, L., Esposito, G., van Hullebusch, E. D., & Fermoso, F. G. (2023). Dynamic modelling the effects of ionic strength and ion complexation on trace metal speciation during anaerobic digestion. Journal of Environmental Management, 343, 118144. https://doi.org/10.1016/j.jenvman.2023.118144.

George, S., Mattei, M. R., Frunzo, L., Esposito, G., van Hullebusch, E. D., & Fermoso, F. G. (2023). Extended ADM1 model to study trace metal speciation and its effects on anaerobic digestion – Under review.

George, S., Mattei, M. R., Frunzo, L., Esposito, G., van Hullebusch, E. D., & Fermoso, F. G. Model based analysis of trace metal dosing strategies to improve methane yield in anaerobic digestion systems – ready to be submitted.

George, S., Mattei, M. R., Frunzo, L., Esposito, G., Hortal, G. C., Gonzalez, E. M. R. & Fermoso, F. G. Application of the trace metal speciation model framework to a full-scale anaerobic digester – in preparation.

Conferences

George, S., Mattei, M. R., Frunzo, L., & Fermoso, F. G. (2023). Model based analysis of trace metal speciation effects in an anaerobic digestion system under different modes of operation. 11th IWA Symposium on Modelling and Integrated Assessment (Watermatex 2023), 2023 (Oral).

George, S., Mattei, M. R., Frunzo, L., & Fermoso, F. G. (2023). Influence of substrate characterization on trace metal dosing to improve biogas yield during anaerobic digestion: a dynamic model-based study. 6th IWA International Conference on eco-Technologies for Wastewater Treatment (ecoSTP2023), 2023 (Oral).

George, S., Mattei, M. R., Frunzo, L., & Fermoso, F. G. (2023). Mathematical modelling trace metal effects on anaerobic digestion to improve process performance and methane yield. 4th International Conference for Bioresource Technology for Bioenergy, Bioproducts & Environmental Sustainability (BIORESTEC), 2023 (Oral).

George, S., Mattei, M. R., Frunzo, L., Esposito, G., van Hullebusch, E. D., & Fermoso, F. G. (2023). Modelling trace metal speciation during anaerobic digestion. International Congress on Metal microbe applications for circular economy (IMAB23), 2023 (Oral).

George, S., Mattei, M. R., Frunzo, L., & Fermoso, F. G. (2023). Effect of Cobalt during propionate degradation in a UASB reactor. International Congress on Metal microbe applications for circular economy (IMAB23), 2023 (Poster).

George, S., Mattei, M. R., Frunzo, L., Esposito, G., van Hullebusch, E. D., & Fermoso, F. G. (2022). Mathematical modelling trace metal speciation effects during anaerobic digestion. VIII Jornadas Doctorales del Programa de Doctorado en Biotecnología, Ingeniería y Tecnología Química de la Universidad Pablo de Olavide (Poster).

Thesis cover designed by Joseph George

UNIVERSIDAD PABLO DE OLAVIDE SEVILLA

UNIVERSITÀ DEGLI STUDI DI NAPOLI FEDERICO II

EUROPEAN JOINT DOCTORATE

M_2-e^x

Metal-Micro exploitation